DOE/MC/30174 -- 5551
(DE97002208)

Rapid Surface Sampling and Archival Record (RSSAR) System

Topical Report

October 1, 1993 - December 31, 1994

Work Performed Under Contract No.: DE-AC21-93MC30174

For

U.S. Department of Energy
Office of Environmental Management
Office of Technology Development
1000 Independence Avenue
Washington, DC 20585

U.S. Department of Energy
Office of Fossil Energy
Morgantown Energy Technology Center
P.O. Box 880
Morgantown, West Virginia 26507-0880

By
General Electric Corporation
Research and Development
P. O. Box 8
Schenectady, New York 12301

Disclaimer

Contents

List of Figures

List of Tables

Executive Summary

This report describes the results of Phase I efforts to develop a Rapid Surface Sampling and Archival Record (RSSAR) System for the detection of semivolatile organic contaminants on concrete, transite, and metal surfaces.

The characterization of equipment and building surfaces for the presence of contaminants as part of building decontamination and decommissioning activities is an immensely large task of concern to both government and industry. Because of the high cost of hazardous waste disposal, old, contaminated buildings cannot simply be demolished and scrapped. Contaminated and clean materials must be clearly identified and segregated so that the clean materials can be recycled or reused, if possible, or disposed of more cheaply as nonhazardous waste.

DOE has a number of sites requiring surface characterization. These sites are large, contain very heterogeneous patterns of contamination (requiring high sampling density), and will thus necessitate an enormous number of samples to be taken and analyzed. Characterization of building and equipment surfaces will be needed during initial investigations, during cleanup operations, and during the final confirmatory process, increasing the total number of samples well beyond that needed for initial characterization. This multiplicity of information places a premium on the ability to handle and track data as efficiently as possible.

GE also has a number of sites requiring building decontamination and decommissioning and recognizes the limitations of currently existing technology to cost-effectively meet surface characterization needs. The most widely used current method involves wipe sampling. In wipe sampling, the surface is wiped with a solvent-soaked piece of cloth, paper or the like, and the wipe is sent to an off-site laboratory for analysis. This method of analysis has a number of problems:

- This method is expensive and highly dependent on the technique used by the operator.
- It cannot be used to lower the cost of a cleanup by providing real-time information to the remediators in a manner that allows them to operate in the most efficient manner.
- The use of solvents raises safety concerns about worker exposure.
- Whenever large numbers of samples are required, characterization by wipe-sampling becomes a logistical nightmare. All samples would have to be manually tracked through the system, increasing the possibility of human errors.
- Off-site analysis with manual manipulation (extraction, etc.) of the wipe sample is very expensive.

- This method requires analysis of all the samples taken and provides no way of effectively screening out a large percentage of the clean samples to reduce analysis costs.

Aware of the shortcomings of traditional surface characterization technology, GE, with DOE support, has undertaken a 12-month effort to complete Phase I of a proposed four-phase program to develop the RSSAR system. The objectives of this work are to provide instrumentation to cost-effectively sample concrete and steel surfaces, provide a "quick-look" indication for the presence or absence of contaminants, and collect samples for later, more detailed analysis in a readily accessible and addressable form. The Rapid Surface Sampling and Archival Record (RSSAR) System will be a modular instrument made up of several components:

- Sampling heads for
  - concrete surfaces
  - steel surfaces
  - bulk samples
- Quick-look detectors
  - photoionization
  - ultraviolet
- Multisample trapping module to trap and store vaporized contaminants in a manner suitable for subsequent detailed lab-based analyses.

GE has assembled a strong team to develop and build the RSSAR system. The EAI Corporation brings an expertise in surface sampling and solid-phase sorbents (as applied to chemical weapons treaty verification) coupled with proven manufacturing and marketing capabilities. Detection Limit Technology, LC possesses state-of-the-art expertise in SERS technology.

In Phase I, GE and its subcontractors, EAI Corporation, Inc., and Detection Limit Technology, LC, have accomplished the goals set out in the RSSAR proposal. Some of the tasks that have been completed dealt with the design, construction, and testing of equipment that will make up the RSSAR system, such as the concrete sampler head, the bulk sampler head, and the near vacuum ultraviolet (NVUV) detector. Other information about critical operating conditions for the sampler and answers to questions such as, "What is the best operating temperature to avoid conversion of polychlorinated biphenyls (PCBs) to polychlorinated dibenzodioxins (PCDDs) and polychlorinated dibenzofurans (PCDFs)?"; "What flow rates provide optimum sample recovery?"; and "What solid phase sorbents exhibit the best trapping efficiency?" have been generated. Still another task determined the feasibility of advanced analytical techniques such as surface-enhanced Raman spectroscopy (SERS) to increase the productivity of subsequent analyses of the samples taking place back in the laboratory. The program involves a

seemingly disparate collection of tasks, but each is critical to the development of a successful, practical, and commercially viable surface sampling system. In somewhat more detail, we have

- Designed, built, and tested a thermal concrete sampler head with appropriate heating rate and heat distribution characteristics.
- Developed a concrete model to aid in understanding the sampling process and interpreting the sampling results.
- Designed, built, and tested a bulk sampler head for characterizing loose materials such as floor sweepings and materials drilled from bore holes.
- Demonstrated a commercially available photoionization detector as a "quick-look" indicator of surface contamination.
- Designed, built, and tested a near vacuum ultraviolet (NVUV) absorption detector as a potential "quick-look" detector.
- Determined that the detection limits for both "quick-look" detectors are sufficient for use in thermal sampling.
- Optimized sampling flow rate conditions using the bulk sampler head by measuring sampling efficiencies using model compounds representing three major classes of pollutants: oil, polychlorinated biphenyls (PCBs) and polynuclear aromatic hydrocarbons (PAHs).
- Tested and identified suitable commercially available solid-phase sorbents for use in trapping and archiving thermally desorbed pollutants.
- Demonstrated the feasibility of using surface-enhanced Raman spectroscopy (SERS) as an analytical tool for detecting PCBs (Aroclor® and single congeners) in the mixture presence of large quantities of oil.
- Demonstrated the feasibility of developing SERS coating technology that favorably absorbs PCBs from oil solutions to allow for detection and quantitation at detection limits of interest in surface sampling.
- Developed a preliminary design for the multitube sample trapping module that will house solid-phase sorbent tubes and will allow for simple, automated subsequent analysis of samples while providing direct transfer of sampling data for data-handling simplification.
- Investigated the temperature dependence of the formation of dibenzofurans from a PCB congener in concrete. In the low temperature region, below 250°C, we found a surprising increase in formation. However, the data in this region is too scattered to be convincing. This region needs to be explored in more detail in Phase 2.

® Aroclor is a trademark of the Monsanto Company.

In Phase II, the team will develop the steel sampling head, the multisample trapping module and will construct a fully integrated lab-scale system. In Phase III, a portable prototype system suitable for field use will be constructed. The system will be used in extensive field tests at a GE site. In Phase IV, the design of a production system will be completed and production units will be built.

The RSSAR system will provide DOE with a new tool to dramatically lower the costs associated with site decontamination and decommissioning activities. It will allow surfaces to be rapidly sampled for the presence of semivolatile organic contaminants, and will provide the means for quickly identifying clean surfaces. It will archive samples in a form that will allow cost-effective laboratory analysis and will provide automated tracking of sampling record and analytical results.

Introduction

The purpose of this effort is to develop a rapid surface contamination measurement system that will provide a "quick-look" indication of contaminated areas, an archival record, and an automated analysis of that record. By providing rapid analyses and a large number of accurate measurements of surface and subsurface contamination, the cost of remediation of large industrial sites will be dramatically lowered by reducing both the characterization time and the material fraction that must be remediated.

The Department of Energy (DOE) sites contain very large areas contaminated with radionuclides and semivolatile organic compounds as the result of decades of nuclear weapon and fuel production activities. Concrete, transite, and metal surfaces have been exposed to these contaminants. Unknown but substantial portions of these surfaces have been contaminated to various depths. Because contamination concentrations can vary widely over adjacent exposed surfaces, these surfaces must be sampled at closely spaced intervals to provide accurate identification of contaminants. Consequently, a huge number of surface regions must be characterized, particularly because remediated areas must be sampled more than once for identification and verification.

Current surface characterization procedures are difficult, expensive, and slow. They require an unacceptably long time to complete and consume a large share, often around 30%, of remediation/disposition resources. Accordingly, they will not meet the challenge of providing low-cost, rapid, quantitative and certifiable surface characterization on the scale required by DOE as part of its decontamination and decommissioning activities.

The objective of this effort is to help develop and demonstrate new and existing technologies that will enable the DOE to decontaminate and decommission their facilities in the most cost-effective manner possible. The costs and environmental risks associated with disposing of structures and equipment as hazardous waste are unacceptably high owing to the nature of the contaminants and the sheer volume of material in question. The DOE recognizes that a large portion of its contaminated material and equipment must be processed in some manner to a state from which it can be recycled and reused. If recycle or reuse proves impossible, then the material must be cleaned in a manner to allow for its disposal as a nonhazardous substance. Disposal of materials as hazardous waste must be minimized.

Characterization technology is key to accomplishing the DOE's decontamination and decommissioning goals. Building materials and equipment must be adequately characterized before, during, and after decontamination and decommissioning activities. The nature and level of contaminants must be initially established to determine whether cleanup is required. During the cleanup, analysis will be required as an element of cleanup process control. Ultimately, the material will have to be certified as clean before it can be recycled or disposed of.

A number of constraints must be met by any technology facing the challenge of characterizing the DOE's sites. It must

- provide rapid results from the enormous amount of surface area to be screened
- be portable
- accurately assess the identity and level of contaminants
- yield valid analytical results that are believed by regulatory agencies
- be robust
- give results in easily understandable form, at least in screening mode
- be operable by persons with minimal amounts of training
- not be overly capital-intensive

Existing technology for analyzing surface contamination does not meet these constraints. The most common and accepted current method for sampling surfaces for hazardous materials is the EPA wipe or swipe test, in which a measured surface area is wiped with a gauze cloth or other absorbent material soaked with an organic solvent. The wipe is then sent off to a laboratory, extracted with solvent, and the extracts are analyzed for the presence of the contaminants. The method, though widely used, suffers from serious limitations:

- It provides extremely variable results, because it relies on the technique and consistency of individual samplers.
- It is inaccurate, with results depending upon the nature of the surface (rough, smooth, porous, rusted, etc.)
- It requires offsite laboratory analysis that can result in delays of days to weeks.
- It analyzes the surface only, not the region below.
- It generates additional contaminated waste that must be disposed: wipes, solvents and sample containers.
- It exposes workers to potentially dangerous and harmful solvents.
- It does not lend itself to efficient data handling.

On porous surfaces, such as concrete, a freshly cleaned surface may pass a wipe test (contain <10 $\mu g/100$ cm^2 contaminant) only to fail it at a later date as material from below the surface migrates upward. In spite of these limitations, wipe sampling is widely used to detect surface contamination.

This program, which concerns the development of a Rapid Surface Sampling and Archival Record (RSSAR) System, was undertaken to provide a solution to the cost and technical shortcomings of conventional methods for characterizing contaminated sur-

faces. It is directed to the development of a portable instrument system capable of sampling a variety of surfaces for semivolatile organic contaminants. The system under development provides

- rapid sampling - one sample per 100 sec.
- "quick-look" indication of contamination level
- a stored record for detailed, automatable analysis

This system is assembled from instruments incorporating several well-established techniques and instruments incorporating innovative techniques. It comprises

- thermal sampler heads
- a "quick-look" module
- an archival multisample trapping module

The RSSAR system is composed of several modular units, as illustrated in Figure 1.

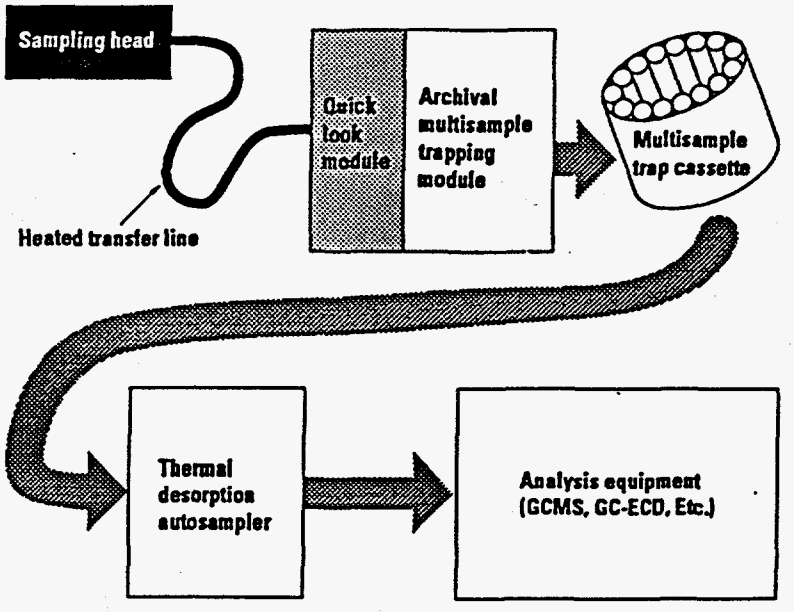

Figure 1. Configuration of RSSAR System. This modular system includes several sampler heads, a quick look facility, an archival record, an organized set of stored samples, and an automated interface to couple this record into various types of analysis equipment.

Thermal sampling for semivolatile compounds has been chosen for development because this technology can provide substantially more reliable readings of surface contamination than wipe sampling. It also minimizes the production of contaminated sampling waste, lends itself to automated processing, separates chemical samples from non-volatile radioactive materials, and is fast. In general, samples are acquired using thermal desorption of contaminants at concrete temperatures between 200 and 250°C generated by radiant heat.

"Concrete," bulk, and "steel" sampler heads are being developed to handle the most frequent sampling requirements. A concrete surface sampler, which has been developed and demonstrated, can be used to determine contamination levels at surfaces and down to at least a few millimeters below the surface for porous, low thermal-conductivity materials, providing information also targeted by the standard wipe test but sampling down to a deeper region. A bulk sampler head has been developed and demonstrated that can be used to measure contaminants in asbestos, paint scrapings, particulate waste, and samples from drilling as well as calibration standards. To determine subsurface contamination, samples from drilling would be placed in the bulk sampler head connected to the RSSAR system for "quick look" and archival analyses. A steel sampler head, which will be developed in Phase II, will be designed for the markedly different sampling conditions provided by nonporous surfaces with high-thermal conductivity.

The purposes of the "quick-look" module are to provide a real-time guide of sampling strategy, a real-time practical indication of system performance, a personnel safety indicator, a redundant indicator channel, and a method to reduce the fraction of samples that are subjected to more time-consuming detailed analysis. The viability of "quick-look" has been demonstrated using both a photoionization detector and ultraviolet absorption.

The archival multisample trapping module traps contaminants and stores them for detailed analysis. This stored record, organized in a cassette format (as shown in Figure 1), is associated with corresponding sample information, to facilitate record-keeping, to minimize handling and training requirements, to reduce errors caused by operator fatigue in the highly repetitive sample acquisition and analysis tasks, and to expedite automated readout. A single sample trapping module is being used in Phase I of this effort, and the results will be used in the design and fabrication of an archival multisample trapping module in Phase II.

The thermal desorption autosampler accepts the organized record format and provides an automated interface to alternative readout instruments such as gas chromatography/mass spectrometry, tandem mass spectrometry, gas chromatography with electron capture detector, or a fast optical readout such as surface-enhanced Raman scattering. Using surface-enhanced Raman scattering, it has been found that PCBs can be detected in solutions containing up to ten times as much transformer oil as PCBs. By manipulating sample and substrate size, quantities of PCBs of interest to the DOE (10 μg on 100 cm^2 surface) should easily be detectable with little additional optimization of techniques that have been developed.

The overall RSSAR System is modular and will use accurate sample acquisition, handling, and analysis techniques. The availability of an archival record that allows detailed analysis (and an occasional backup check on the quick-look detector) will expedite material disposition planning and regulatory approval. Consequently, the RSSAR System will provide a cost-effective approach for the measurement of semivolatile contamination required for large industrial site remediation.

This report provides details on Phase I tasks. Accordingly, the discussion that follows describes the development and demonstration of sampler heads for concrete surfaces and bulk samples, which have been integrated with analytical components to form a quick-look and single sample trapping module. In the quick look module, both a photoionization detector and an ultraviolet absorption cell have been demonstrated to provide target detection limits. In addition, surface-enhanced Raman scattering has been demonstrated to provide fast detection of PCBs in oil. Finally, a conceptual design for an archival multisample trapping module has been prepared.

In Phase II, an archival multisample trapping module will be developed to replace the single-sample trapping module. The modification will allow trapping of up to 50 separate samples and will allow for their transfer to a modified thermal desorption autosampler for subsequent analyses. A steel surface sampler head will be built and demonstrated, and a fully integrated laboratory-scale system will be constructed.

Task 1.2 Sampling Artifact Experiments

This section describes experiments that were done to determine the temperature window for safe thermal sampling of PCBs. The temperature of the thermal sampler needs to be controlled within some bounds to prevent or at least to minimize thermally induced decomposition or alteration of the sample. Although all compounds are subject to thermal decomposition at some temperature, based at a most fundamental level upon bond dissociation energies, the thermal stability of materials vary enormously. A number of the compounds of interest in sampling surfaces at governmental and industrial manufacturing sites are those that were used as heat transfer agents (such as oils and PCBs) and therefore possess considerable inherent thermal and oxidative stability. This stability, though has limits. Even PCBs, noted for their stability and persistence, are known to undergo thermally promoted reactions at temperatures above 300°C. The purpose of these experiments was to characterize the behavior of thermally treated, PCB-contaminated concrete samples in an effort to find temperatures that minimize conversion of the PCBs to polychlorinated dibenzodioxins (PCDDs) or polychlorinated dibenzofurans (PCDFs).

There are two problems associated with thermally induced changes in the sample. First, any change in the sample will serve to complicate subsequent analyses. Second, there is a potential to convert relatively benign substances into more hazardous ones. The possible conversion of PCBs to PCDDs and PCDFs is a good example. Although some changes in the sample may be unavoidable, all reasonable care must be taken to minimize those changes.

A worst case scenario was chosen for these studies. That is, 2,2′,5,5′-tetrachlorobiphenyl contains two chlorine atoms in the ortho and ortho′ positions, ideally set up for a reaction to form a dibenzofuran. Less than half of the structures which make up a typical Aroclor mixture contain this ortho-ortho′ substitution pattern. Dibenzofuran forming reactions from these non-ortho-ortho′ substituted congeners are expected to be much more difficult. As a result, the experiments described in this section will overestimate the formation of dibenzofuran products.

Experimental

Materials – 2,2',5,5'-tetrachlorobiphenyl (nominally 99+% pure by GC/FID) was obtained from AccuStandard, Inc., New Haven, CT, and was used as received. An aged, structural grade concrete sample containing large aggregate (up to 1.5 in.) was obtained as a core sample from a floor in the Engineering Physics Building at GE's Corporate Research and Development Center in Schenectady, NY. The section of flooring was poured in 1954. Analyses of sections of the core showed it to contain no PCBs. Samples of 2,4- and 2,8-dichlorodibenzofuran were obtained from AccuStandard, Inc., and were used as obtained, p-terphenyl was obtained from Aldrich. All solvents were obtained from Baker as pesticide grade, or suitable for organic residue analysis and were used as

received. Standard solutions of 2,4-dichlorodibenzofuran and p-terphenyl in pesticide grade toluene were used as internal standards in the GCMS analysis of the concrete extracts.

Preparation of contaminated concrete samples – A section (0.95 cm thick) of the core concrete sample was broken up using a hammer and crushed using a hand-operated grinder. The concrete was sieved and the fraction of 250-850 μm was retained for use. This size range was chosen to permit rapid diffusion of the analytes through the concrete microstructure without completely removing the effects that the microstructure could have upon chemical conversion. To a glass jar equipped with a magnetic stir bar was added 58.1 g of the concrete, 3.6 mg of 2,2',5,5'-tetrachlorobiphenyl, 75 mL of ethyl acetate and 25 mL of hexane. The jar was covered with aluminum foil and contents were stirred overnight. The suspension was poured into a clean crystallizing dish and was allowed to evaporate at ambient conditions in a fume hood. The crystallizing dish was covered with a paper towel to help avoid contamination.

Analysis of the contaminated concrete samples – The concrete was contaminated with enough 2,2',5,5'-tetrachlorobiphenyl to result in a 62 ppm concentration (62 μg/g). Four samples (approximately one gram, each, weighed to the nearest milligram) of the contaminated concrete were sent to an outside contract laboratory (Northeast Analytical, Inc.) for congener specific analysis. The average concentration was determined to be 34 μg of 2,2',5,5'-tetrachlorobiphenyl per gram of concrete.

Sample ID No.	2,2',5,5'-Tetrachlorobiphenyl Concentration (μg/g)
1500-57-1	29
1500-57-2	31
1500-57-3	42
1500-57-4	33
Average	34

The discrepancy illustrates a well-established difficulty of quantitatively determining species in concrete—a very tenacious matrix.

Thermolysis of the Concrete Samples – To determine the effect of sampling conditions on the production of dibenzofurans and dibenzodioxins in PCB-contaminated concrete samples, experiments using a single PCB congener as a model were performed. Concrete samples contaminated with 2,2',5,5'-tetrachlorobiphenyl were prepared, sealed in glass ampoules (under air), and heated to various temperatures for either 100 or 600 sec. The contaminants were extracted from the concrete, and the solvent extract was analyzed by gas chromatography-mass spectrometry. Thermal gravimetric analysis of un

contaminated concrete samples indicated that a weight loss of approximately 10%, presumably caused by volatilization of water, would be observed at 400°C. To avoid any potential environmental contamination and safety issues associated with the rupture of sealed tubes upon heating, the scale of the experiments was decreased by a factor of ten from those originally proposed, from 1.0 g to 0.1 g. Contaminated concrete (approximately 0.1 g, but each sample accurately weighed to the nearest 0.01 mg) was placed in a pyrex tube (approximately 15 cm × 1 cm, with a wall thickness = 2 mm), previously sealed on one end. The tubes were tapped on a counter top to minimize the amount of concrete adhering to the walls, and were sealed using a natural gas/ oxygen flame. The tubes were sealed under air at atmospheric pressure. The samples sat sealed for a maximum of five days at room temperature prior to thermolysis.

The tubes were individually dipped into a preheated nitrite/nitrate salt bath for the required 100- or 600-sec. time period. To ensure that the sample was actually at temperature for the required 100 or 600 sec., a heatup time, as determined below for ~300 and ~400°C temperatures, was added to the time each sample was in the salt bath. A sample of 2-mercaptobenzimidazole (melting point = 301-305° C), which was sealed into a tube and placed into a salt bath at 310°C, required 1.5 minutes to begin melting. A sample of 1,3,5-benzenetricarboxylic acid (melting point = 380°C), treated similarly and placed in a 390°C bath, required 1.25 minutes to begin melting. One and a half minutes was taken as a rough measure of the time necessary for the tubes to come to temperature. This amount of time was added to the 100- and 600-second time increments that each of the samples were immersed in the salt baths.

After cooling to room temperature, the tubes were rinsed in water to remove any residual salt and opened. The contents of the tubes were poured into 10-mL tapered centrifuge tubes and each section of the halved thermolysis tubes was rinsed with a combined total of 3 mL of a mixture of 3 parts pesticide grade toluene to 1 part pesticide grade ethyl acetate. The rinsings were added to the concrete samples in the centrifuge tubes. The solvent/concrete suspensions were sonicated for 3 minutes using one of two different models of lab-scale ultrasonic generators (Heat Systems Ultrasonics, Inc. Model W185D or W-225), equipped with tapered horns. The centrifuge tubes were immersed in ice water during the sonication step to prevent them from overheating. The tubes were centrifuged for 4 minutes and the supernatant liquid was transferred using a Pasteur pipette in stages to 1-mL volume conical vials (Wheaton) and blown down at ambient temperature under an argon stream. The extractions were repeated a total of three times and all the extraction liquids for each sample were combined. The extracts were analyzed by gas chromatography/mass spectrometry. Levels of polychlorinated dibenzofuran (PCDF) and polychlorinated dibenzodioxin (PCDD) were measured against added standards. The standard used for residual 2,2'5,5'-TCB quantification was p-terphenyl. The standard used for the 2,8-PCDF determination was 2,4-PCDF. Recovery of 2,2'5,5'-TCB was determined using a total ion chromatograph. Analysis of 2,8-PCDF was accomplished by using selective ion monitoring at mass 237.9765.

The GC/MS consisted of a Hewlett-Packard 5890 GC coupled to a JEOL HX110 mass spectrometer. The GC was equipped with a 30-meter DB-5 column (0.32 mm id, 0.5-μm film thickness) operated under isothermal conditions.

Results and Discussion

Thermolysis of the concrete samples contaminated with 2,2',5,5'-tetrachlorobiphenyl (TCB) gave rise to measurable amounts of a single dichlorodibenzofuran isomer at some of the temperatures tested. The results are shown in Table 1.

The table displays the temperature and heating time for each sample, the initial weight of 2,2',5,5'-tetrachlorobiphenyl present in the sample, the recovery of unaltered tetrachlorobiphenyl, the weight of 2,8-dichlorodibenzofuran found in the sample, the percent conversion that amount of dibenzofuran represents, and a percent conversion normalized to the amount of 2,2',5,5'-tetrachlorobiphenyl recovered. This last column is included in an attempt to diminish the effect that variations in extraction efficiency might have on the results. The assumption is made that the solubility and extraction efficiency of the dibenzofuran and tetrachlorobiphenyl are similar. Since significant variability in tetrachlorobiphenyl extraction was encountered, it was surmised that this measure was a more accurate representation of the conversion of 2,2',5,5'-tetrachlorobiphenyl to 2,8-dichlorodibenzofuran. Small amounts of 2,8-PCDF are detected in some of the control samples which were not spiked with 2,2',5,5'-tetrachlorobiphenyl. This may be due to cross contamination of samples during the extraction process, although attempts were made to carefully clean the extraction equipment between runs.

Several important points have emerged. First, the major "product" is unchanged 2,2',5,5'- tetrachlorobiphenyl. In other words, the vast majority of the PCB model is unaffected by the thermolysis conditions. This is shown in Figure 2 which is the total ion chromatogram for one of the samples. Second, there is a temperature dependence on the production of 2,8-PCDF, which is not as simple as originally expected. Additionally only a single PCDF isomer was found.

Table 1. Production of 2,8-Dichlorodibenzofuran from 2,2'-5,5' Tetrachlorobiphenyl: Thermolysis of Contaminated Concrete Samples

Sample	temp(°C)	time (sec)	µg 22'55' -TCB on concrete	% recov of 22'55' -TCB	ng PCDF produced	Conversion (%)	Normalized to PCB Recovery
1500-20-1	200	100	7.4524	40.2	57.3	0.95	2.35
1500-20-1C	200	100	control		0.0		
1500-20-2	200	100	6.0636	29.8	10.8	0.22	0.74
1500-20-3	200	600	6.572	25.0	21.6	0.40	1.62
1500-20-3C	200	600	control		0.0		
1500-22-4	200	600	7.192	6.2	0.0	0.00	0.00
1500-22-5	250	100	8.6862	8.1	0.0	0.00	0.00
1500-22-5C	250	100	control		0.0		
1500-22-6	250	100	8.7172	14.2	0.0	0.00	0.00
1500-22-7	250	600	7.068	23.1	0.0	0.00	0.00
1500-22-7C	250	600	control		0.0		
1500-24-8	250	600	6.2434	14.5	0.0	0.00	0.00
1500-24-9	300	100	7.6074	15.6	1.3	0.02	0.14
1500-24-9C	300	100	control		0.0		
1500-24-10	300	100	6.0202	12.5	0.2	0.00	0.04
1500-24-11	300	600	7.4276	31.8	2.4	0.04	0.13
1500-24-11C	300	600	control		0.0		
1500-24-12	300	600	8.4382	16.7	1.3	0.02	0.11
1500-24-13	350	100	5.5614	36.1	4.5	0.10	0.28
1500-24-13C	350	100	control		0.0		
1500-24-14	350	100	7.9174	31.9	7.5	0.12	0.37
1500-24-15	350	600	6.3674	14.0	3.7	0.07	0.51
1500-29-15C	350	600	control		0.0		
1500-29-16	350	600	6.107	29.1	9.0	0.18	0.63
1500-29-17	400	100	6.6092	16.4	11.2	0.21	1.27
1500-29-17C	400	100	control		5.1		
1500-29-18	400	100	8.587	19.6	14.0	0.20	1.02
1500-29-19	400	600	6.8262	18.6	15.5	0.28	1.51
1500-29-19C	400	600	control		0.3		
1500-29-20	400	600	5.8776	21.4	17.0	0.36	1.67
1500-29-23C	not heated		7.8988	32.0	1.2	0.02	0.06

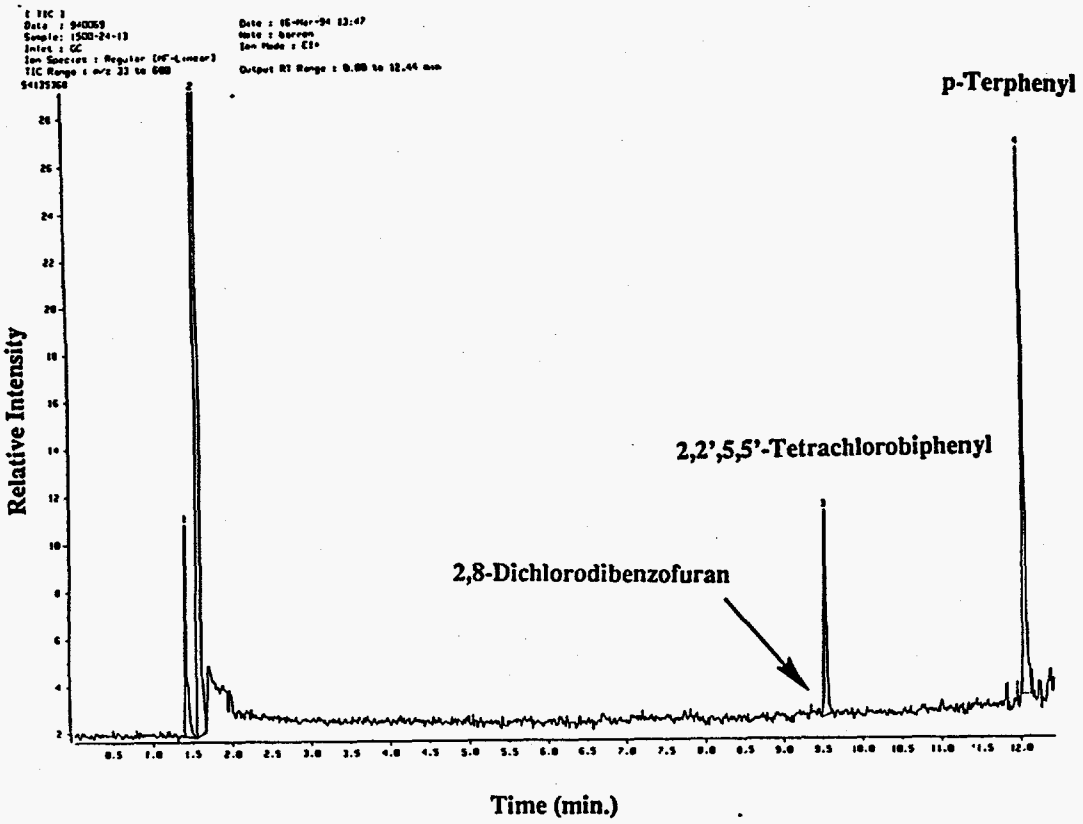

Figure 2. GC-MS total ion chromatograph obtained on solvent extracts of thermolyzed concrete.

Temperature dependence – Most of the literature on the conversion of PCBs to PCDFs and PCDDs is directed at understanding PCDF formation in incineration processes and focuses on high temperature (300 to 700°C) regimes [1,2]. Earlier work has been done at GE on the lower temperature thermolysis of PCBs in soils [3]. This work also used 2,2'5,5'-tetrachlorobiphenyl as a model system, taking advantage of its known conversion to PCDF isomers. When heated in soil for up to a week, 2,2'5,5'-tetrachlorobiphenyl is converted slowly to a number of products, but not to dibenzofurans. This is true even in the case of lime-amended soils with pH = 11, similar to the pH of concrete. The results of heating contaminated soils are shown in Figure 3. Even with extended heating, the major material recovered was unchanged 2,2'5,5'-tetrachlorobiphenyl. Products resulting from hydroxylation, dechlorination and methylation were observed, but no dibenzofuran isomers were detected. Given this evidence, we predicted that no PCDF or PCDD isomers would be detected in the heated concrete samples. This turned out not to be the case.

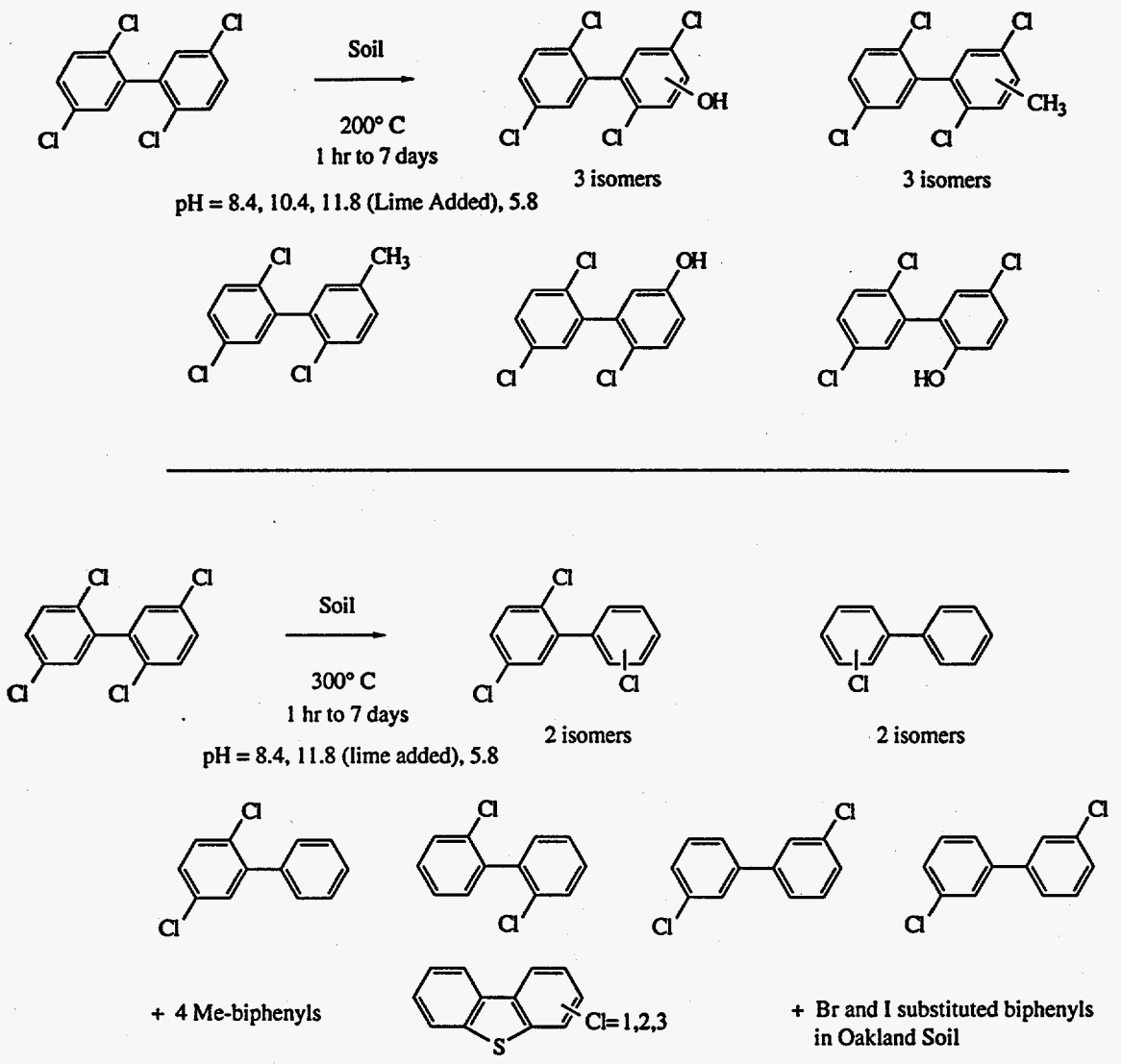

Figure 3. Results of Heating 2,2',5,5'-tetrachlorobiphenyl on soils at 200 and 300°C.

It was expected that if PCDF isomers were formed in thermolyzed concrete samples, they would be seen only at higher temperatures (>300°C). Instead the formation of PCDF gave evidence of being more complicated, demonstrating the behavior shown in Figure 4.

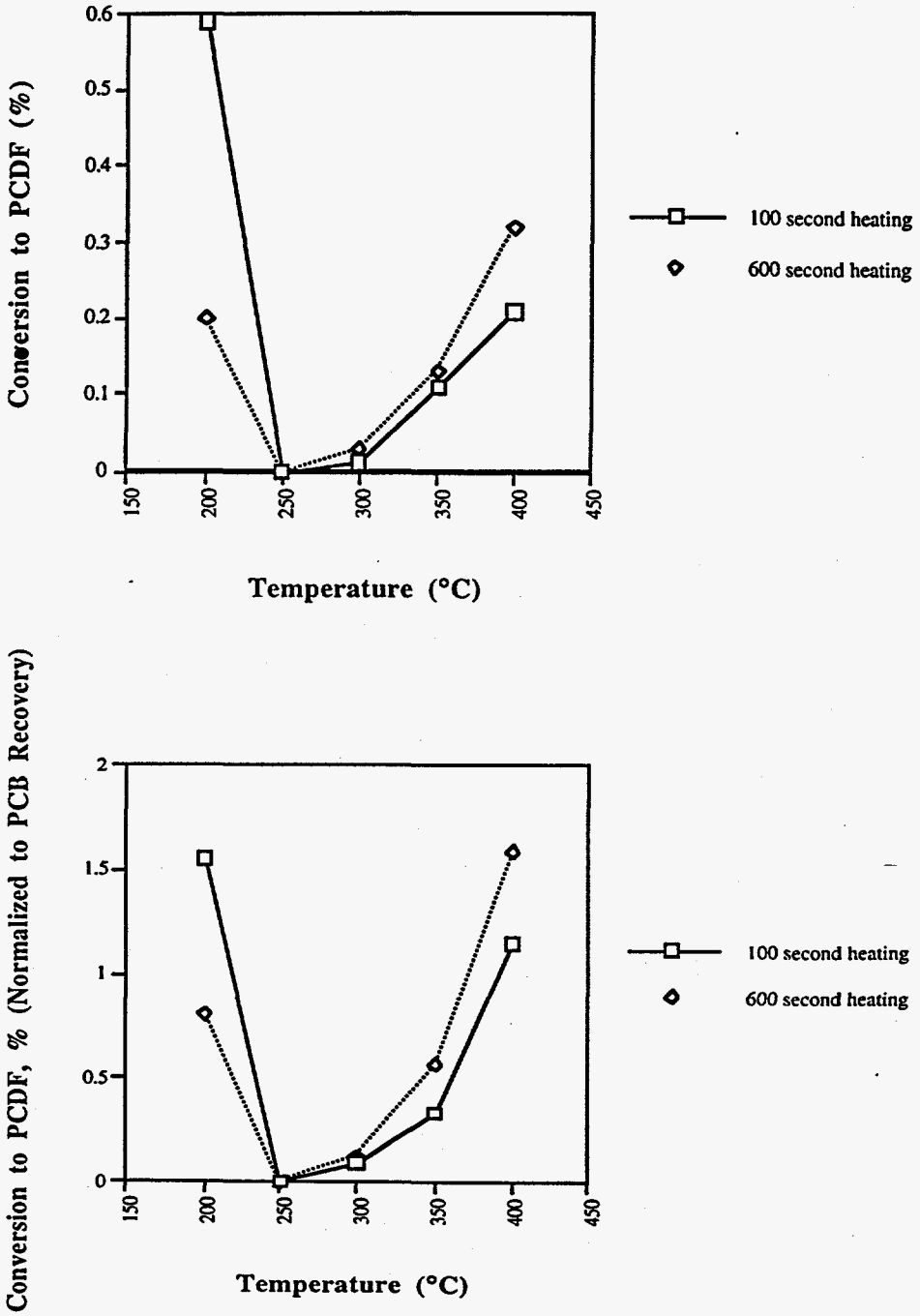

Figure 4. Conversion of 2,2',5,5'-tetrachlorobiphenyl to 2,8-dichlorodibenzofuran as a function of temperature.

These graphs show the expected increase in 2,8-PCDF formation as the temperature increases from 250°C to 400°C, but also suggest the very unexpected result of 2,8-PCDF formation at 200°C.

However, careful examination of the data in Table 1 calls into question the results for the 200°C runs. The scatter in the data, as measured by the range of the values obtained, is extremely high for both the 100 sec. and 600 sec. measurements at 200°C. Table 2 shows the ranges for all the experiments. At 200°C, the ranges are higher than the average measurement. Samples 1500-20-3 and 1500-22-4 (600 sec. at 200°C) are a case in point. In one measurement, 14.19 ng of 2,8-PCDF was detected. In the duplicate, no 2,8-PCDF was found. At the higher temperatures, the ranges are much more reasonable. For this reason, we suggest that the 200°C runs be repeated at the beginning of Phase 2 under conditions outlined later in this section.

Table 2. Range of Values Associated with the Thermolysis Data.

Sample	Temp. (°C)	Time (sec)	% Conversion to PCDF, Normalized to TCB Recovery	Average Conversion For Both Runs	Range of Values
1500-20-1	200	100	2.35	1.545	1.61
1500-20-2	200	100	0.74		
1500-20-3	200	600	1.62	0.81	1.62
1500-22-4	200	600	0		
1500-22-5	250	100	0	0	0
1500-22-6	250	100	0		
1500-22-7	250	600	0	0	0
1500-24-8	250	600	0		
1500-24-9	300	100	0.14	0.09	0.1
1500-24-10	300	100	0.04		
1500-24-11	300	600	0.13	0.12	0.02
1500-24-12	300	600	0.11		
1500-24-13	350	100	0.28	0.325	0.09
1500-24-14	350	100	0.37		
1500-24-15	350	600	0.51	0.57	0.12
1500-29-16	350	600	0.63		
1500-29-17	400	100	1.27	1.145	0.25
1500-29-18	400	100	1.02		
1500-29-19	400	600	1.51	1.59	0.16
1500-29-20	400	600	1.67		

Single PCDF Congener Formed

Only one PCDF congener was detected in all of the thermal reactions studies. The parent PCB congener, 2,2',5,5'-tetrachlorobiphenyl, was selected because its conversion to dibenzofurans had been studied previously [3]. Mechanisms for the production of a number of dibenzofuran isomers have been proposed and are shown in Figure 5 [4].

In theory, these pathways can operate to provide a variety of PCDF isomers, involving formal chlorine, hydrogen or hydrogen chloride loss. Concrete is a very alkaline environment and certain pathways are probably favored under high pH conditions. The extracts were examined and carefully monitored for the production of each of these six PCDF isomers and also related polychlorinated dibenzodioxins (PCDDs). The fact that only one PCDF isomer was observed in any of the experiments gives some evidence that the results are a worst case situation and predict more PCDF formation than one would likely see in the thermolysis of an Aroclor mixture, because less than 50% of the PCB congeners in an Aroclor mixture such as 1242 or 1248 contain the 2,2'-dichloro functionality necessary for the observed type of dibenzofuran formation. PCBs containing a single or no ortho chlorines would apparently require more forcing conditions for PCDF forming reactions to take place.

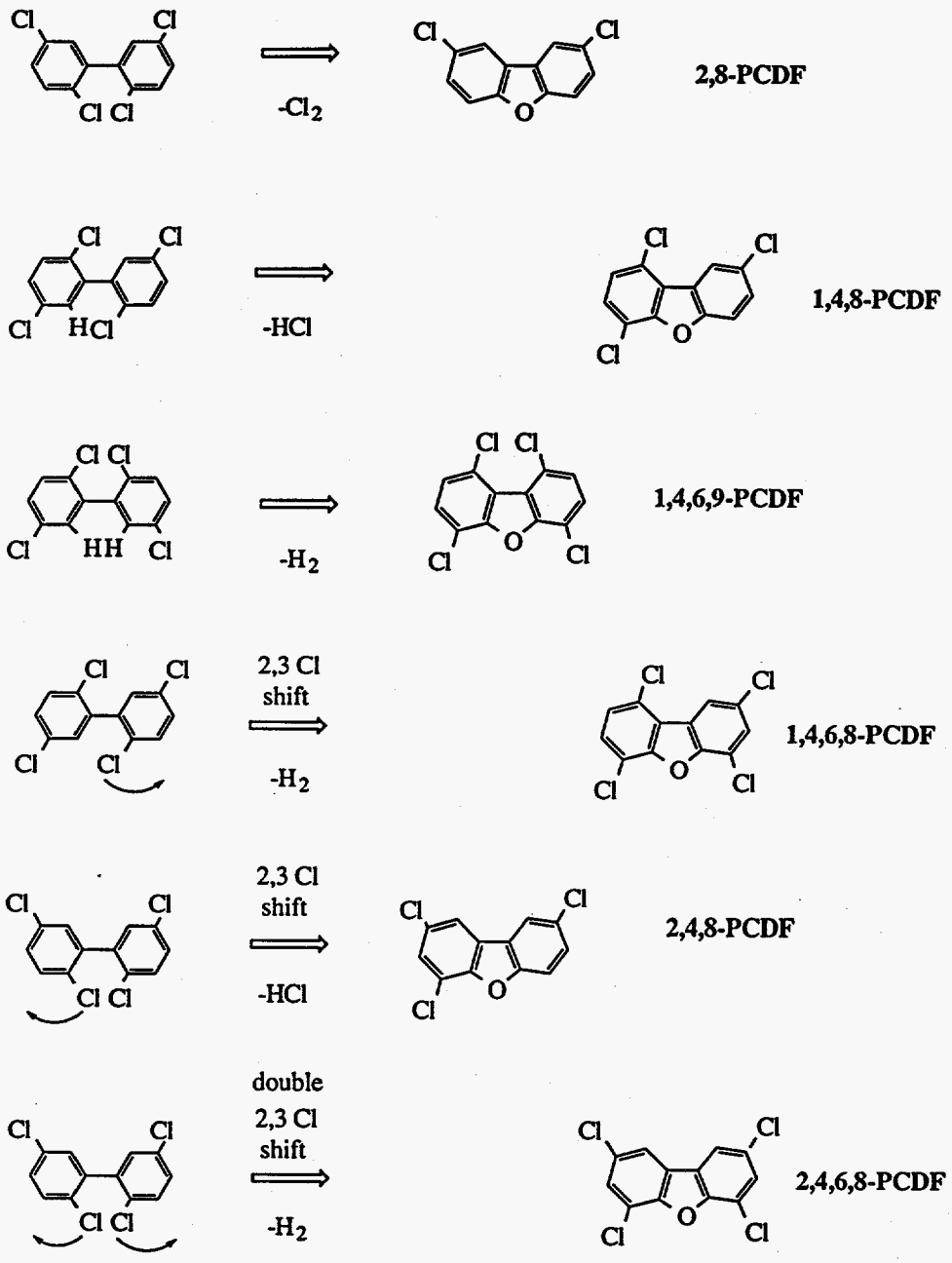

Figure 5. Possible pathways for PCDF formation from 2,2',5,5'-tetrachlorobiphenyl.

Figure 6 shows our proposed mechanism for the formation of 2,8-dichlorodibenzofuran in concrete involving displacement of chloride by hydroxide (concrete is an extremely alkaline environment), followed by proton loss and a second, intramolecular displacement of chloride ion.

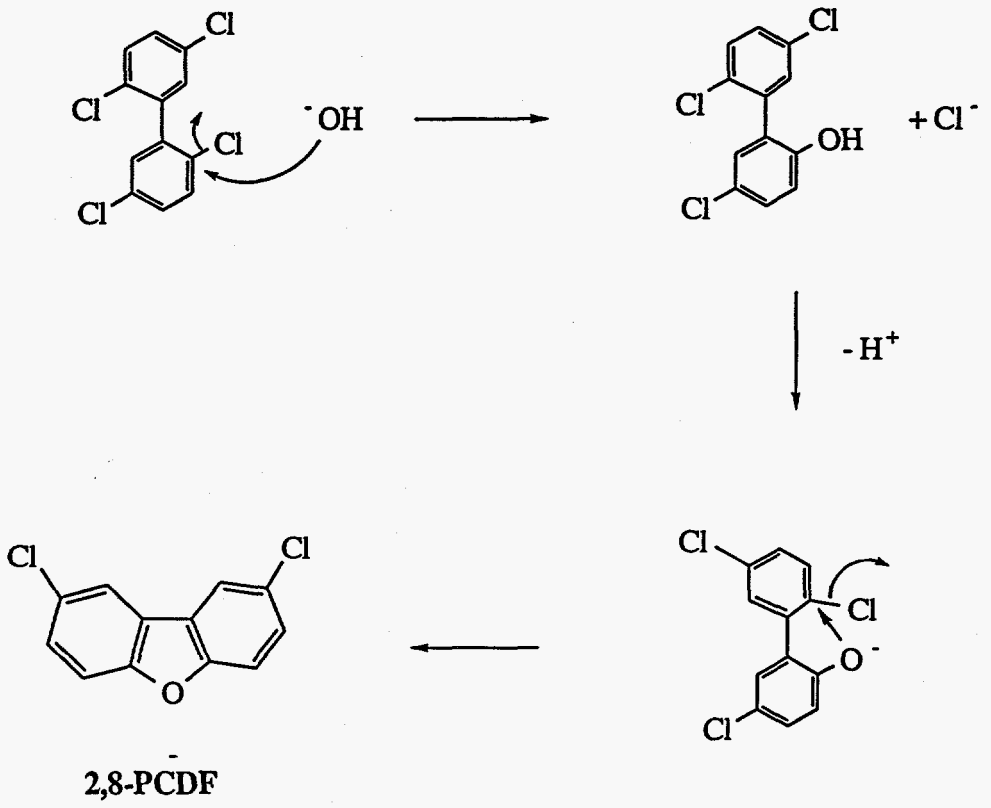

Figure 6. Proposed mechanism of formation of 2,8-dichlorodibenzofuran in concrete sample contaminated with 2,2',5,5'-tetrachlorobiphenyl.

Suggestions for Further Experiments

To improve the quality of the data from this experiment, we recommend that these experiments be repeated with the concentration of PCBs on the concrete increased by a factor of 100 to approximately 5000 ppm, and the scale of the reaction increased by a factor of five to 0.5 g, thus allowing for much better detection capabilities. The larger scale should diminish errors associated with sampling a heterogeneous matrix while partitioning the concrete into individual aliquots for thermolysis. We recommend also that the temperature range around 200°C be explored in 20°C steps to establish the temperature dependence of PCDF formation rate precisely.

Finally, a congener lacking the 2,2'-chlorine functionality should be tested to determine whether other PCDF formation mechanisms become operative at temperatures of interest in sampling.

Conclusions

Additional experiments on PCB sampling at temperatures less than 250 °C need to be carried out during Phase 2 to determine whether present results are anomalous, and to better characterize the time and temperature dependence of any significant PCDF formation processes. Even if PCDF formation rates near 200°C are found to be negligible, it may be necessary to control sampler heads to within fairly rigorous tolerances (< 250° C surface temperature) to avoid formation of small amounts of PCDFs at high temperatures when sampling PCBs.

We note that the results of these studies will be significant both for thermal sampling and for thermal cleanup strategies.

Task 1.3 Design of the Concrete Sampler Head

Performance Requirements

Design of the concrete sampler head was driven by a number of requirements, among which are

- ability to sample a sufficient area to obtain a statistically significant result
- ability to obtain a sample rapidly on the order of 100 sec.
- need to sample horizontal and vertical surfaces with some degree of roughness and departure from flatness
- uniformity or at least predictability of analyte extraction over sampled area
- ease of maintenance and cleaning
- acceptable weight and power requirements;
- separation of analyte vapors from surfaces at temperatures over 250°C
- ability to transport vapors unchanged (insofar as possible) to the quick look and archival storage modules;
- a collection volume that is small compared to the volume of gas pulled through the sampler in the sample time
- safety (i.e., safe to touch)

Consideration of these requirements led to preliminary choice of a concrete sampler head based on concrete surface heating by radiation from a tungsten-halogen light bulb. These considerations were reviewed and expanded in Phase 1, as discussed below, producing a confirmation of this choice with several modifications of the original design.

Consequence of the Rapid Sampling Requirement

For our initial calculations of the absorbed power density at the concrete surface necessary to satisfy the rapid sampling requirement, the following characteristic thermal parameters were used for cured concrete.

Thermal conductivity $k = 0.011$ W/(cm°C)

Heat capacity $C = 0.88$ J/(g°C)

Concrete density $\rho = 2.1$ g/cm^3

The one-dimensional heat conduction equation gives the following result for surface temperature for a surface described by the constants above absorbing a power density of P (watts/cm^2).

$$T = T_o + \frac{2Q}{k}\left(\frac{\alpha t}{\pi}\right)^{1/2} \quad (1)$$

where T_o is the initial surface temperature, Q is the absorbed power density on the surface, and the thermal diffusivity α=k/cρ.

According to this equation, an absorbed power density of 6 W/cm^2 will warm the surface from 20°C to 300°C in 100 sec.. Actually, as discussed in the Concrete Modeling Section, the heating effect is more complicated, depending significantly on the moisture fraction, porosity and permeability of the concrete. Nevertheless, we have found experimentally that a power density on the order of 6 W/cm^2 is needed to provide the requisite surface heating rate.

Selection of the Heating Method

Heating by conduction from a hot plate in contact with the surface

The transfer of a power density on the order of 6 W/cm^2 by conduction from a hot plate to a concrete surface would require that the hot plate temperature be well above the concrete surface temperature, particularly for a concrete surface that is not unusually smooth and flat. In that case the conduction must occur predominantly across a still air (or air and vapor) film with an thickness which is typically larger than 100 µm (0.004 in.). The necessary temperature difference can be estimated from the equation describing conductance across the film:

$$Q = k\Delta T / x \quad (2)$$

where ΔT is the temperature difference between the concrete surface and the hot plate, and x is the average film thickness. Using a typical value for the conductance of air at 100°C, k = 3.1 × 10^{-4} W/(cm°C), we find that the temperature difference necessary to maintain a heat flow of 6 W/cm^2 across 100 µm of air is approximately 200°C. It can be shown that the radiation heat transfer is much smaller than the conduction for this temperature difference; therefore, radiation can be neglected for this estimate. However, as reported in Task 1.2 Sampling Artifact Experiments, a hot plate temperature which is nearly 200°C over the elevated concrete surface temperature (which is expected to reach 200°C) can cause significant conversion of analytes to other chemical species, which may

be hazardous or go undetected. Therefore, surface heating by conduction from a hot plate does not appear to be a desirable method. This conclusion is reinforced by consideration of the uneven heating effects produced by a slight departure from flatness in the surface.

Heating by IR radiation

Commercial sources operating in the temperature range around 1000°C can provide an incident power density in the required range of 6 W/cm^2. There are several other types of commercially available radiant heat sources in this range. The problem with all these sources is that it is difficult to shield the analyte vapors from undesirably high temperatures when they are used. In addition, most of the radiation from these sources lies in the 3 to 10 μm band, where windows with high transmission and chemical stability are relatively expensive and delicate. If windows with intermediate transmission are used, the windows themselves overheat. Consequently, we have not been able to generate an economic design for a concrete sampler head based upon this type of power source.

Heating with a laser source

A laser heating source was considered, with a fiber optic coupler allowing the source to be remote and flexibly transmitted to the sampler head. However, in order to illuminate an area of 100 cm^2 with a power density of 6 W/cm^2, a laser with average source power greater than 600 W is required. Although lasers at this power level (and higher) are available, at present they are expensive ($100,000). The most efficient lasers operate at wavelengths that cannot be coupled conveniently by fibers. Extensive cooling facilities are required to reject the waste heat. Therefore, we do not recommend a laser source for concrete sampling. (The situation may be different, however, for metal sampling, because of the much greater thermal conductivity, the lower permeability of most metals, and the smaller sampling area necessary to accommodate curved surfaces.)

Heating with radiation from a tungsten-halogen lamp

Since a large fraction of the radiation from a tungsten-halogen lamp is radiated into the spectral band from 0.4 to 4 μm where it can be coupled efficiently to the surface, we expected that a 1000-W lamp of this type would be able to irradiate 100 cm^2 of concrete surface with sufficient power density to satisfy the 100-second sampling condition. In practice, this expectation has proved to be correct; in fact, it appears to be possible to operate the lamp somewhat below its design power input and still obtain satisfactory surface heating rates. This result is advantageous because it extends lamp lifetime and shifts the lamp spectrum toward the infrared, contributing to heating uniformity as will be discussed in the Section Task 1.3.1 Thermal Tests on Concrete Sampler Head. The fact that the tungsten-halogen lamp provides somewhat more light power than needed also suggests that a lower temperature 1000-W incandescent lamp might also suffice. However, it would probably be necessary to use a lamp with a quartz envelope to make available the 2 to 4 μm band of emission not transmitted by standard envelope glasses.

One thousand watt tungsten halogen lamps are available with 350-hour rated lifetimes that can be operated in any position. (For example, see Oriel Corp. Light Sources Catalog Vol. II, pages 46-47.) Typical cost per lamp is $60, which is acceptable for this application. At rated power, this lamp is specified to operate at a filament temperature of 2900°C; a typical output spectrum is shown in Figure 7. Suitably mounted, we have found this lamp to be sufficiently rugged for field operations.

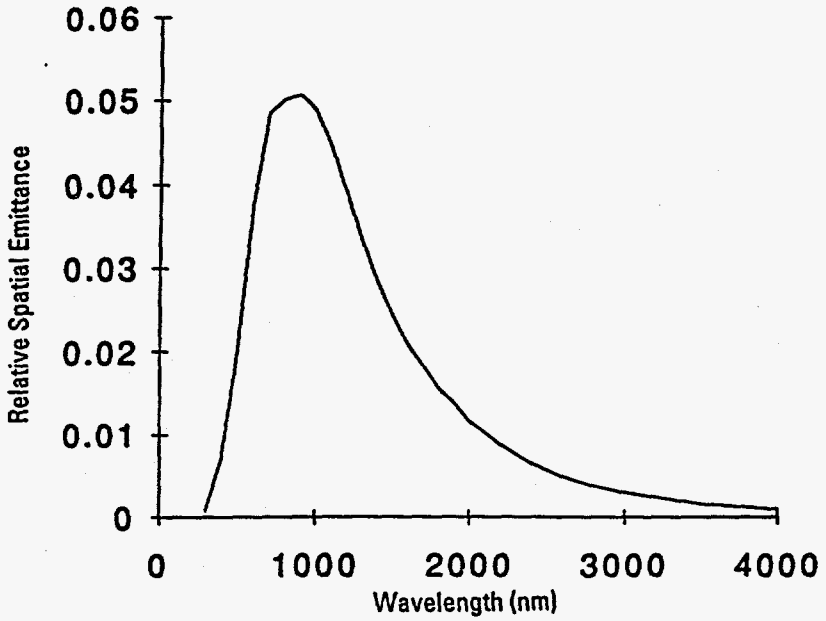

Figure 7. Emission spectrum from a tungsten-halogen lamp operating at a filament temperature of 2900°C.

Initial Prototype Concrete Sampler Head

An initial prototype concrete sampler head was designed and built before the start of this contract, primarily for risk reduction. A plan view of this head is shown in Figure 8. It is based upon a fairly massive reflector body in the form of an aluminum cylinder approximately 15 cm in diameter and 12 cm high, into which a concave reflector cavity was turned. The 1000-W lamp is mounted on spring-loaded pins inside this cavity, which is closed by a quartz window. The collection zone is enclosed by this window and by a slightly raised ring which contacts the surface to be sampled. The inner diameter of this ring is 11.3 cm, defining a sampled surface area of 100 cm^2. Air is drawn past this ring and the surface at a typical rate of 5 cm^3/sec, eventually passing between the ring and quartz window into heated conduits that are coupled into the rest of the sampling system. The head is heated by heating tapes wrapped around the cylinder periphery. Cylinder temperature is typically controlled to 250°C ± 10°C, as sensed by buried thermocouples. Solid construction was chosen to add thermal mass, simplifying control when the lamp is turned on and several hundred watts of waste heat is added to the assembly. Insulation and an outer metal shell complete the head. Total weight of the first prototype sampler head is approximately 10 lb.

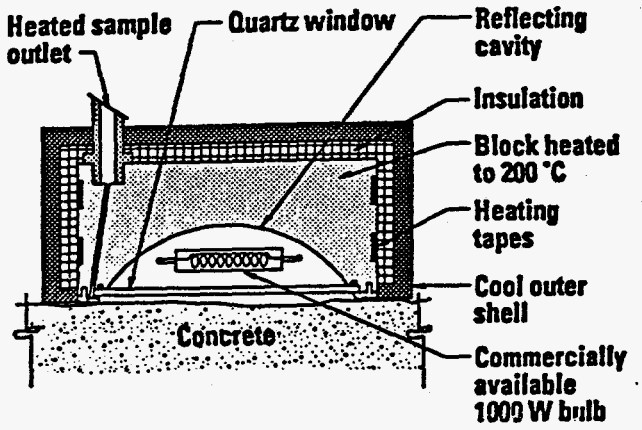

Figure 8. Initial prototype concrete sampler head.

This concrete sampler was used in preliminary tests at a GE site on a concrete floor known to contain high concentrations of oil and PCBs. Analyte vapors were collected in liquid nitrogen double cold traps. These tests were successful, producing large collected samples showing reasonable correlation with wipe tests. However, the tests indicated two improvements needed in the sampler head: first, the heating appeared to be uneven, producing a discolored region in the central 4 cm of the sampled area suggesting a hot spot. This suggestion was confirmed by thermocouple tests, and supported by a Monte Carlo radiation model described later in this section. The second needed improvement, brought up at the contract kickoff meeting, was to modify the mechanical design to avoid exposed screw heads on the bottom plate, which could create an opportunity for transfer of contamination.

Second Iteration Concrete Sampler Head

Modifications to improve heating uniformity

A standard Monte Carlo technique [5] was used to calculate the illumination pattern at the exit surface of the concrete sampler head. This technique was chosen because it is the most reliable way to calculate illumination patterns when diffuse surfaces play a significant role in the behavior of the ray paths. The basic methodology is to simulate the illumination process by calculating a large (>50,000) number of random ray paths that have characteristic probabilities determined by the physical nature of the optical surfaces.

Figure 9 shows a graphical output from a Monte Carlo calculation for the case when the number of initial rays was restricted to 200 rays. It is important to note that this number is actually the number of rays launched from the lamp. Each ray launched will generate multiple suitably weighted ray-paths at dielectric interfaces where reflected and transmitted rays are possible.

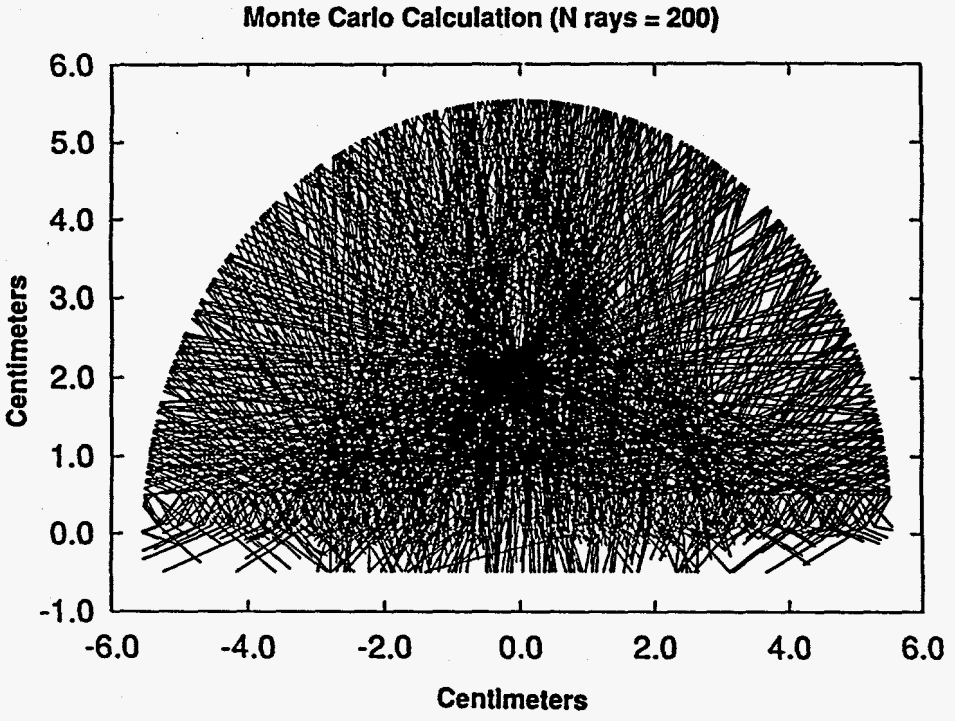

Figure 9. Monte Carlo ray simulation cross section (N = 200).

All calculations were done using values corresponding to a single representative wavelength in the mid-visible spectrum. We assumed that reflection and refraction values would not change fast enough over the wavelength range emitted by the lamp to require multiple wavelength values. (However, see later comments in the Concrete Sampler Head Thermal Tests Section.)

The reflectivity of the reflector surface, integrated over all angles, was taken to be 0.83 based upon measured optical values. Dielectric surfaces were modeled using an index of refraction of 1.5. Diffuse surfaces were modeled by using a random number generator as input to a generating function chosen with parameters to represent the diffuse scattering patterns we measured for ground glass and sandblasted aluminum surfaces similar to those that would be used in the concrete sampler. In one dimension, the underlying distribution takes the form

$$P(\theta) = \rho\cos(\theta) + (1-\rho)\cos((\theta_j)/\rho) \qquad 0 \le \rho \le 1 \tag{3}$$

where θ is the angle of reflection, θ_j is the angle of incidence and ρ is the parameter indicating the degree of diffuseness of the scattered light.

The appropriate value of ρ was determined by laboratory measurements. For example, Figure 10 shows actual measurements for a sandblasted sample of aluminum, compared to the scattering distribution predicted by Eq. (3) with $\rho = 0.7$ and $\theta_j = 45$

degrees. The only significant deviation is a component due to backscattering, but even that component, when integrated over angle, represents a small fraction of the scattered rays.

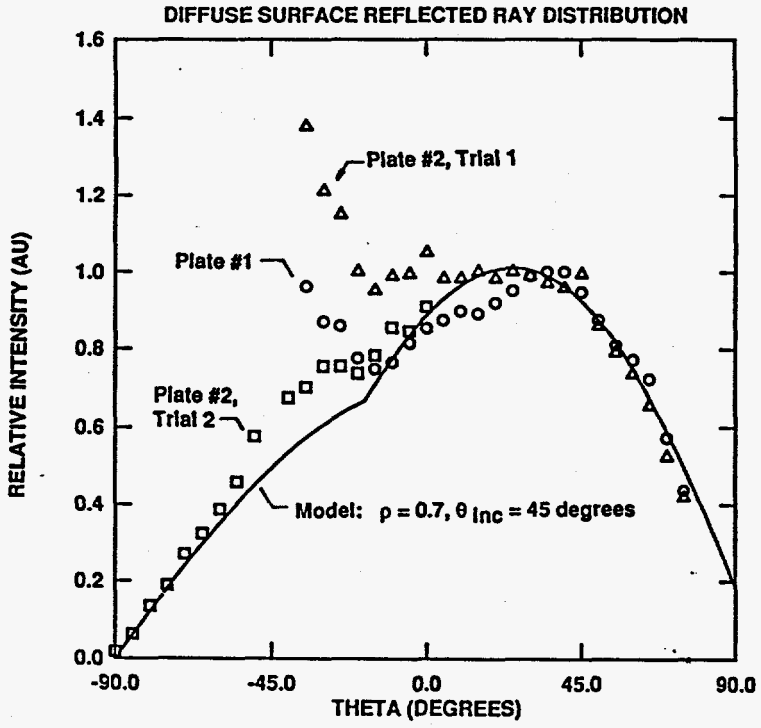

Figure 10. Reflected ray distribution (model and measured values).

On a SPARCStation LX, the speed of execution of this calculation was between 500 and 1400 initial rays per minute. A typical run of 50,000 rays, describing the irradiation distribution for one optical design, required about 1 hour.

Result for the baseline configuration

Figure 11 shows a cross section of the initial prototype sampler head. The predicted irradiance distribution at the sampled surface is shown in Figure 12 in the form of a cross-section distribution in the X- and Z-directions along with a contour plot of the irradiance distribution. This calculation predicts the hot spot in the center observed experimentally with this configuration. Other conclusions from this calculation are summarized in Table 3. One significant conclusion is that total power on the target can be increased by about 25% by using a polished reflector instead of a diffuse (sandblasted) one.

Design calculations for the second head

Calculations for different lamp positions and reflector characteristics produced the following general conclusions:

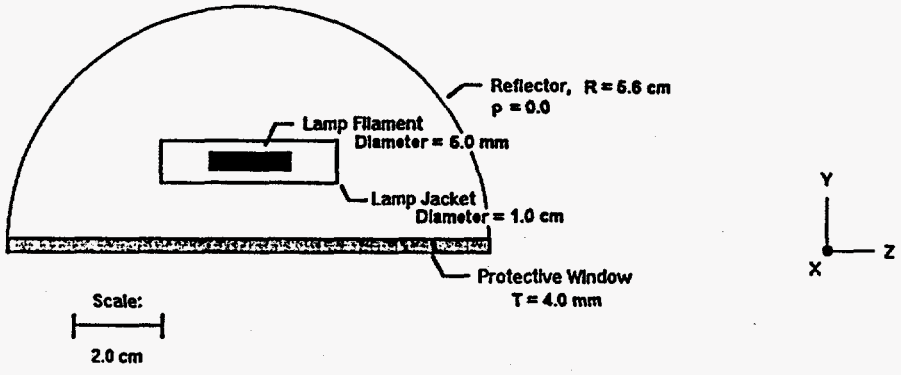

Figure 11. Baseline configuration—the initial prototype sampler head.

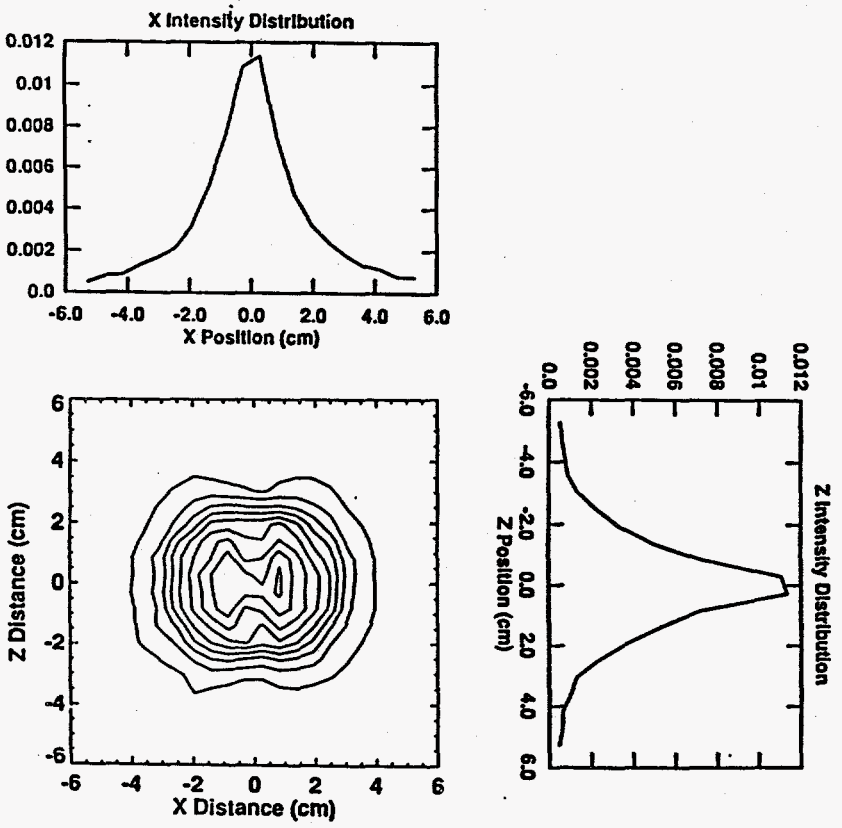

Figure 12. Performance of baseline configuration.

Table 3. Results of Monte Carlo Analysis.

Category	Percent of Optical Power in Category	
	(Reflector $\rho = 0.7$)	(Reflector $\rho = 0.0$)
Lost out ends of lamp	8%	7%
Absorbed in metal reflector	30%	15%
Incident on Target Area	62%	78%

- A smooth reflector with the lamp located near the top leads to efficient coupling with much improved uniformity, eliminating the central hot spot.
- The lamp ends, which are absorbing surfaces, do not account for more than 7% of the waste energy.
- The mechanical structure that holds the lamp in place is not a significant loss.
- There is a relatively strong asymmetry of reduced radiation along the lamp axis, which results primarily from the smaller filament projected area along the axis.

This predicted asymmetry was reduced significantly in the Monte Carlo model by including a diffuser plate located just below the lamp. The resulting configuration is shown in Figure 13. The lamp axis is positioned 4 cm above the target surface with a ground glass quartz plate (both sides ground) mounted as close to the lamp as possible. The resulting illumination patterns are shown in Figure 14. In Table 4 the efficiency values for this configuration are shown. These results were sufficiently encouraging to lead us to adopt this optical configuration for the second concrete sampler head prototype.

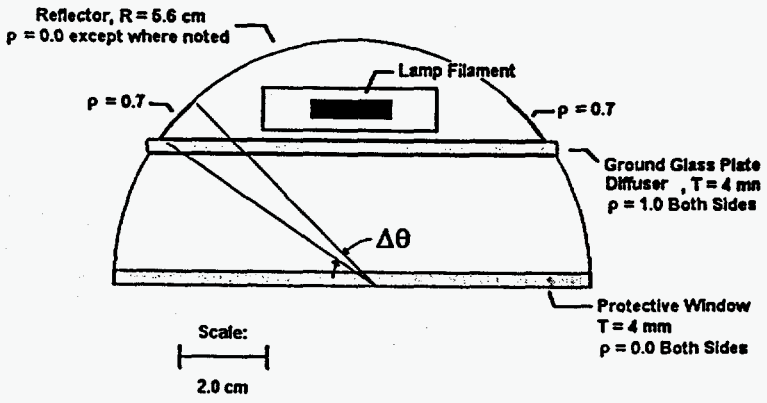

Figure 13. Optimum configuration according to Monte Carlo analysis.

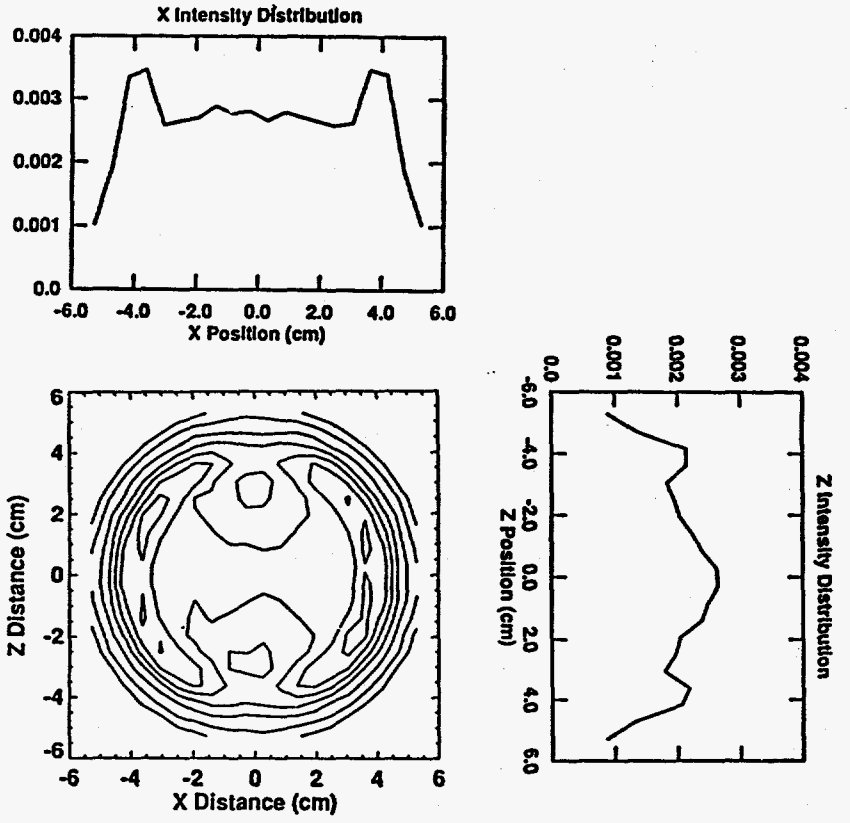

Figure 14. Monte Carlo simulation for optimum configuration.

Table 4. Loss Characteristics for Optimum Configuration According to Monte Carlo Analysis.

Category	Percent of Optical Power in Category
Lost out ends of lamp	7%
Absorbed in metal reflector	18%
Incident on target area	75%

Mechanical design considerations and modifications

The most important mechanical goals for the second head are

- The bottom surface should have no cavities such as those in screw heads or other features that could trap debris or contaminated substances.
- It should be possible to change the cover glass and the lamp without disassembling the entire head.
- The sampler should work well in all orientations.
- The outer shell should be sufficiently cool to touch comfortably.

These criteria were met using the design illustrated in cross section in Figure 15, and the mechanical drawings included in Appendix 1 Design Drawings. This design consists of a central heating block, a 3-piece chassis (upper and lower caps and a cylindrical side section), and associated hardware. The heating block is constructed from aluminum, while the chassis is made from stainless steel because of its low thermal conductivity and high strength. An additional doughnut-shaped ceramic spacer provides insulation between the top of the heating block and chassis. Protruding nuts, which are welded onto the lower chassis, fit into recessed holes on the bottom of the heating block. Shoulder bolts are placed through the heating block from the top and screw into the nuts, holding the lower cap snugly and sealing the cover glass against the bottom of the heating block. Spring washers are used to allow for differential expansion between the bolts, the heating block, and the lower cap. The bolts are extended through the top of the upper chassis cap, allowing the lower cap to be removed for maintenance of the glass and heating lamp without any other disassembly. Insulating material is wrapped around the heating block and protected by the cylindrical side section of the chassis. The upper cap is attached to the heating block through the ceramic spacer by eight screws, supplying the necessary rigidity and strength so that the entire assembly may be used in any orientation. The cylindrical side section fits inside the rims on both the upper and lower caps, so that it does not need to be fastened to the heating block. Air flow for sample collection is accomplished through 8 slots in the lower chasis, which mate to a recessed circular channel cut out from the heating block. Air flow is drawn through a clear hole cut through the heating block to the recessed channel.

These optical and mechanical design considerations defined the configuration of the second prototype concrete sampler head. Results of thermal and sampling performance tests are reported in subsequent sections.

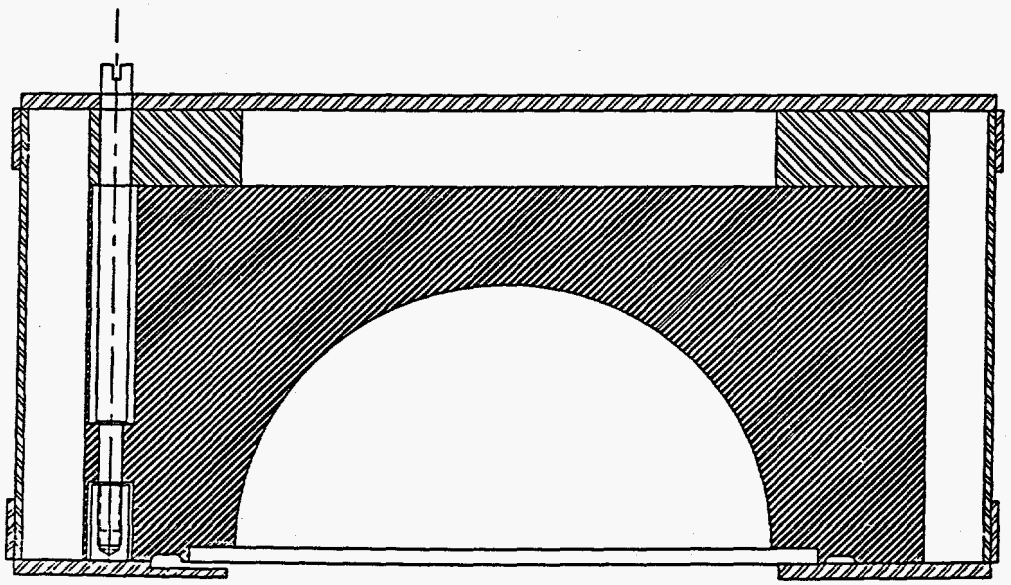

Figure 15. Cross-sectional view of the revised mechanical design for the concrete sampler head.

Task 1.3.1 Thermal Tests on Concrete Sampler Head

Introduction

Task 1.3.1 involves testing the thermal performance of the Concrete Sampler Head on concrete. The purpose of these tests is to determine

- the uniformity of heating over the sample area
- the thermal distribution within a concrete disk as a function of time during the surface heating
- the predictability of the average surface temperature in the sampling region
- alterations to the sampler head to improve uniformity and predictability

The data will be used to evaluate attainment of the original goal specifications for concrete sampler head performance, and will be compared with predictions of the numerical concrete model developed to guide interpretation of the measurement results.

Test Methods

Concrete sample preparation

The tests were begun in late April 1994 using concrete disk samples prepared in March 1994. In the preparation process, three disk samples, 30 cm in diameter by 2.5 cm thick, were constructed for thermal tests using one part Portland cement to two parts sand, with no additional filler material. Since we decided to produce the contamination test disks and the thermal test disks to the same dimensions to simplify preparation and modeling, dimensions were chosen to keep the total disk volume to just under 2L, a restriction for preparation of contaminated samples under our PCB license.

Spring form pans with a mold release made of Teflon sheets were used for preparation of the samples. To create channels for thermocouples, Teflon pieces approximately 10 cm long by 1 cm wide by 1 to 10 mm in thickness were pressed into the sample surface before the concrete began to set up. These channel pieces were removed just after setup. Holes 1/16 in. in diameter by 1/2 in. deep were pressed horizontally into the concrete at the ends of these channels with a metal rod. A Type K thermocouple with wire diameter of 0.040 in. and woven fiberglass insulation was inserted into each hole and then led out through the bottom of the corresponding channel to the edge of the disk. The thermocouple lead orientation parallel with the surface was chosen to keep the leads parallel to anticipated thermal gradients, so that heat conducted along the leads would not distort the measurements. A new mix of concrete with the same component ratios was then pressed tightly into each hole and channel and the surface was leveled. Subsequently, the concrete cured in 100% relative humidity at room temperature for 14 days, and then was left

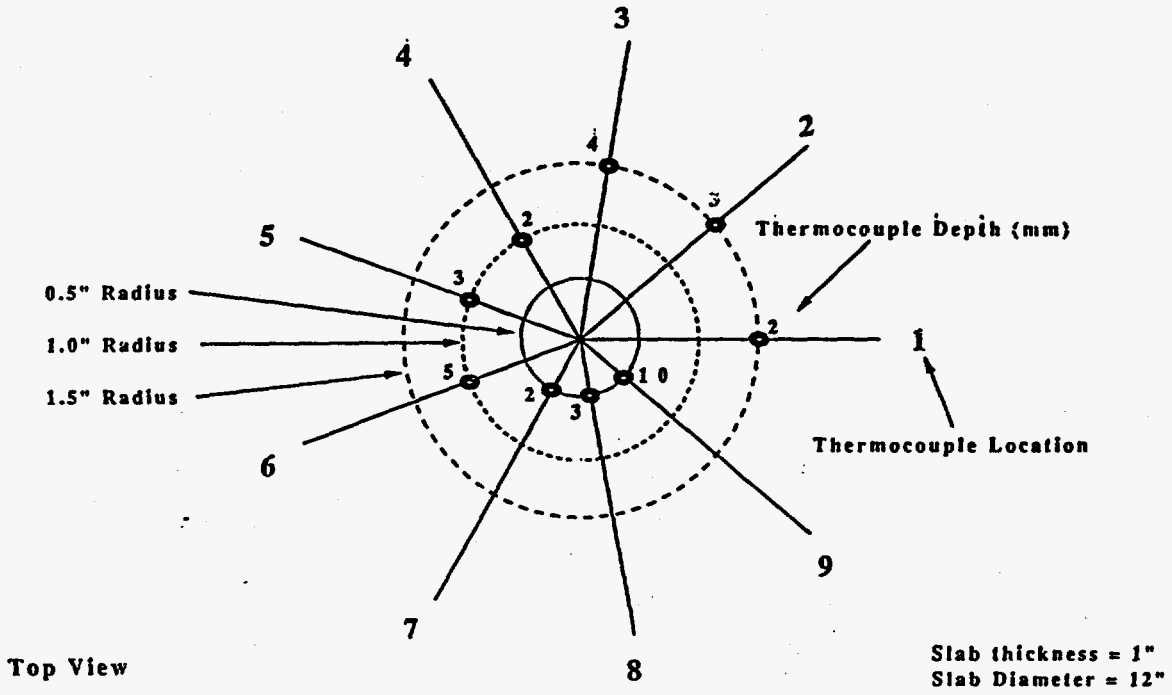

Figure 16. Thermocouple locations and depths in RSSAR concrete samples.

out in room air for 14 days to dry. The configuration of channels and the resulting measurement point locations are shown in Figure 16.

Figure 17 shows a photograph of one of the test samples after the curing and drying processes. It is evident that the concrete in the fill channels is darker, even though the same materials were used. This difference may have resulted from different mixing techniques—the larger amounts of concrete used for the samples were mixed in a small-scale mechanical mixer whereas the channel fill was mixed by hand.

Thermal imaging test methods

After the thermal test samples had undergone the scheduled curing and drying periods, we began thermal tests. The concrete samples were heated with the concrete sampler head, and, in calibration tests, with a hot plate. Air was drawn through the concrete sampler head during these tests to remove water vapor. However the air flow (and water vapor evaporation rate) are too small to significantly affect the surface temperatures. Temperatures within the sample were measured with the buried thermocouples described

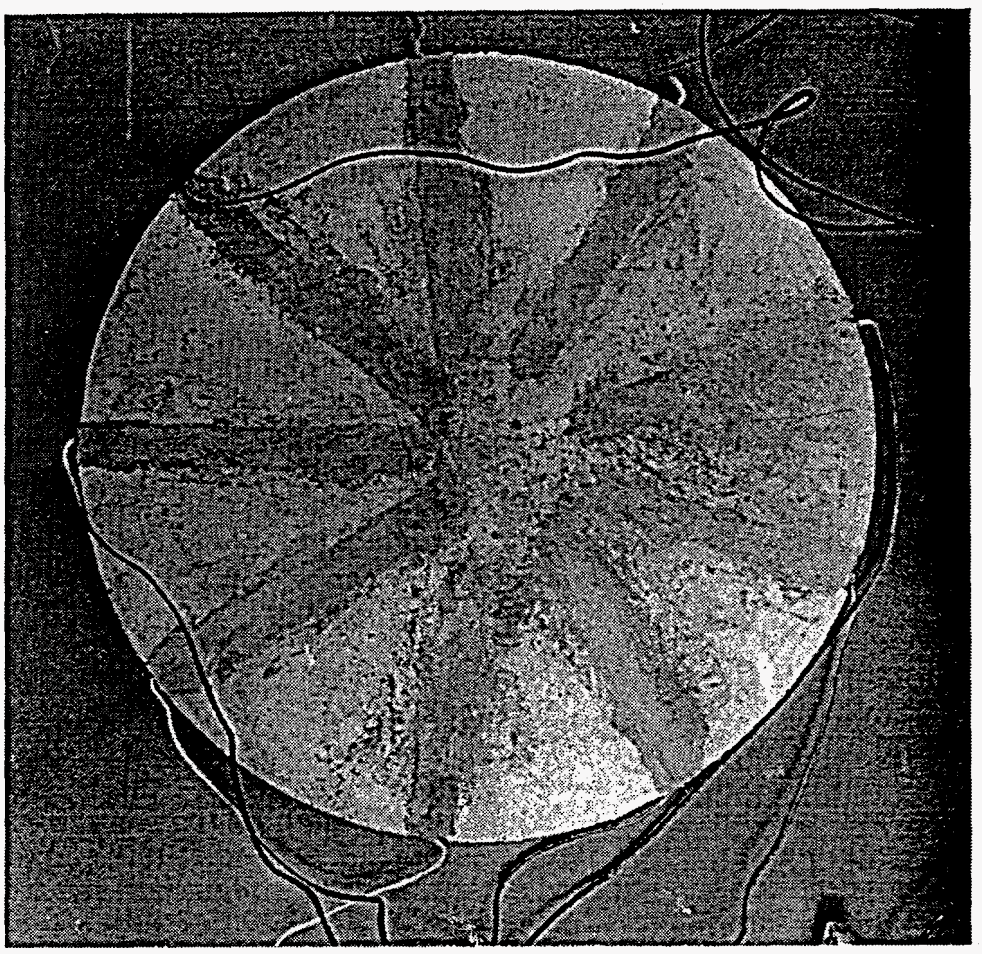

Figure 17. Photograph of one of the test samples after the curing and drying process.

above. Temperatures on the faces of the sample were measured with an AGEMA Thermovision 970 SW/TE imaging infrared radiometer operated within the 2- to 5.2-μm wavelength band. An image of IR emission from the heated face of the concrete sample was obtained using the imaging pyrometer immediately after the 90-sec. exposure period, and at 10-sec. intervals thereafter for 200 sec. Each image is fully acquired in the much shorter interval of 1/20 sec. In separate experiments, the thermal emissivity of the concrete sample face was determined on the channeled and unchanneled backside of the concrete sample disk within the 2- to 5-μm band in order to convert the radiance measurements into surface temperature measurements. Thin strips of black plastic electrician's tape (3M Super-33) were fastened to the disk's faces. A hot-air gun was used to heat the reference tape and unknown concrete surfaces to approximately 100°C. Spectral emissivity of the concrete was found to be 0.93 ± 0.01 by comparing the radiance of the reference tape (emittance previously found to be 0.96) with that of the concrete in locally isothermal areas on the sample.

Experimental Results

We will discuss the results obtained using the imaging radiometer first, because they will help to explain the results obtained using the thermocouples.

The first thermal test is designated by the code RSSR042694_1, where the date is given by the six numbers before the underscore, and the experiment number on that date by the first number after the underscore. For this test, one of the concrete samples was heated for 90 sec. using the concrete sampler head at full power (1 kW).

The resulting temperature distribution over the face of the concrete sample from data taken within 2 sec. after the 90-sec. heating cycle is shown in Figure 18. From this result, and similar ones obtained from other sample faces, it is clear that the concrete sampler head provides ample irradiation to raise the average surface temperature to 200 to 250°C in less than 90 sec. However, the temperature distribution is not sufficiently uniform. In fact, the temperature variation is substantially greater than that calculated from the Monte Carlo radiation distribution model.

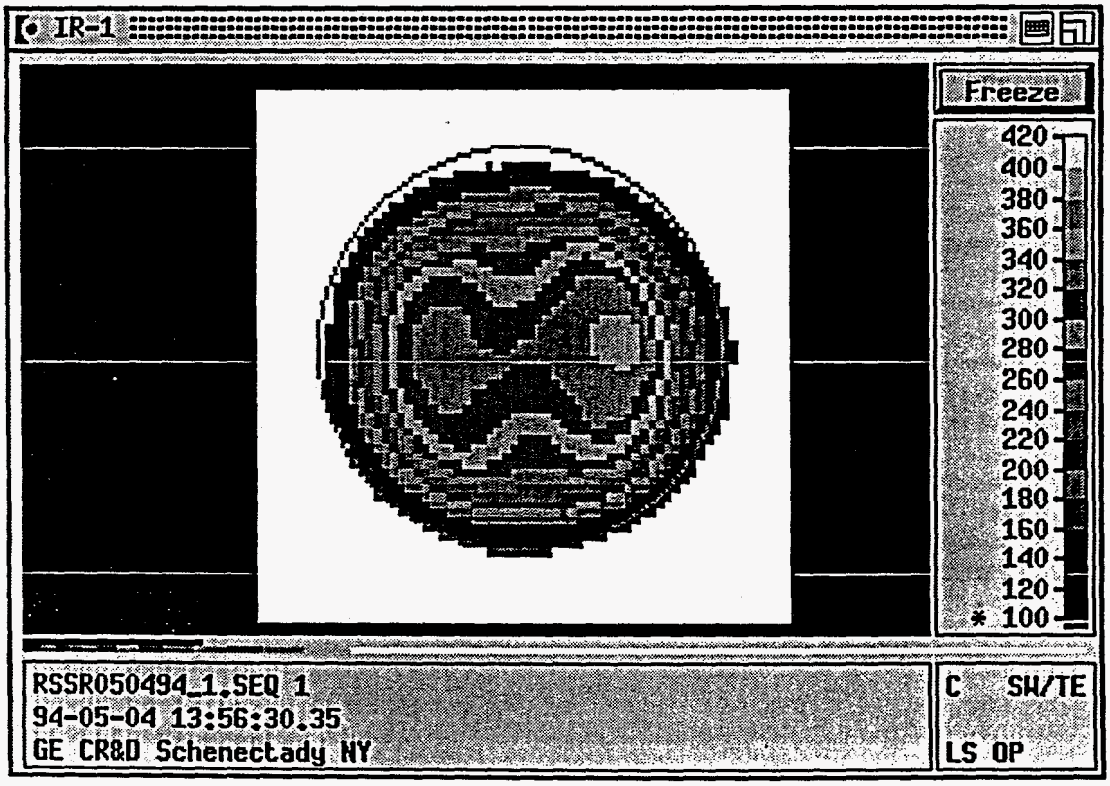

Figure 18. Temperature distribution on concrete sample surface generated by 90-sec. exposure to the concrete sampler head. Second iteration head design. The peak temperature appearing in a small region in the right-hand lobe is between 340 and 360°C.

According to Figure 18, the peak temperature 3 sec. after the 90-sec. heating period is between 340 and 360°C, dropping off to 100 to 140°C near the 11.4 cm boundary indicated by the outer ring on the image. Approximately 20% of the sampling area (100 cm^2) is within 320 to 360°C. This area is in the form of a double lobe (dumbbell-shaped), with its long axis of symmetry located parallel to the heating lamp axis, as expected from the Monte Carlo model. There are several conclusions that can be drawn from this initial result.

- This concrete sampler head configuration provides a substantial heating margin, which will probably allow lower lamp temperatures, a consequent longer life, and a consequent shift of lamp irradiation to the IR, where we expect more even heating will result (see the section of this report entitled Uniformity of Heating).
- To at least a first approximation, surface temperature differences produced in the heating process can be expected to be proportional to the peak temperature rise. In that case a range of ± 20°C over a 220°C rise should correspond to a ± 30°C range over a 340°C rise. The initial heating results shown in Figure 18 indicate that *approximately 35% of the sample area* is within the equivalent of the success criterion range. This is too small a fraction to provide reliable sampling. Both temperature asymmetry and rapid temperature falloff towards the edges are problems.

In order to improve the radiation pattern, a quartz diffuser plate was added just above the clear quartz window. The purpose of this plate is to scatter light away from the hottest regions back toward the reflector, where a portion of it will be re-reflected into the cooler regions. A first trial plate was sandblasted in a pattern mimicking the temperature distribution. This plate increased the area meeting specifications from 35% to 45%. A second plate was sandblasted over a slightly larger area, producing the temperature distribution shown in Figure 19. This pattern meets the success criterion for temperature uniformity over 60% of the heated surface, and another 15 to 20% of the area is very close to that level, encouraging expectations of further substantial improvement.

We have identified four purposes to seek a reasonable level of heating uniformity:

1. To avoid hotspots where chemical conversion of analytes could be accelerated
2. To prevent recondensation of analytes onto colder surface regions before they can be entrained in the sampling air flow
3. To maximize the collected sample
4. To provide a simple temperature distribution for heating control and sampling models.

At the present level of heating uniformity, the performance of the concrete sampling head has been very encouraging. As noted in the Final Report under Task 1.3.2 (Concrete Sampler Head Functional Tests), collected amounts of analytes have been high and closely correlated to original contamination levels. No recondensation or pronounced

Figure 19. Improved temperature distribution with second iteration concrete sampler head and diffuser plate No. 2. The peak temperature shown in two small regions in the upper central lobe is between 230 and 240°C.

hotspots have been observed. On the other hand, the artifact experiments indicate a need to provide positive temperature control to limit the concrete surface temperature to levels no higher than 250 °C. Some redesign of the concrete sampler head will be needed to include a temperature sensor, and it will be possible during this step to introduce further evolutionary improvements in heating uniformity. A proposed change in bulb orientation and reflector design incorporating an IR concrete surface temperature and cylindically symmetric radiation source is shown in Figure 20.

Thermocouple measurements of interior temperatures

The buried thermocouple data results for the first test on one of the concrete samples RSSR042694-1 is shown in Figure 21. The thermocouple locations are shown in Figure16 and the depths are also shown in the key to Figure 21. The depths are estimated to be accurate to ± 0.5 mm. The uncertainty arises primarily from the roughness and slight waviness of the top surface, which makes determination of the surface level more difficult. Also, the effective depth will be affected by the exact position of the thermocouple junction within the slightly oversize hole that accommodates it (the pressed holes have diameters of 1/16 in., whereas the thermocouple bead diameters were 0.050 to 0.055 in. in diameter).

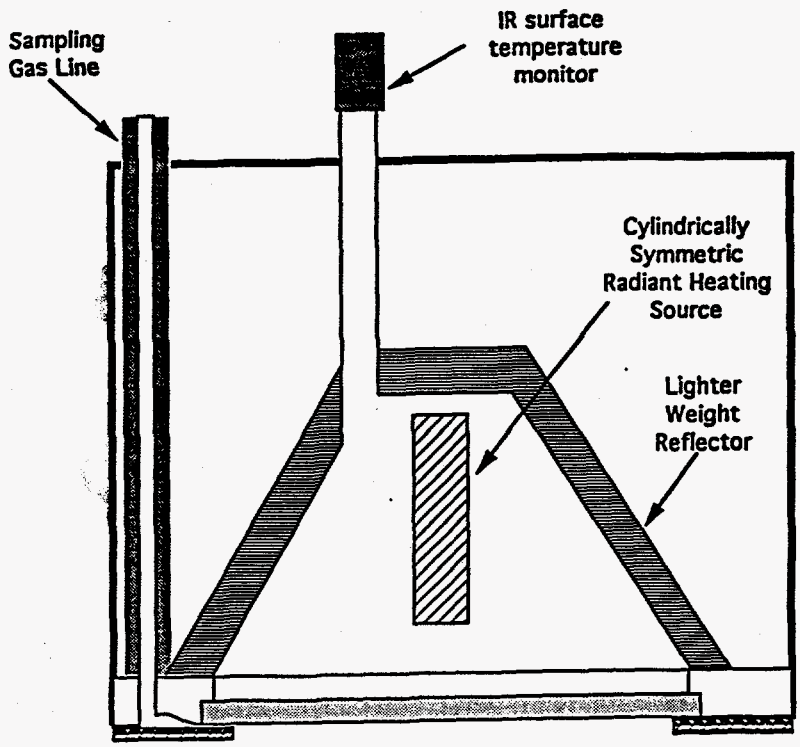

Figure 20. Schematic of proposed changes in the concrete sampling head incorporating an IR surface temperature monitor and cylindrically symmetric radiation source.

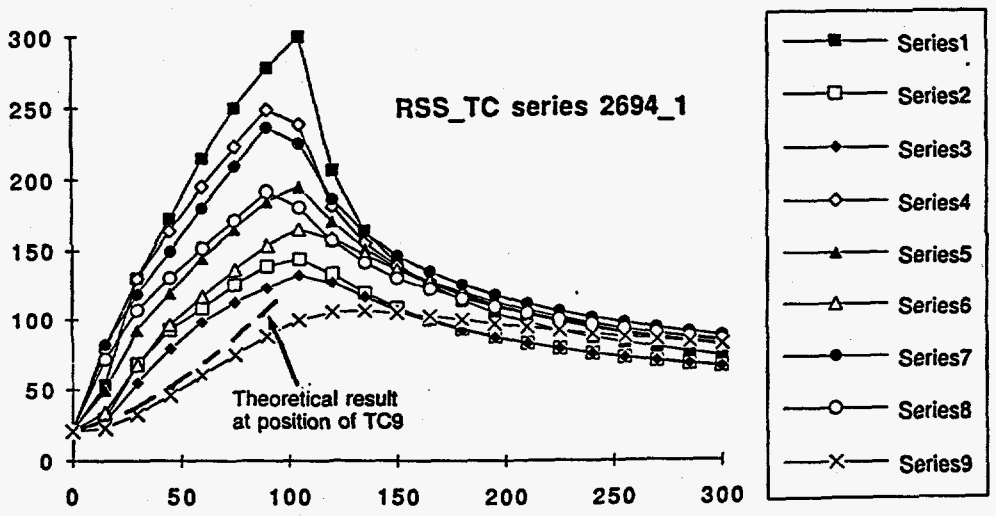

Figure 21. RSSR042694_1.dat. 1 KW at 90 sec. TC side, slab 3-21. Buried thermocouple results after heating concrete for 90 sec. using concrete sampler head.

Taking into account the heating patterns revealed in the IR surface temperature map in Figure 18, the gross features of the thermocouple readings can be explained. The three top traces in Figure 21 all correspond to nominal thermocouple depths of 2 mm below the heated surface. Furthermore, the trace reaching the highest temperature was produced by a thermocouple lying directly under the hottest lobe, as shown in the corresponding radiometer image of the surface [Figure 18]. Two of the three thermocouples at the 3-mm depth also group closely, but the third one follows a substantially lower trajectory. Again, this difference can be explained at least partially by the variation in surface temperature, because in this case the two higher readings from TCs No. 2 and No. 5 in Figure 21 correspond to positions under the higher temperature lobes on the surface, whereas the third thermocouple (No. 8) is located under a cooler region. Finally, slightly higher temperature indicated by the 5-mm-deep thermocouple in comparison to the 4-mm-deep thermocouple can be correlated with a high-temperature lobe position over the former.

The temperature traces and time variations are consistent at least to a first approximation of a simple thermal conduction model. For example, we show a 1-D constant coefficient thermal conduction prediction for the 10-mm-deep TC as a dotted line in Figure 21. This calculation uses the values of conductivity, heat capacity, and density assumed as typical concrete values in our proposal and included in Section 1.3 Design of the Concrete Sampler Head and the well-established result [6] for a constant coefficient semi-infinite solid exposed to constant heat flux at its surface:

$$T(x) = \frac{2Q}{k}\left\{\left(\frac{\alpha t}{\pi}\right)^{1/2} e^{-\frac{x^2}{4\alpha t}} - \frac{x}{2}\,erfc\left(\frac{x}{2\sqrt{\alpha t}}\right)\right\} \qquad (4)$$

Here x is the depth into the solid, and $erfc(x)$ is the complementary error function. The other quantities are as defined for Eq. (1).

We know that the concrete samples have a high moisture content, relative to typical aged concrete, because they had been subjected to ambient drying for only 10 days before the thermocouple tests. It has been established in the literature that vaporization and diffusion of water vapor must be taken into account in concrete heating to temperatures above 100°C, and these effects tend to increase the thermal conduction substantially [7]. The effects of free water vaporization within the bulk concrete are evident in a number of the thermocouple temperature measurements. A particularly dramatic example is shown in Figure 22 where the temperature rise is produced by a 15-minute exposure at reduced incident power density on the back side of the slab. Since the thermocouple depths are indicated from the front of the 25-mm-thick slab, thermocouple TC9 at an indicated depth of 10 mm is actually 25 mm - 10 mm = 15 mm from the heated surface; the others are

farther away and as one would expect, increase in temperature more slowly. Thermocouple TC9 shows a reduction in heating at 100°C, and then a sudden increase just before its peak temperature, whereas thermocouples TC7 and TC8 in one group, and TC4, TC5 and TC6 show a distinct shelf near 100°C. We believe that the plateau effects near the water boiling point represent free water vaporizing and escaping without a large pressure rise, either to the surface or to other regions within the concrete. The sudden rise in TC9 data near the peak may be attributable to condensation of water vapor from nearby hotter regions at high pressure. A similar effect at lower pressure may account for the sudden rise before the 100°C plateau shown by the TC7 and TC8 data. The variation in temperature beyond these effects probably resulted predominantly from the statistical variation of pore distribution (and consequent water vapor pressure rise) at the different thermocouple sites. Thus, we believe that the prominent plateaus are associated with extended pores or cracks reaching from the thermocouple sites to the surface, allowing water vapor to escape to the surface with only a small temperature rise. This type of feature can be expected as a result of the method by which the thermocouple channels were produced, since that method introduced an interface between concrete with different cure periods that extends nearly to the thermocouple bead.

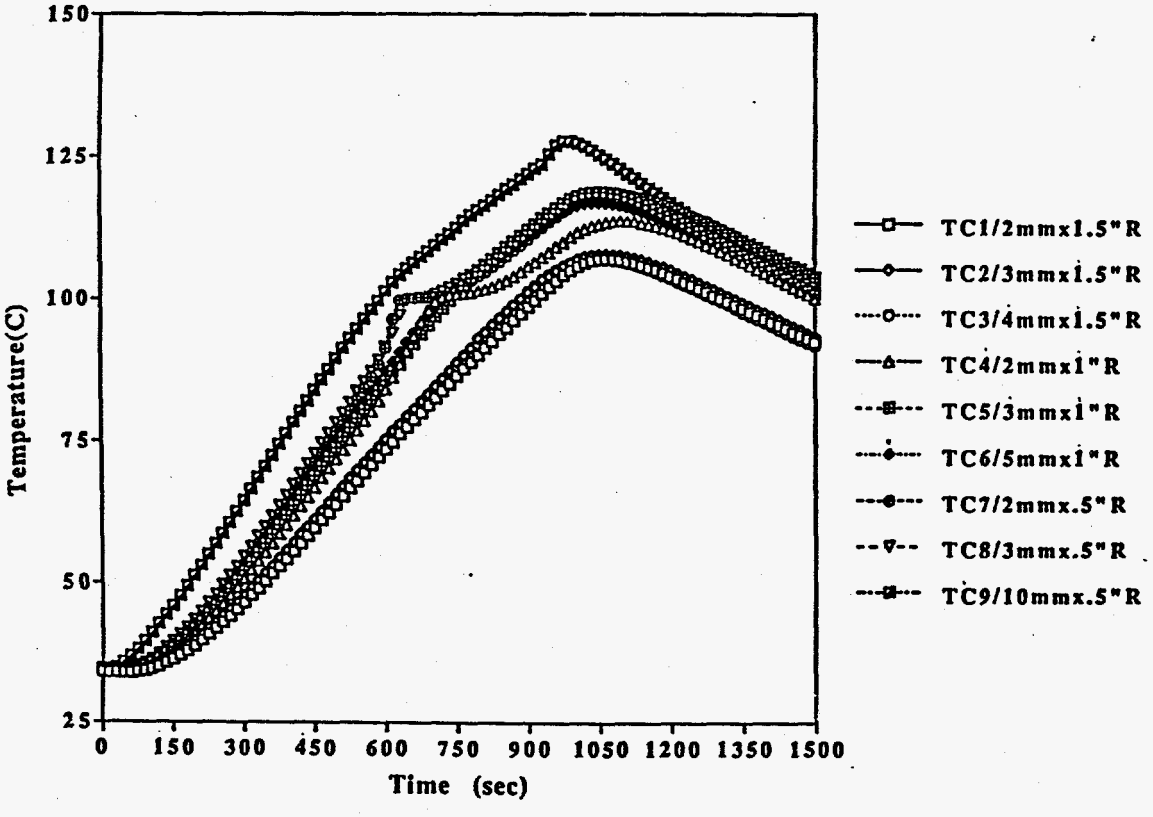

Figure 22. Buried thermocouple results after heating for 15 min. using reduced incident power density on the back of the slab.

It should be noted that the temperature variations from the dependence predicted by a simple model are not enormous, and they are accentuated by the long heating period of 900 sec. versus the 90-sec. period envisaged for the sampling duration. Nevertheless, it is clear that concrete heating and analyte extraction to several hundred degrees centigrade are not so simple as to be interpreted with a simple closed form solution. Therefore, we have developed a finite-element model incorporating thermal conduction along with vapor and air diffusion through the concrete. This model will predict temperature and pressure distributions within the concrete, and gas and vapor (including PCB analyte) emission from the concrete, allowing us to calculate the effects of porosity, diffusivity, and free water content on the sampling depth and efficiency.

Uniformity of heating

The surface-temperature measurements described above were performed on the back side of the concrete samples, opposite the side containing the thermocouple channels, because the channel side showed strong differences in visible light absorption where fill concrete had been pressed into the thermocouple channels; these regions were much darker. Thus the measurements may not be representative of field conditions where one can encounter concrete surfaces inhomogenously stained with oil, accumulated dirt, old paint, etc. Those surfaces might be expected to show larger temperature variations because of variations in absorptivity. However, during the course of the IR temperature measurements we found that the absorptivity of the clean concrete surface in the 2- to 5-μm band is very high, with an average of 0.92. Since most coatings and stains can also be expected to have high absorptivity in this IR band, it is reasonable to anticipate that heating in that band will be more uniform than visible inspection would suggest. It is fortunate that the present design of the concrete sampler head provides a somewhat higher heat flux than needed to meet heating rate requirements. That situation makes available the opportunity to reduce power to the lamp, shifting a larger fraction of its output to the IR where more uniform heating can be anticipated. That opportunity will be studied in Phase II to support the design tasks of that phase.

Thermal and Diffusion Model for Cement

Modeling of concrete heating

The thermal desorption process considered here involves heating a semi-infinite concrete slab from its exposed surface so that the contaminants within the concrete are volatilized and subsequently removed from the slab and collected by the sampler. In this process heat is transferred by radiation to the surface of the concrete and then by conduction into the concrete where water and contaminants in the pores are heated and vaporized. The gases within the pores will flow from regions of high pressure to regions of low pressure. The pressure gradients result from the evaporation of liquids and the thermal expansion of gases. In addition to the pressure-driven flow, the vapors will diffuse down their concentration gradients. A mathematical model has been developed to help understand the thermal desorption process within concrete.

Governing equations

The one-dimensional equation for transient heat transfer with conduction, convection, and heat sinks from evaporation is

$$\frac{\partial T}{\partial t} = \frac{k'}{\rho' c'} \frac{\partial^2 T}{\partial x^2} - \frac{n}{\rho' c'} \frac{\partial}{\partial x} (uT \sum_i \rho_i c_i + \rho T \sum_i D_i c_i \frac{\partial \omega_i}{\partial x}) - \frac{n \dot{m} h_{fg}}{\rho' c'} \tag{5}$$

where T is temperature, t is time, x is position, u is mass-averaged velocity and n is porosity of the material. The quantity ρ_i is the concentration of species i in the vapor phase, ω_i is the mass fraction and c_i is its thermal capacity. The quantities k', ρ' and c' are the thermal conductivity, density and thermal capacity of the concrete, while $\dot{m}$ is an evaporation (or condensation) rate. In Table 5, quantities involved in equations in this section are further defined.

The derivation of Eq. (5) involves an assumption that the thermal mass and conductivity of the gases are negligible compared to the solid concrete. The heat sink term associated with evaporation represents evaporation of any species such as free water, water of hydration, or PCBs. The heat of hydration for cement is typically about 400 J/g of unhydrated cement. Because hydrated cement consists of about 20% water by weight, the heat of hydration per unit mass of water is about 1600 J/g of water or about the same order of magnitude as the latent heat of evaporation of free water (2300 J/g). The distinction between free water and hydrated water is presumed to be relatively unimportant. Furthermore, because the expected concentration of contaminants is low compared to water, only evaporation of water is considered in the energy equation. Of course evaporation of the contaminant is accounted for in its mass balance equation below.

The equation for the transport of noncondensable gases like air is given by

$$\frac{\partial \rho_1}{\partial t} = \frac{D_1}{\tau^2} \frac{\partial}{\partial x} \rho \frac{\partial \omega_1}{\partial x} - \frac{\partial (u \rho_1)}{\partial x} \tag{6}$$

where ρ_1 is the concentration of the noncondensable species, ω_1 is the mass fraction of the noncondensable species. The diffusion coefficient for this mixture of gases D_1 is taken to be that of air. For species i that have the potential to evaporate and condense such as water and PCBs, the mass transfer equation is

$$\frac{\partial \rho_i}{\partial t} = \frac{D_i}{\tau^2} \frac{\partial}{\partial x} \rho \frac{\partial \omega_i}{\partial x} - \frac{\partial (u \rho_i)}{\partial x} + \dot{m}_i \tag{7}$$

where $\dot{m}_i$ is the evaporation rate of species i. Equation 7 is applied to regions where the vapor phase is in equilibrium with its liquid phase. At some point during the heating pro

Table 5. Model Parameters in Numerical Simulation.

Model input parameters	Value	Definition
A1	$9.25 \cdot 10^{10}$ Pa	coefficient in water vapor pressure relation, [Eq. (9)]
A2	$1.06 \cdot 10^{11}$ Pa	coefficient in PCB vapor pressure relation, [Eq. (9)]
B1	5121.1 K	exponent in water vapor pressure relation, [Eq. (9)]
B2	9070 K	exponent in PCB vapor pressure relation, [Eq. (9)]
C_{p0}	1.0 kg m^{-3}	assumed initial liquid PCB concentration
C_{w0}	87.5 kg m^{-3}	assumed initial liquid water concentration
C_A	1050 J kg^{-1} K^{-1}	heat capacitance of air
C_w	2016 J kg^{-1} K^{-1}	heat capacitance of water vapor
C'	1000 J kg^{-1} K^{-1}	heat capacitance of concrete
D	10^{-5} m^2 s^{-1}	contaminant and air diffusion coefficient
h_{fg}	$2.32 \cdot 10^6$ J kg^{-1}	heat of vaporization of water
K	10^{-17} m^2	hydraulic permeability
Mw_{PCB}	0.300 kg mol^{-1}	molecular weight of PCB (kg/mole)
Mw_w	0.018 kg mol^{-1}	molecular weight of water
n	0.1	porosity
P_0	10^5 Pa	initial pressure
T_0	300 K	initial absolute temperature
α	$7 \cdot 10^{-7}$ m^2 s^{-1}	thermal diffusivity of concrete
ρ'	2300 kg m^{-3}	density of concrete
τ	1.5	tortuosity
μ_0	$1.3 \cdot 10^{-5}$ kg m^{-1} s^{-1}	viscosity of vapor at T_0

cess, all of the condensed phase may have been evaporated in which case Eq. 7 reverts to the form of Eq. 6. The mass transfer equation of condensed species such as water or PCBs is

$$\frac{\partial \rho_i}{\partial t} = -n\dot{m}_i \tag{8}$$

where n is the porosity of the concrete. The condensed species are assumed to be immobile in terms of diffusion and convective transport and unlike the vapors which exist only in the pore space, the condensed species are assumed to be distributed throughout the matrix. Thus the concentration of condensed species is given in units of mass per volume of concrete while vapors are given in units of mass per volume of pore space.

The equilibrium relation between the vapor and liquid phases is approximated by the vapor pressure relation

$$p_v = Ae^{-B/T} \tag{9}$$

where p_v is the partial pressure of the vapor phase, T is the absolute temperature and A and B are empirical coefficients identified for each species. The partial pressure of the contaminant vapor is related to its concentration by the ideal gas relation

$$\rho_i = p_{vi} Mw_i / RT \tag{10}$$

where Mw_i is the molar weight of species *i*.

The flow rate of vapors through porous media is modeled by the Darcy equation which states that the pore velocity u is proportional to the pressure gradient and inversely proportional to the viscosity of the fluid:

$$u = -\frac{K}{n\mu}\frac{\partial P}{\partial x} \tag{11}$$

The fluid flowing through the concrete is composed of air, volatilized contaminants and water. We assume that the gaseous mixture can be modeled by the ideal gas relation

$$P = \rho RT \sum_i \frac{\omega_i}{Mw_i} \tag{12}$$

Because the flow of the gases through concrete is a strong function of the gas viscosity, the ideal gas viscosity is employed, where the viscosity is proportional to the square root of absolute temperature .

$$\mu = \mu_0 \sqrt{T/T_0} \tag{13}$$

Finally the equation for conservation of mass of vapors in the pore space is given by

$$\frac{\partial \rho}{\partial t} = -\frac{\partial (u\rho)}{\partial x} + \dot{m}_{H_2O} + \dot{m}_3 \tag{14}$$

where m_{H2O} and m_3 are the evaporation rate of water and contaminant, respectively.

Example

The governing equations have been discretized in a finite difference algorithm, programmed in FORTRAN, and run on a Convex computer. The parameters input into the model are listed in Table 5 for an example simulation. The predicted temperature, pressure, and water distributions are shown in Figures 23-25. It is clear from this simulation that high pressures in the concrete are predicted and the location of the maximum pressure occurs at the wet/dry interface. This pressure distribution will cause transport of water vapor both into and out of the slab. The water vapor that moves farther into the slab recondenses in the cooler regions. This effect near the wet/dry interface is similar to a heat pipe in which the energy is transferred by evaporation/condensation of water.

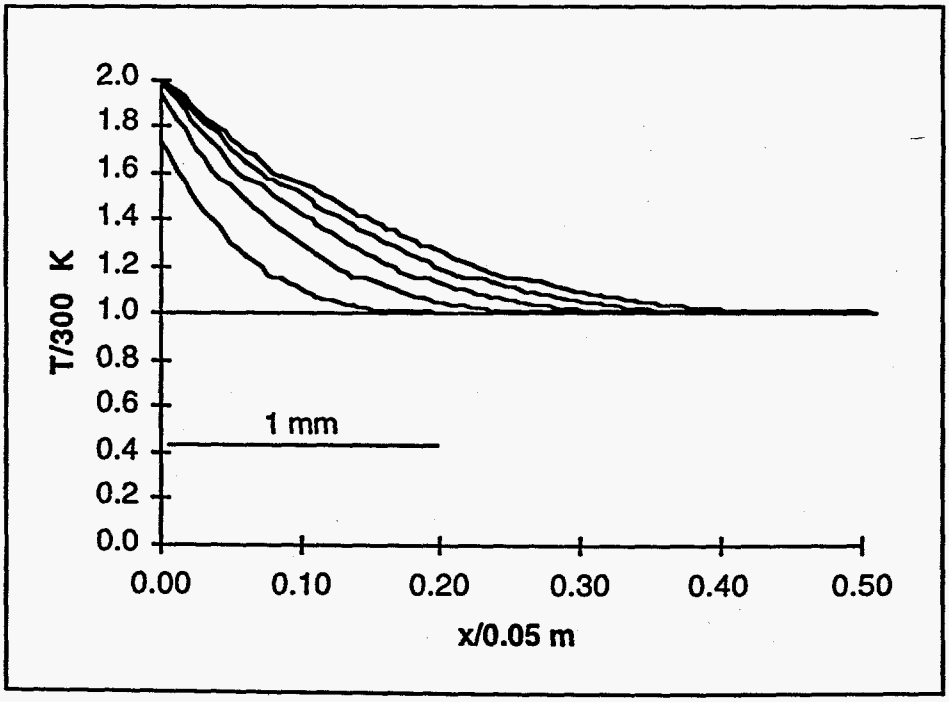

Figure 23. Temperature distribution at 13 s intervals.

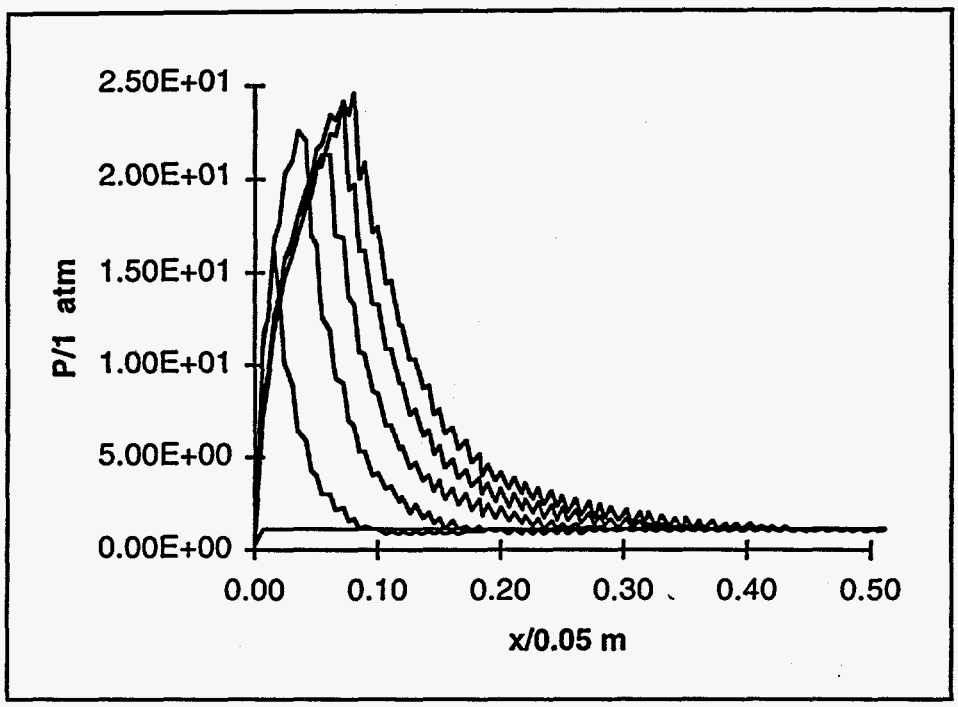

Figure 24. Pore pressure distribution at 13 s intervals.

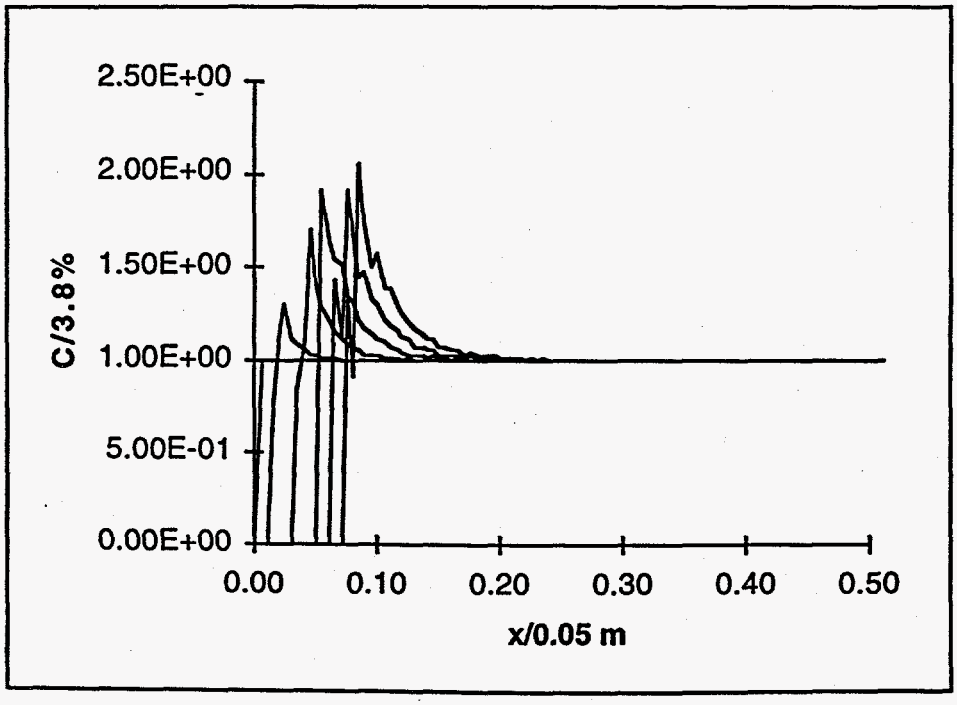

Figure 25. Liquid water concentration, normalized to an initial concentration of 3.8% at 13 s intervals.

Plans

The present computer model exhibits some "ringing" in the concentration profiles that can only be eliminated if very high spatial and temporal resolution is used. Different numerical techniques will be investigated to permit larger time steps and a coarser grid. Additional simulations will be made to verify the accuracy of the model. The model predictions will be compared to experimental data obtained from heating tests on concrete slabs. Model parameters will be adjusted to account for a range of permeabilities, water content, and heat flux rates. The model will be used to determine appropriate heating rates and exposure times for rapid field analysis. Modifications will address issues such as the effect of condensed phases on effective porosity and the effect of dehydration on permeability, long term migration of PCBs in concrete at rear-ambient temperatures, and the effects of surface cracks..

Conclusions regarding thermal tests of the concrete sampler head

The concrete sampler head is suitably rugged and maintainable for laboratory and limited field testing at its present level of development and is upgradable in these qualities without difficulty. In its present form, initial thermal measurements support an expectation that it will meet heating uniformity criteria over at least 60% of the sampling area. Efforts to increase this fraction are under way and do not appear to present any serious difficulty. Initial measurements indicate that peak temperatures are predictable within 10°C on our prepared samples. Effects of variation in concrete absorption resulting from composition variation, surface contamination, and coatings, and effects caused by variation in porosity and water content are being evaluated experimentally and by numerical models. Provided that artifact effects can be controlled, the thermal performance of this equipment indicates that it should provide an excellent sampling method.

Task 1.3.2 Concrete Sampler Head Functional Tests

The purpose of this task is to test the performance of the concrete sampler head using well-defined concrete samples. These samples, containing known amounts of three model compounds, allow sampling efficiency data to be obtained. The samples are analyzed in a manner that provides information about the time dependence of the sampling process.

Preparation of Concrete Samples

Concrete "cakes" 30 cm in diameter and approximately 2.5 cm thick, contaminated with known amounts of three model compounds, were prepared in May 1994. To contaminate the concrete, we used clean sand (800 g) treated with a solution of anthracene (4.0010 g), phenyldodecane (3.9999 g) and 2,4,5-trichlorobiphenyl (3.9870 g) in a mixture of methylene chloride (250 mL) and hexane (250 mL). The solvent was allowed to evaporate over a 24-h period, and the sand slurry was stirred occasionally during the evaporation process.

Analysis of the dried sand (24-h soxhlet extraction with toluene followed by GC analysis) gave the results listed in Table 6.

Table 6. Analysis of Dried Contaminated Sand

Contaminant	Amt Detected (g/kg)	Std Dev	Amt Spiked (g/kg)
Anthracene	5.68	0.79	5.0013
Phenyldodecane	4.97	0.29	4.9999
2,4,5-trichlorobiphenyl	5.06	0.22	4.9838

All analyses gave acceptable results. The results were essentially the same as the spiked amounts given the standard deviation for the measurements. These results are averages of three separate sand samples, each sand sample extract being analyzed three times.

The master batch of dry, contaminated sand was used to prepare concrete samples containing varying concentrations of the model contaminants, by mixing varying amounts of clean and contaminated sand in the concrete (Table 7).

The contaminated cakes were numbered one through six. In addition, two uncontaminated cakes were prepared and instrumented with thermocouples. After the concrete was mixed and poured, the cakes were allowed to sit in the cake tins for 5 days. After 5 days they were stacked in a metal can separated with blocks of teflon. Water was added to the bottom of the metal can to allow the cakes to cure in high humidity. A week later the cakes were transferred to a polypropylene tray for storage. They were aged in an average relative humidity of 45% for approximately 6 months prior to these tests.

Table 7. Mixtures of Contaminated Sand Used to Prepare Concrete Cakes.

Sample A used to prepare cakes 1 and 2

Ingredients		Contaminant Concentration (ppm)	
Clean sand	2700 g	Anthracene	426
Contaminated sand	300 g	Phenyldodecane	373
Portland cement	1000 g	2,4,5-Trichlorobiphenyl	380
Water	590 g		

Sample B used to prepare cakes 3 and 4

Ingredients		Contaminant Concentration (ppm)	
Clean sand	2920 g	Anthracene	114
Contaminated sand	80 g	Phenyldodecane	99
Portland cement	1000 g	2,4,5-Trichlorobiphenyl	101
Water	590 g		

Sample C used to prepare cakes 5 and 6

Ingredients		Contaminant Concentration (ppm)	
Clean sand	2980 g	Anthracene	28
Contaminated sand	20 g	Phenyldodecane	25
Portland cement	1000 g	2,4,5-Trichlorobiphenyl	25
Water	590 g		

Initial Heating Experiments

One of the concrete cakes that is instrumented with buried thermocouples was used in initial experiments to determine the lamp voltage necessary to bring a surface layer of the cake to 250 °C in 4 min. Results for 65 V input are shown in Table 8. This setting was used in subsequent experiments.

Experimental Configuration and Procedure

The experimental configuration for the concrete sampler head performance tests is shown in Figure 26. The heated lines shown in the figure are 1/8-in stainless steel silica-lined tubing. These lines, and the UV absorption cell, were wrapped with aluminum foil, then heating tapes, then with quartz fiber insulation encased with an outer aluminum foil layer. Temperatures were maintained using three Omega temperature controllers. Temperature uniformity was monitored by 9 additional thermocouples. These instruments indicated temperature uniformity within ±20 °C.

Two sets of experiments were performed. In the first set, a single solvent trap was used to collect evolved species over a 5-min heating period. Thermal samples were obtained from concrete cakes 4 and 6. Cake 4 was contaminated to 100 ppm nominal with each of these materials. Cake 6 was contaminated to a level 25 ppm (nominal) each with anthracene, 2,4,5 trichlorobiphenyl and phenyldodecane.

Table 8. Average Temperature Reading from Three Thermocouples Buried 2 mm Deep in Concrete Cake, as a Function of Time After Heating Lamp was Energized. Lamp Setting: 65 V, Corresponding to about 450 W.

Time (min)	Ave. thermocouple reading (°C)
0	33
0.5	106
1	138
1.5	166
2	184
2.5	204
3	221
3.5	236
4	250

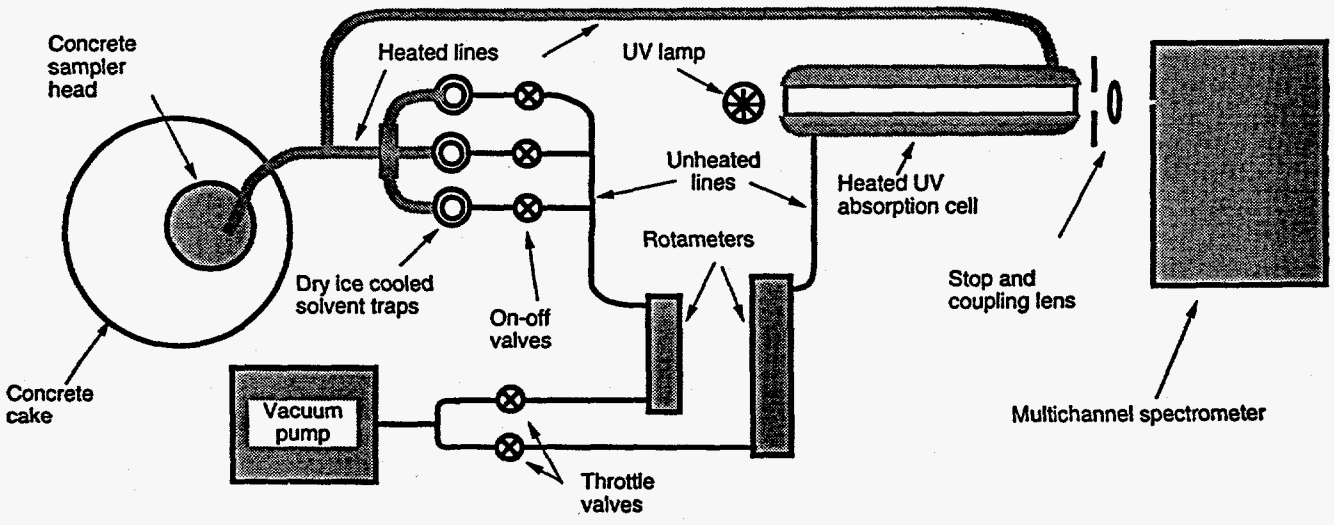

Figure 26. Experimental configuration for the concrete sampler head functional tests.

The experimental sequence is summarized below:

1. Sampler head, heated line, and UV absorption cell heaters were turned on and warmed up to 250 °C.

2. The solvent traps were cooled using dry ice.

3. An initial UV absorption spectrum was acquired to serve as the zero absorption standard.

4. The head was placed on a concrete "cake" sample.

5. The lamp was then energized to a voltage setting near 65 V chosen to warm the block surface (at a point 2 mm below the surface) to an average temperature of 250 °C in 4 min.

6. Simultaneously the throttle valves were opened and adjusted to establish the 10:1 split flow through the UV absorption cell and solvent trap. The total noncondensable flow rate was 165 cm^3/min. The distinction of noncondensable flow is important because a substantial amount of water vapor evolves during the thermal extraction of concrete. This vapor is condensed in the solvent traps before the flow is measured. The water vapor evolution is one of the reasons why the flow rate is set relatively high—to ensure that the water vapor does not set up a back flow to carry analytes away from the sampling head. Because of concern about efficient trapping with such a high flow rate, we chose to split the flow, such that 1/11 of the noncondensable flow passed through the collection solvent trap and the rest passed through the UV absorption quick-look detector and then through a backup solvent trap. The flows were measured by rotameters calibrated under closely similar pressure and temperature conditions with a bubble flow meter.

7. UV absorption spectra were acquired at 1-min intervals after lamp ignition for 1 to 5 min.

8. At 5 min the head was removed from the concrete block and flow through the solvent trap was stopped.

9. The solvent trap was removed, emptied, rinsed with a measured amount of additional solvent, and all solvent was analyzed using a Shimadzu 9A GC to determine solvent concentrations of the three analytes.

In the second set of experiments the procedures were similar except that all three solvent traps shown in the figure were used. The flow was directed through one of these traps for the first minute of heating. The second trap received the flow from minute 1 to minute 5. The last trap received the flow from minute 5 through minute 10.

Collection Results

The UV quick-look detector provided sensitive semiquantitative measurements of the analyte concentrations in the flow as a function of sample time. Results for cake 6 at 1-min intervals are shown in Figure 27. Here the highest trace is the spectral signal recorded for clean air just before the heating period. The absorption bands evident at the shortest wavelengths (around 180 nm) are Schumann Runge bands of oxygen, which determine the long wavelength limit of the vacuum ultraviolet. The oxygen absorption bands shown here were produced by a total pathlength of 50 cm in air. Subsequent traces are labeled with the time (in minutes) after the heating power is turned on. The analyte concentrations are determined by the reduction in transmission, which reaches a lowest value of approximately 0.22 at the 3-min point at 191 nm, and then begins to increase. This behavior is consistent with thermal desorption from a shallow surface layer nearing completion, while desorption from deeper layers follows a slower rate both because of the slower temperature rise and the greater diffusion distance. The behavior of this collection rate will be studied in Phase 2, when detailed concrete sampling models are developed from the preliminary model in Phase 1.

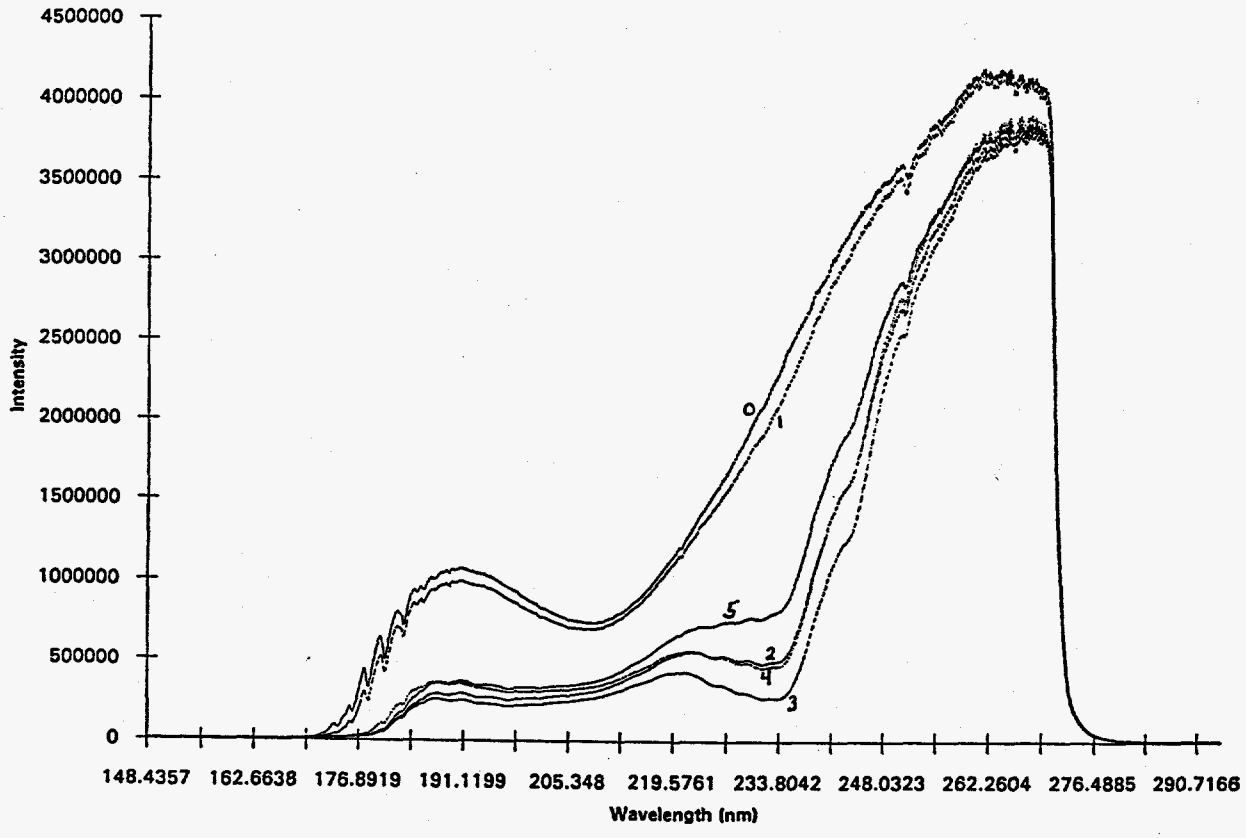

Figure 27. UV transmission spectra at 1-min intervals for initial cake 6 experiments.

Precontract work established that molar extinction coefficients for PCB congeners range from 10^4 to greater than 10^5 cm L/mol, at 191 nm, with the highest coefficients corresponding to the most halogenated congeners. Although absolute coefficient measurements have not been obtained for the specific congener used in these tests, a reasonable value is 1×10^4. For a simple illustration we assume that the 2,4,5-trichlorobiphenyl congener accounts for all the observed absorption. Then from the data in Figure 27, which shows the absorption in a 25-cm pathlength, the average concentration of that congener in the sample air as 560 µg/L. Multiplying this concentration by an effective collection time of 3.5 min, and total flow rate of 165 mL/min, we estimate that the sampled mass is 323 µg.

This value for total collected mass compares with a calculated value, based upon original analyte loading, and the measured trapped masses, as follows: The mass of each analyte that should be collected is estimated by assuming that all of the analyte masses in the first 1 mm of depth (or equivalently, half the analytes in the first 2 mm of depth) are collected over the full heated area of 100 cm^2 during the first 5-min heating period. In this case, for cake 6, with a measured density of 1.87 g/cm^3, the estimated mass is 472 µg.

In comparison, the total solvent volume used in each trap, including trap rinses, was 20 mL. For the initial experiment on cake 6, the concentration of the 2,4,5–trichloro-biphenyl in this solvent was measured using a calibrated Shimadzu GC, which indicated 1.6 µg/mL. Thus the total trapped PCB analyte mass was 32 µg. Taking into account the 10:1 split ratio, the indicated collected PCB mass is 352 µg, which compares very favorably with the values obtained by estimate from the original loading, and from UV absorption. Additional measurements are listed in Table 9.

Table 9. Anthracene, 2,4,5-Trichlorobiphenyl, and Phenyldodecane Recovered by the Concrete Sampler Head from Concrete Cakes 4 and 6 and Measured by GC-FID.

Cake	Compound	µg in 1 mm thickness	Total collected (µg)
#6	Anthracene	529	121
	2,4,5-Trichlorobiphenyl	472	352
	Phenyldodecane	472	477
#4	Anthracene	2116	355
	2,4,5-Trichlorobiphenyl	1888	1194
	Phenyldodecane	1888	1022

In these simple experiments, where the analytes are known, the UV absorption data has the potential to produce quantitative specific results. This capability exists because each of the analytes has a distinct absorption band shape. The quantitative calculation presented above could be low because of the presence of water vapor in the measured

stream, since that vapor will dilute the concentration of analyte. On the other hand, the estimate is biased high because the absorption of the other analytes was not included. It is relatively straightforward to correct for the presence of other *known* analytes by using data from multiple wavelengths. Correction for water vapor dilution is more difficult, but could be estimated. We did not attempt either of these corrections because it is not clear that either would be helpful in an actual measurement situation where the specific analytes and their relative concentrations are unknown. For these situations the UV absorption technique, at least at its present level of development, is proposed only as a quick-look detector. The quick-look capability is based on the observation that all of the highly controlled analytes we have measured have strong absorption in the near vacuum UV, whereas analytes determined to be less harmful, or innocuous, have much weaker or negligible absorption. Nevertheless, it is encouraging to find the technique provides at least semiquantitative results in known situations.

In the second set of experiments, all three solvent traps shown in Figure 26 were used. One valve was opened for the first minute of collection. That valve was closed and the next opened for minutes 1 to 5. Then the second valve was closed and the third opened for minutes 5 through 10. In this way, time resolution of the trapping rates was obtained. These experiments were run in duplicate. Time-resolved UV absorption results for representative experiments on cakes 1 and 3 are shown in Figures 28 and 29. It is clear that the absorption levels are consistent with the original loadings of the cakes. Concentrations calculated from the solvent trap measurements are shown in Figure 30. As illustrated in these figures, for the most part the results at the 5-min collection time correlate to within a factor of approximately two with an assumed uniform mix of the original analyte loadings into the first millimeter depth of the cake. It should be noted that the assumption that measured levels should be compared with complete removal of analyte from a 1-mm depth (or equivalently, 50% removal from 2 mm) is reasonable but arbitrary at this point. A model of the extraction process, and comparison with other types of measurements on particular concrete samples will be needed to establish a quantitative correlation with bulk analyte loadings. However, we believe that these experiments show that the thermal sampling approach has sufficient potential accuracy to justify this careful approach. These results are very encouraging when compared with the well-known variability of wipe measurements. On the other hand, it should be noted that these measurements show one persistent anomaly: the anthracene results are consistently low.

Differences in vapor pressure for the three species are not sufficient to explain the apparent reduction of anthracene near the surface. However, anthracene is, by far, the most chemically reactive of the analyte species. We have observed oxidation of anthracene to anthraquinone at room temperature in solution and in the heated vapor stream. It is quite possible that the anthracene is substantially converted to other chemicals, in addition to anthraquinone, which are not monitored in our GC measurements. In fact, several uncalibrated, late-eluting peaks have been observed frequently. In contrast, the oxidation products of the PCB congener and phenlydodecane

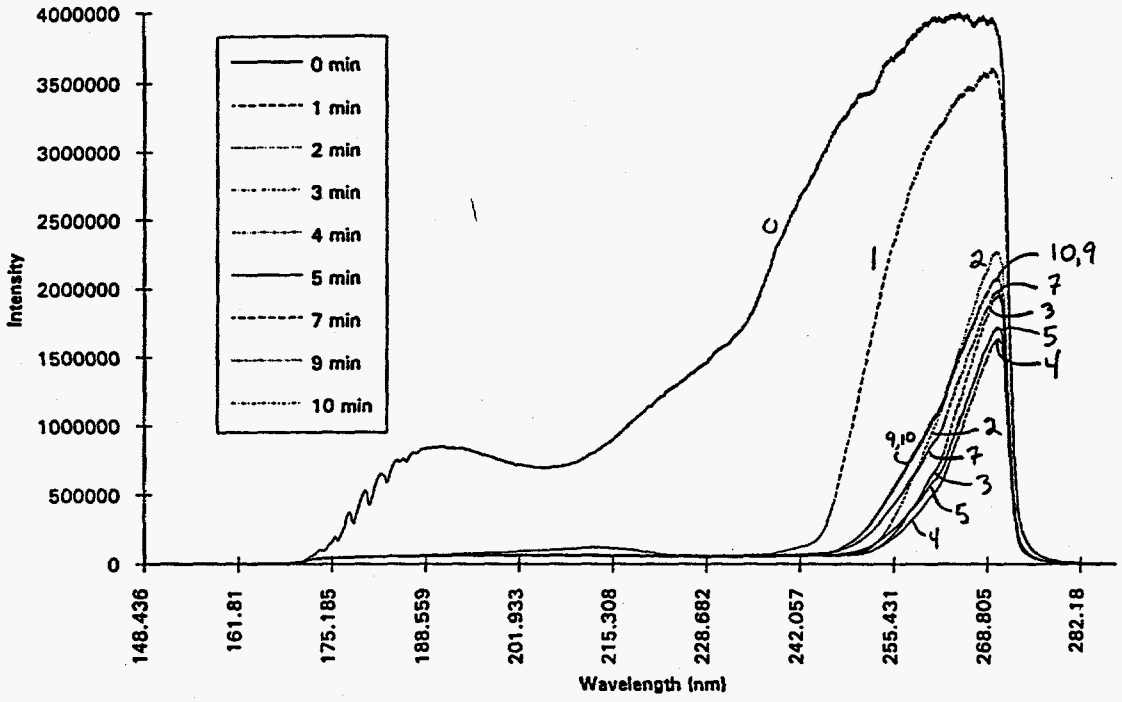

Figure 28 UV transmission spectra at 1-min intervals for cake #1 experiment.

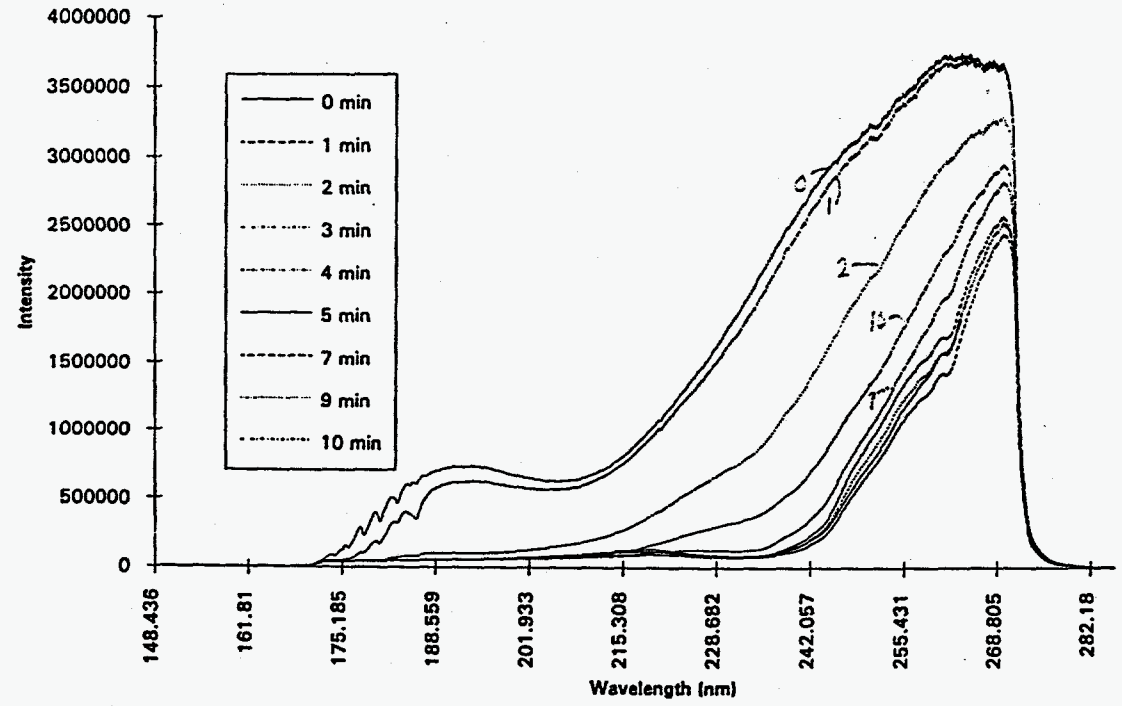

Figure 29. UV transmission spectra at 1-min intervals for cake #3 experiment.

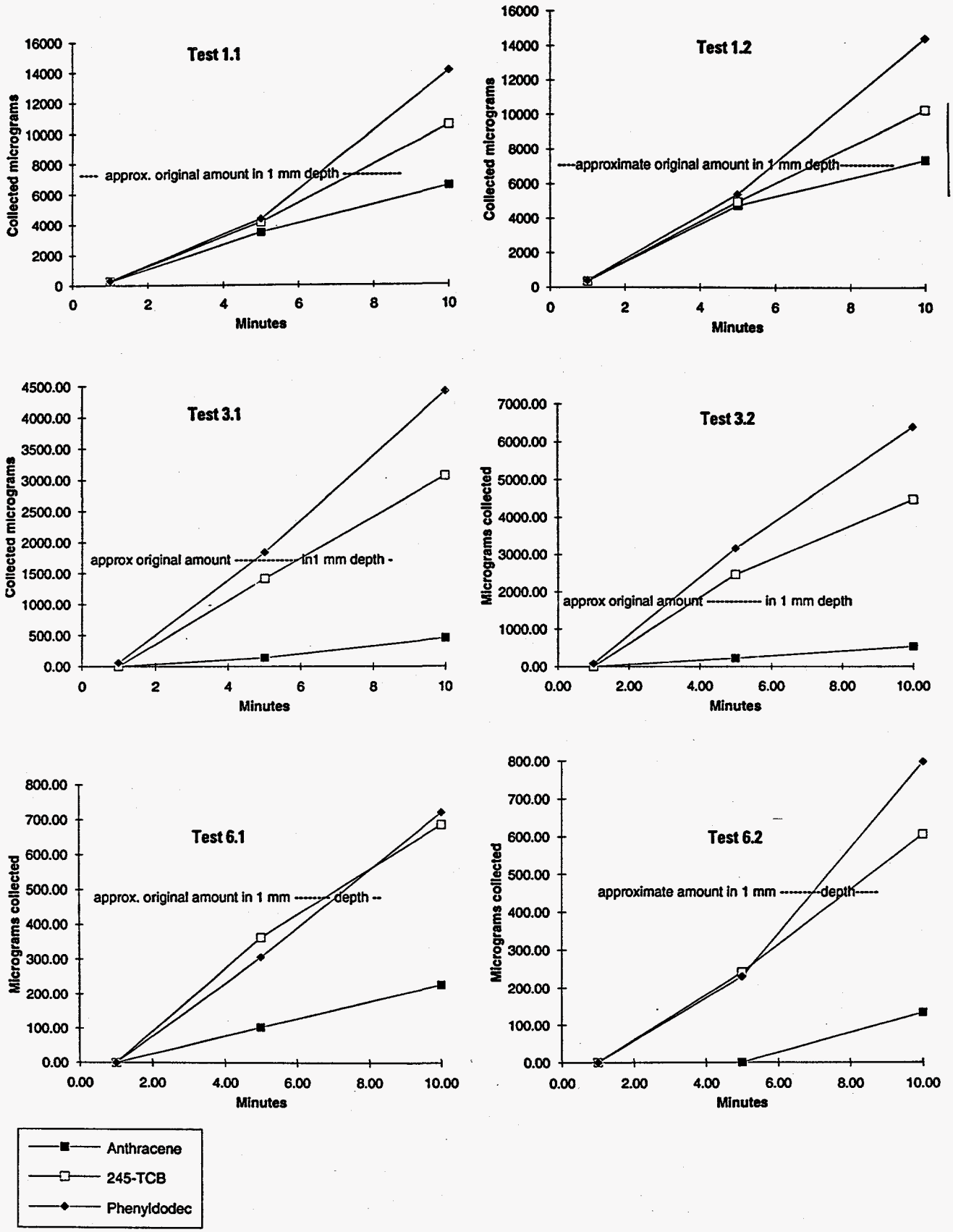

Figure 30. Total extraction amounts versus time-determined from GC analysis of solvent traps. The first test number refers to the cake number and the second to the specific experiment, two experiments were run on each cake.

have not been observed in these tests. Further, we have been informed that anthraquinone is unusually tightly bound to a concrete matrix. Either or both of these effects could account for the low levels of observed anthracene.

Core Analysis Results

Concrete cake 3 was analyzed by coring for comparison with the thermal extraction data. A tungsten carbide-tipped hole saw was used to obtain nominal 1-in diameter cores from sampled and unsampled areas on these concrete cakes. Surface layers at the top and bottom of each core were chipped off to obtain some spatial resolution in the core analysis. The samples were crushed and subjected to soxhlet extraction. Results are shown in Table 10.

Table 10. Results of Drilled Core Analyses of Concrete Cakes

Sample	Thick mm	Section	Mass (g)	Dil. Vol. (mL)	Anthra-cene µg/mL	2,4,5-TCB µg/mL	Phenyl dodecane µg/mL	Anthra-cene µg/g	2,4,5-TCB µg/g	Phenyl-dodecane µg/g
3.H.1	3	T	4.18	200	<0.1	<0.1	<0.1	<5	<5	<5
3.H.1	15	M	15.65	200	2.59	2.37	2.85	33.1	30.3	36.4
3.H.1	3	B	2.53	100	<0.1	<0.1	<0.1	<5	<5	<5
3.H.2	2	T	3.48	100	<0.1	<0.1	<0.1	<5	<5	<5
3.H.2	17	M	12.87	200	1.68	1.39	2.07	26.1	21.6	32.2
3.H.2	7	B	4.66	200	1.01	0.71	1.01	43.3	30.5	43.3
3.C.1	4	T	3.69	200	<0.1	<0.1	0.64	<5	<5	34.7
3.C.1	18	M	12	200	2.44	2.84	2.56	40.7	47.3	42.7
3.C.1	5	B	3.45	200	<0.1	0.6	1.31	<5	34.8	75.9
3.C.2	4	T	3.85	200	<0.1	<0.1	0.53	<5	<5	27.5
3.C.2	20	M	13.08	200	2.55	2.84	2.55	39	43.4	39
3.C.2	10	B	6.02	200	0.85	0.9	1.25	28.2	29.9	41.5

Concrete cake 3
H = heated section, C = unheated section
B = bottom, T = top, M = middle slice of core section

Taking into account that cake 3 was contaminated to 100 ppm (nominal) with each of the analytes, the results shown in the last three columns of Table 10 indicate that only in one case was as much as 75% of the original average contamination concentration was recovered. The rest of the results vary widely, either near 0 or near 40% of the original average loading. We have the following comments regarding these results.

First, the low readings on all six of the heated top regions are expected, since these regions should have been depleted by the thermal sampling. However, four of the top readings and one of the bottom readings on unheated sections are also effectively zero.

Low values for anthracene might be expected on the basis of the arguments made previously, regarding the chemical reactivity of anthracene. However, two surface readings for anthracene are relatively high.

A possible explanation for the distribution of these results is that the coring operation may have heated the samples sufficiently to move the analytes from original locations. There was substantial variability in this coring process, and core temperatures were not monitored. The act of coring with a tool having slightly oversize tungsten carbide inserts tends to insulate the core, particularly near the end drilled last. Although these experiments cannot be repeated because there is insufficient remaining sample, in subsequent work we will monitor core temperatures and control drilling speeds if necessary.

Conclusions

When comparison is made to results from other sampling techniques (drilled cores, wipe sampling) it appears that the thermal sampling approach gives evidence of being substantially more closely correlated to bulk contamination levels. The essential steps of the proposed sampling process: semiquantitative (at least) performance of the UV quick-look detector; trapping of evolved products in solvents or a sorbent trap; efficient transfer of these analytes to a GC column; and close quantitative correlation between concentration determinations and original *bulk* contaminant loadings *all* have given positive results in these experiments.

Task 1.4 Design and Test of the Bulk Sampler Head

Bulk Sampler Head Design and Construction

The purpose of the bulk sampler head is to extract analytes from 1 to 5 mL of a bulk sample by thermal desorption. Typical bulk samples are drillings, pulverized concrete, and particulate waste. The bulk sampler can be used, for example, for deep sampling of concrete wherein the samples are acquired by drilling a concrete wall or floor. It can also be used to characterize general debris and soils. Another major use is to provide samples to test and calibrate quick look modules and sorption devices. Consequent requirements are to provide

- Rapid sample heating (~100 seconds)
- Convenient cleaning and quick sample insertion
- Heated connection to the rest of the RSSAR system
- Safe and rapid handling of samples

A photograph of the resulting bulk sampler head prior to heating design and insulation application is shown in Figure 31. Detailed drawings are presented in Appendix 1 (Design Drawings). The oven is formed from a solid aluminum block into which a rectangular channel is milled. Two additional milled blocks made of stainless steel are used to provide thermal breaks from the heated oven portion. The heated aluminum is wrapped with a 700-W calrod heater of 1/16 in. in diameter. The calrod is clamped along with a type K thermocouple onto the oven and wrapped with aluminum foil for uniform thermal transfer to the sample chamber. A stainless steel bellows is connected to the bulk sampling oven with a swagelock fitting. The bellows has a 600-W heating tape wrapped around its entire length, is fitted with three type K thermocouples, and also is wrapped with aluminum foil for uniform thermal heat transfer. The entire oven and bellows are wrapped with fillerless glass matting and cloth for insulation. The oven is packaged into an aluminum housing with electrical and thermocouple terminations. The rectangular sample holder is formed of solid aluminum with a cylindrical well for the sample. Like the oven, the sample holder which consists of two rectangular pieces and a hollow stainless steel rod has three stainless steel thermal breaks. A hole through the thermal breaks and the sample holder allow for a thermocouple to be inserted for monitoring the sample temperature. The bulk sampling oven is connected to the photo-ionization detector (PID) using swagelock fittings between the heated bellows from the oven and the PID input tubing. Since the PID input and output tubing extends out of the PID housing, the tubing is also wrapped with a calrod heater and is insulated in the same fashion as the bulk sampling oven and bellows. The output of the bulk sampling oven is terminated with swagelock fittings to two solvent cold traps, which are in turn connected to a pump that pulls a vacuum at the required flow rates. Temperature control is provided by temperature controllers from Omega Engineering. The temperature controllers are self calibrating and automatically adjust the control parameters as flow rates are changed.

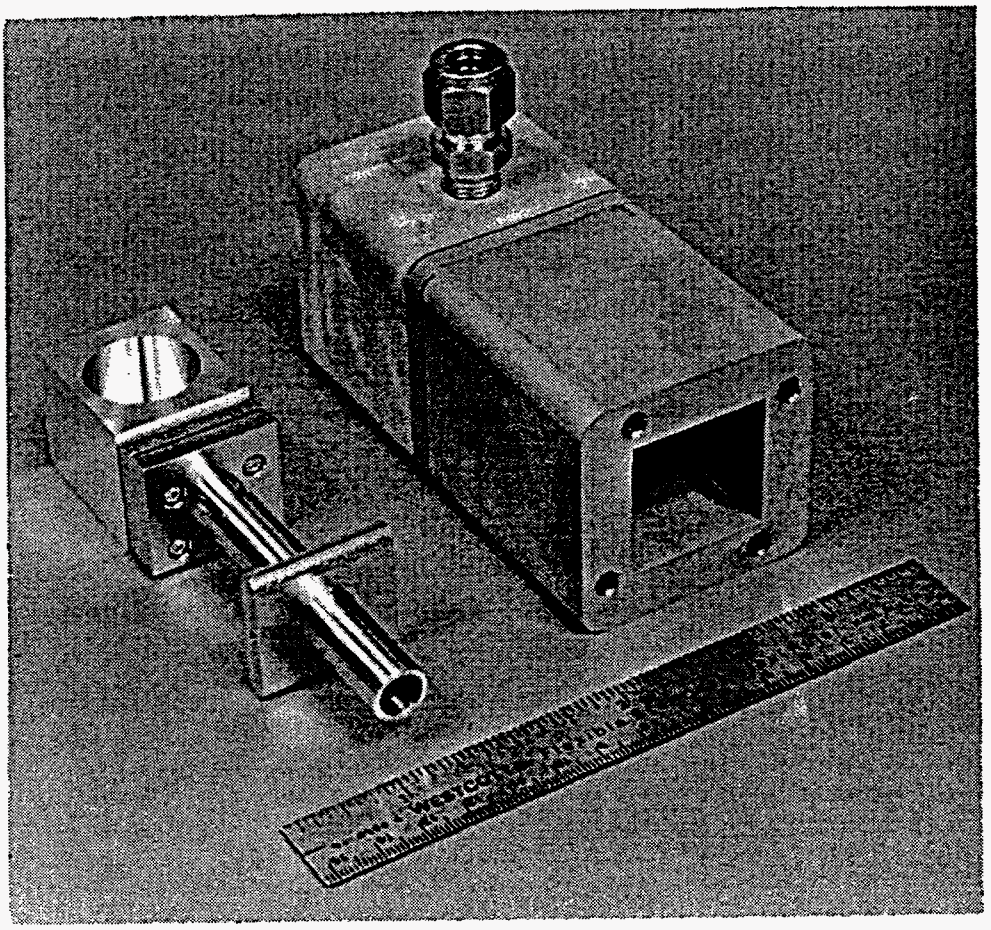

Figure 31. Photograph of the bulk sampler head prior to heater design and insulation application.

Performance Tests

The performance of the bulk sampler oven has been tested extensively in experiments on desorption with the photoionization detector (PID) and the UV absorption detector. One typical result is presented in this section. Figure 32 shows the PID trace resulting from a sample of 10 μg of phenyldodecane. In experiments of this type, the majority of desorption products detected by an in-line photoionization detector are evolved 4 minutes after which the signal returns rapidly to background levels. Other results are shown in the Task 1.5.1 Section. The oven is convenient to use in its role as the workhorse instrument for calibration and recovery fraction experiments. Problems common to other thermal sampling techniques, dealing with incomplete recovery and chemical conversion, are discussed in the section entitled Task 1.5.1 Photoionization Detector.

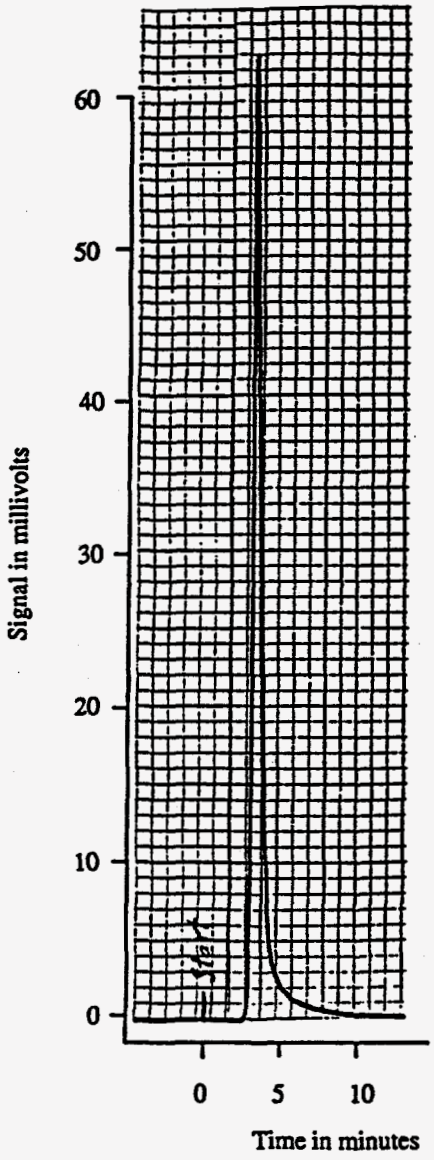

Figure 32. Response of photoionization detector to 10 µg of phenyldodecane.

Task 1.5.1 Photoionization Detector

This section describes the trials that were conducted with the bulk sampling oven/photoionization detector (PID) assembly to demonstrate that the PID assembly can be used to detect the presence or absence of contaminants in real time in bulk pieces of concrete, transite, and the like. Known amounts of contaminant model compounds were placed in the bulk sampler head and were volatilized; detector response was determined, and purge gases were collected and analyzed for determination of mass balance. The experimental details that follow describe the evaluation of this assembly with three model compounds at three different air flow rates. The model compounds were chosen to represent a polynuclear aromatic, a polychlorinated biphenyl, and an oil-like material—compounds likely to be encountered as contaminants in a manufacturing facility.

Experimental

System Components

The components of this system, an oven, a photoionization detector (PID), and traps were arranged in series such that materials volatilized in the oven could be carried through a vapor transport tube, past the PID and into the solvent-filled traps for recovery. A small aluminum oven, equipped with a removable tray in the oven compartment, was designed and built as described in section Task 1.4. It was connected to a stainless steel bellows, 0.95 cm in diameter and 90 cm long, that functions as a transfer line for volatilized compounds. Subsequently the bellows was replaced by a 3 mm stainless steel tube lined with quartz. This tubing had an ID of 1 mm and is quite flexible. An HNu Corporation photoionization detector with a 10.2 eV ultraviolet lamp was connected to the other end of the stainless steel bellows. The exit port of the photoionization detector was equipped with Swagelok® fittings to allow for gas-tight connection to the traps. The traps, made from glass and modified with metal inlet and outlet tubes, were also equipped with Swagelok fittings. Two traps were placed in series. A carbon-filled trap was attached to the exit port of the terminal solvent trap using Tygon tubing and the other end of the carbon trap was similarly connected to a vacuum pump. The vacuum pump was equipped with a calibrated rotameter that allowed adjustment and measurement of the air flow through the entire system. Fluke readout thermometers equipped with type K thermocouples were connected to the oven, the bellows transfer line, and the PID. Omega temperature controllers were used to maintain set temperatures.

Materials

All reagents except anthraquinone were used as received. Anthracene, anthraquinone, phenyldecane, and phenyldodecane were obtained from Aldrich Chemical Co., Inc. 2,4,5-trichlorobiphenyl was obtained from Accustandard, Inc. Anthraquinone was sublimed in an oil bath heated to 160°C under a vacuum of 1 torr. Pesticide grade solvents (methylene

® Swagelok is a trademark of Swagelok Co., Solon, OH.

chloride and acetone) were used. Solutions of the model compounds were prepared in methylene chloride. Ultrapure nitrogen (Air Products, 99.9993%) was used as the blow down gas in the Turbo-Vap® assembly. All glassware was washed with detergent, rinsed with tap water, and then rinsed several times with deionized water. A final acetone rinse followed the deionized water rinse steps. The glassware was dried in a 104°C forced air oven for at least 30 min prior to use.

In a typical experiment, the equipment was assembled and brought to temperature using the thermal controllers. The oven tray was removed from the oven to keep it at room temperature. The traps were each filled with approximately 20 mL of methylene chloride, and were attached to the system and cooled in a dry ice-isopropyl alcohol bath. The vacuum pump was started and the rotameter was adjusted to give the desired airflow. The compound of interest was placed in an aluminum pan (made for use in differential scanning calorimetry [DSC] work) in the following manner. A solution of the compound was made up in methylene chloride generally on the order of 1 μg/μL in concentration. From 10 to 40 μL of solution was transferred to the aluminum pan using a Gilson Microman positive displacement pipettor. The methylene chloride was allowed to evaporate, leaving the contaminant behind. The pans were made up an hour or less before use and were not used if more than one hour old, in case some material might be lost through evaporation or sublimation. The contaminant-loaded pan was placed into the oven tray (at <30°C); the strip chart recorder connected to the PID was started and zeroed; and the tray was inserted into the oven. The response of the PID was logged on the chart recorder. After several minutes, the tray was removed and the section connecting the PID exit port to the traps (an unheated zone where contaminant might condense) was heated with a heat gun. The traps were then removed, the methylene chloride from each trap was poured into a separate Turbo-Vap tube, and the traps were rinsed four times with methylene chloride, making sure that the methylene chloride rinse material contacted all of the interior surfaces of the traps. These rinsings were added to the Turbo-Vap tubes. A Turbo-Vap unit from Zymark, Inc. was used to concentrate the solvents prior to gas chromatographic (GC) analysis. Solutions were blown down to the optical end point of 0.5 mL. The sides of the Turbo-Vap tube were rinsed with 3 mL of methylene chloride after the initial volume reduction. The material in the tube was blown down again to a volume of 0.5 mL and the sides of the tubes were rinsed with two mL of methylene chloride. After another volume reduction to 0.5 mL, a final rinse was done with 1 mL of solvent and the volume was reduced to 0.5 mL. A known amount of an accurately prepared internal standard solution was added, and the resulting solution was analyzed by GC [Shimadzu GC equipped with a flame ionization detector and DB-5 (J&W,5% phenyl 95% dimethylsiloxane, 30 meter) column, He carrier gas, split mode (ratio approximately 1 to 50), isothermal, 210°C]. A CR4A data handler (Shimadzu Instruments) was used to collect and integrate data.

® Turbo-Vap is a trademark of Zymark, Corp., Hopkinton, MA.

Blanks, made by dispensing 20 µL of methylene chloride into a DSC pan and allowing it to evaporate, were run before and after each series of runs. One blank was run for every three contaminant runs.

Results and Discussion

The volatilization and trapping of three model compounds have been studied at three loadings and three flow rates. One purpose of the experiments was to determine whether the photoionization detector (PID) was sensitive enough to act in the capacity of a quick-look detector for the RSSAR system. The goal is to be able to detect 1 µg of each of the model contaminants. A second purpose was to determine how efficiently samples volatilized in the bulk sampler oven could be recovered after passing through the sample transport tube. A third purpose was to determine the effect of air flow rate on sampling efficiency.

The model compounds were chosen to represent contaminants likely to be found in contaminated industrial sites. Phenyldodecane was chosen as a model for an aryl-alkyl oil. We chose 2,4,5-trichlorobiphenyl to represent a simple Aroclor mixture. Anthracene was chosen to represent a typical polynuclear aromatic hydrocarbon. The results for each compound will be discussed separately.

2,4,5-Trichlorobiphenyl

The PCB model compound was volatilized in an oven at 250°C. Flow rates of 0.4, 2, and 4 standard cubic feet per hour (SCFH) were examined. The results are shown in Table 11. The table shows the results for runs involving 0, 10.3, 20.6, and 41.2 µg of 2,4,5-Trichlorobiphenyl. The results from three separate analyses of each trap are included. Significant levels of blow-by were observed, where material was swept past trap one and into trap two, which occurred at high flow rates and loadings. At least one blank was run at each flow rate (Runs 1, 6, 10, 11 and 15). At no time was any carryover from a run to a blank observed.

The PID was very capable of detecting 1 µg of this compound. The response of the PID was determined to be fairly linear over the range tested. Doubling the concentration of the model contaminant doubled the signal. The response of the PID to 10.3 micrograms of 2,4,5-trichlorobiphenyl is shown in Figure 33. The analyte signal is essentially complete after four minutes. Taking into account the large signal-to-noise ratio of the PID response, it is clear that quantities much smaller than one microgram of this material can be detected with the bulk sampling oven system.

The best flow rate, as measured by sampling efficiency [(total weight of compound detected in both traps/weight of compound placed in aluminum pan) × 100] was 2 SCFH. The sampling efficiency was lower at both lower and higher flows.

In general, sampling efficiency was lower than was hoped for. Subsequently, in work for Task 1.5.3, Sample Trapping Efficiency, we found the primary cause for the low sampling efficiency obtained in this task: a leak in the PID gauge which caused intermittent gross changes in the flow through the sampling oven, substituting unexposed air.

Apparently OH and atomic O radicals generated by the UV lamp from moist air caused chemical breakdown of the elastomeric gasket in the PID exposure chamber. As a result, the flow rates and collection efficiencies quoted herein are not accurate. A different gasket material must be chosen for extended operation of the PID in moist air..

Table 11. 2,4,5-Trichlorobiphenyl Sampling Efficiency Results

Run	Trap	Flow Rate (scfh)	2,4,5-TCB Analysis 1 (micrograms)	2,4,5-TCB Analysis 2 (micrograms)	2,4,5-TCB Analysis 3 (micrograms)	Average	Sample Weight (micrograms)	Sampling Efficiency (%)
1	1	2	0.0	0.0	0.0	0.0	0.0	NA
1	2		0.0	0.0	0.0	0.0		
2	1	2	3.1	2.9	3.0	3.0	10.3	39
2	2		1.0	1.0	1.1	1.0		
3	1	2	5.8	5.8	5.8	5.8	20.6	38
3	2		2.0	1.9	1.9	1.9		
4	1	2	16.0	15.2	16.5	15.9	41.2	49
4	2		4.7	4.3	4.2	4.4		
6	1	4	0.0	0.0	0.0	0.0	0.0	NA
6	2		0.0	0.0	0.0	0.0		
7	1	4	0.7	0.8	0.7	0.7	10.3	7
7	2		0.0	0.0	0.0	0.0		
8	1	4	1.4	1.5	1.5	1.5	20.6	7
8	2		0.0	0.0	0.0	0.0		
9	1	4	6.8	6.9	6.6	6.8	41.2	16
9	2		0.0	0.0	0.0	0.0		
10	1	4	0.0	0.0	0.0	0.0	0.0	NA
10	2		0.0	0.0	0.0	0.0		
11	1	0.4	0.0	0.0	0.0	0.0	0.0	NA
11	2		0.0	0.0	0.0	0.0		
12	1	0.4	0.0	0.0	0.0	0.0	10.3	0
12	2		0.0	0.0	0.0	0.0		
14	1	0.4	0.0	0.0	0.0	0.0	20.6	0
14	2		0.0	0.0	0.0	0.0		
15	1	0.4	0.0	0.0	0.0	0.0	0.0	NA
15	2		0.0	0.0	0.0	0.0		
16	1	0.4	4.8	4.8	4.8	4.8	41.2	12
16	2		0.0	0.0	0.0	0.0		

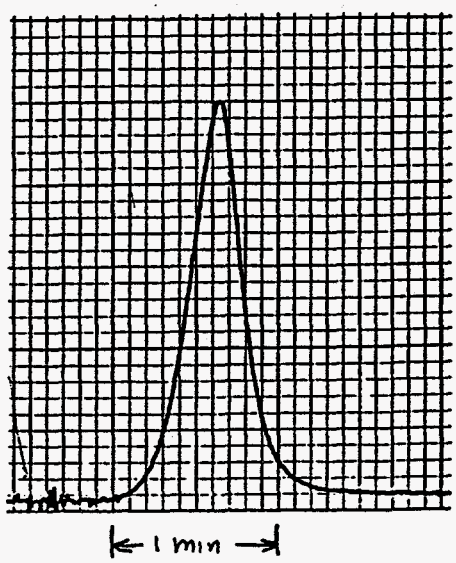

Figure 33. Photoionization gauge response for 10.3 µg of Trichlorobiphenyl evaporated from a microsample pan into a 2.5 SCFH air flow by the bulk sampler head.

Phenyldodecane

Phenyldodecane is a fairly volatile compound. It is a liquid with a boiling point of 179-180°C at 13 torr. It was noted that if phenyldodecane samples were allowed to stand for extended periods of time, significant evaporation occurred. For this reason, phenyldodecane samples were placed in the aluminum DSC pans less than one hour before use. In spite of this volatility, the sampling efficiency was low. The reason for low sampling efficiency is discussed in the previous section on trichlorobiphenyl (Table 12). Normal flow rates of 0.1, 0.2-0.3, and 0.4 SCFH were used. Sample loadings of 0, 10.1, 20.3, and 40.5 were used. The higher the flow, and the higher the sample loading, the better the sampling efficiency. No sample blow-by was observed using phenyldodecane because no phenyldodecane was seen in trap number two for any of the phenyldodecane trials.

The photoionization detector was easily capable of detecting a 1 µg change of phenyldodecane under all the sampling conditions. Taking into account the linearity and signal-to-noise, we estimated a minimum detectability of 0.1 µg under these conditions.

Anthracene

Anthracene is a semivolatile solid with melting a point of 216 to 218°C. The results from the sampling process were complicated by an oxidation reaction that was found to occur. The results are shown in Table 13. When anthracene was volatilized and trapped, anthraquinone was found to be the major product.

Table 12. Phenyldodecane Sampling Efficiency Results

Run	Trap	Flow Rate (scfh)	Phdodecane Analysis 1 (micrograms)	Phdodecane Analysis 2 (micrograms)	Phdodecane Analysis 3 (micrograms)	Average	Sample Weight (micrograms)	Sampling Efficiency (%)
1	1	0.4	0.0	0.0	0.0	0.0	0.0	NA
1	2		0.0	0.0	0.0	0.0		
2	1	0.4	0.0	0.0	0.0	0.0	10.1	0
2	2		0.0	0.0	0.0	0.0		
3	1	0.4	1.5	1.5	1.5	1.5	20.3	7
3	2		0.0	0.0	0.0	0.0		
4	1	0.4	8.2	7.8	7.5	7.9	40.5	20
4	2		0.2	0.0	0.2	0.1		
5	1	0.4	0.0	0.0	0.0	0.0	0.0	NA
5	2		0.0	0.0	0.0	0.0		
6	1	0.2-0.3	0.0	0.0	0.0	0.0	10.1	0
6	2		#	#	#	#		
7	1	0.2-0.3	1.4	1.5	1.5	1.5	20.3	7
7	2		0.0	0.0	0.0	0.0		
8	1	0.2-0.3	6.8	6.9	6.6	6.8	40.5	17
8	2		0.0	0.0	0.0	0.0		
9	1	0.2-0.3	0.0	0.0	0.0	0.0	0.0	NA
9	2		0.0	0.0	0.0	0.0		
10	1	0.2-0.3	0.5	0.5	0.5	0.5	20.3	2
10	2		0.0	0.0	0.0	0.0		
11	1	0.2-0.3	0.0	0.0	0.0	0.0	10.1	0
11	2		0.0	0.0	0.0	0.0		
15	1	0.1	0.1	0.0	0.0	0.0	10.1	0
15	2		0.0	0.0	0.0	0.0		
16	1	0.1	0.3	0.3	0.3	0.3	20.3	2
16	2		0.0	0.1	0.1	0.0		
17	1	0.1	1.2	0.9	0.8	0.9	40.5	2
17	2		0.0	0.0	0.1	0.0		
18	1	0.1	0.0	0.0	0.0	0.0	0.0	NA
18	2		0.0	0.0	0.0	0.0		
# Trap broken during experiment								

Table 13. Anthracene Sampling Efficiency Results

Run	Trap	Flow Rate (scfh)	Anthracene Analysis 1 (micrograms)	Anthracene Analysis 2 (micrograms)	Anthracene Analysis 3 (micrograms)	Average	Anthraquinone Analysis 1 (micrograms)	Anthraquinone Analysis 2 (micrograms)	Anthraquinone Analysis 3 (micrograms)	Average	Sample Weight (micrograms)	Sampling Efficiency %
1	1	0.4	0.0	0.0	0.0	0.0	2.4	2.4	2.2	2.3	11.4	18
1	2		0.0	NA	NA	0.0	0.0	NA	NA	0.0		
2	1	0.4	0.0	NA	NA	0.0	0.0	NA	NA	0.0	0.0	NA
2	2		0.0	NA	NA	0.0	0.0	NA	NA	0.0		
3	1	0.4	0.0	0.0	0.0	0.0	8.7	9.0	8.6	8.8	22.8	33
3	2		0.0	NA	NA	0.0	0.0	NA	NA	0.0		
4	1	0.4	3.9	3.7	3.6	3.7	17.8	17.1	16.9	17.3	45.6	41
5	1	0.4	0.0	NA	NA	0.0	0.0	NA	NA	0.0	0.0	NA
5	2		0.0	NA	NA	0.0	0.0	NA	NA	0.0		
6	1	0.2-0.3	0.0	0.0	0.0	0.0	2.1	2.2	2.3	2.2	11.4	17
6	2		0.0	NA	NA	0.0	0.0	NA	NA	0.0		
7	1	0.2-0.3	0.0	0.0	0.0	0.0	4.9	4.7	4.8	4.8	22.8	18
7	2		0.0	NA	NA	0.0	0.0	NA	NA	0.0		
8	1	0.2-0.3	0.0	0.0	0.0	0.0	12.1	12.0	11.7	11.9	45.6	22
8	2		0.0	NA	NA	0.0	0.0	NA	NA	0.0		
9	1	0.2-0.3	0.0	NA	NA	0.0	0.0	NA	NA	0.0	0.0	NA
9	2		0.0	NA	NA	0.0	0.0	NA	NA	0.0		
10	1	0.1	0.0	0.0	0.0	0.0	3.0	3.0	3.1	3.0	11.4	23
10	2		0.0	NA	NA	0.0	0.0	NA	NA	0.0		
11	1	0.1	0.0	0.0	0.0	0.0	4.3	4.1	4.0	4.1	22.8	16
11	2		0.0	NA	NA	0.0	0.0	NA	NA	0.0		
12	1	0.1	5.4	5.8	5.4	5.5	6.8	6.9	6.6	6.8	45.6	25
12	2		0.0	NA	NA	0.0	0.0	NA	NA	0.0		
13	1	0.1	0.1	0.2	NA	0.1	0.0	0.0	NA	0.0	0.0	NA
13	2		0.0	NA	NA	0.0	0.0	NA	NA	0.0		
14	1	0.4	18.5	18.4	18.3	18.4	10.7	10.7	10.6	10.7	45.6	60
14	2		0.0	NA	NA	0.0	0.0	NA	NA	0.0		
15	1	0.4	0.0	0.0	NA	0.0	3.4	3.5	NA	3.4	22.8	13
15	2	(no PID)	0.0	NA	NA	0.0	0.0	NA	NA	0.0		

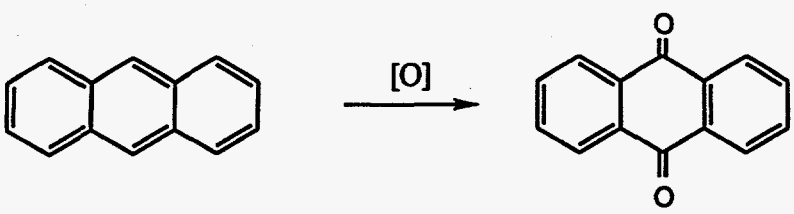

This oxidation appears to be fairly rapid, and only at high loadings (runs 4,12 and 14) is any anthracene detected in the traps. Traces of other products were seen in the chromatograms, but were present in too small a quantity to be identified. Flow rates of 0.1, 0.2-0.3, and 0.4 were examined. Loadings of 0, 11.4, 22.8, and 45.6 micrograms were used. The sampling efficiencies were calculated by determining the conversion to anthraquinone and by summing the anthraquinone yield and anthracene yield where appropriate. Once again, the sampling efficiency was lower than hoped for and ranged from 16% to 60%. Sampling efficiency was higher at the higher loading levels and generally higher with higher flow rate. An experiment was done showing that sample loss during the blow-down process was less than 5%. Sampling efficiencies were reduced by the PID leak discussed previously. Nevertheless, the photoionization detector was easily capable of detecting 10 μg of anthracene under the range of sampling conditions examined. Again, PID response was linear. Based upon this linear response and the signal-to-noise provided by a loading of 10.0 micrograms, as shown in Figure 32, we estimate a minimum detectability of 200 nanograms in this system. The actual minimum could be substantially lower because of the PID leak discussed previously.

Conclusions and Recommendations

The bulk sampling oven has been used to volatilize three model contaminants. A number of conclusions have been reached.

- The sensitivity of the photoionization detector has been shown to be very adequate to detect these materials at levels of interest in surface sampling applications. The response is rapid and linear.
- Sample trapping efficiencies are lower than hoped for. However, subsequent to the work on this task, in Task 1.5.3, we discovered the reason for this problem. A large leak had developed around an internal gasket in the PID reaction chambers, causing clean air to be pulled through the traps in place of most of the analyte laden air.
- Sample trapping efficiencies were affected by the loading of the contaminant and by the flow rate used during sampling. However, these levels reflected the PID leak and so were not correct in an absolute sense. More accurate flow rate results and much higher trapping efficiencies were obtained and are reported under Task 1.5.3.

Task 1.5.2 Near Vacuum UV Quick-Look Detector

The UV absorption spectra of PCB congeners and polyaromatic hydrocarbons (PAHs) in vapor form have strong absorption bands in the 180-220 nm region. In the case of PCBs, the very limited existing literature describes this feature as the "main" band [8]. We refer to this spectral region as the near vacuum ultraviolet (NVUV) region, since the region between 100 and 180 nm is often described as the vacuum UV (VUV). Measurement of absorption in the NVUV band has the potential for quick identification of a likelihood of PCB or PAH presence at actionable levels, since the NVUV absorption is much stronger per molecule for these species than that for many relatively benign species likely to be co-present in a sample. In particular, our measurements indicate that the molar extinction coefficient ratio between PCBs and water vapor at 200 nm is over 10^8. Therefore, it is possible to detect low concentrations of PCBs in vapors thermally desorbed from samples containing large amounts of water, such as concrete. Furthermore, the UV absorption band can be chosen such that the absorption per gram of PCB volatilized into a container is nearly independent of the PCB mixture, or such that it is approximately proportional to the chlorine content. Thus, a quick-look application based on NVUV absorption can be tailored to the environmental action definition.

Experimental Technique

In work primarily accomplished prior to the awarding of this contract, we measured UV absorption spectra for a number of PCB congeners, Aroclor mixtures, and other species. Relative spectra were obtained by measuring the absorption through a heated cell as a function of temperature. Absolute absorption spectra were obtained by carefully weighing a small amount of a sample introduced into a cell of known volume and then measuring the transmission as a function of wavelength. The sample weight was chosen such that we expected complete vaporization. Ultraviolet radiation from a deuterium arc source was passed through the cell and then was focused on a 1/4-meter spectrometer. A multichannel detector (EG&G PARC model 1460) was used to obtain the entire spectrum simultaneously, generally from 180 to 240 nm, with a spectrometer slit function with 0.3 nm full width at half maximum. We determined that the derived extinction coefficients as a function of wavelength were nearly independent of vapor pressure, which is characteristic of a smooth intrinsic wavelength dependence (as opposed to a resolvable line spectrum).

In work supported by this contract, in order to demonstrate quick-look measurements with the concrete and bulk sampler heads, we constructed a 25-cm absorption cell constructed of glass with quartz end windows. The interior absorption length of this cell is 24 cm. The configuration of the cell and associated optics is shown in Figure 34. The cell was interconnected with the bulk sampling oven and PID quick look detector as shown in Figure 35. A similar configuration is being used to obtain signals from the concrete sampler head.

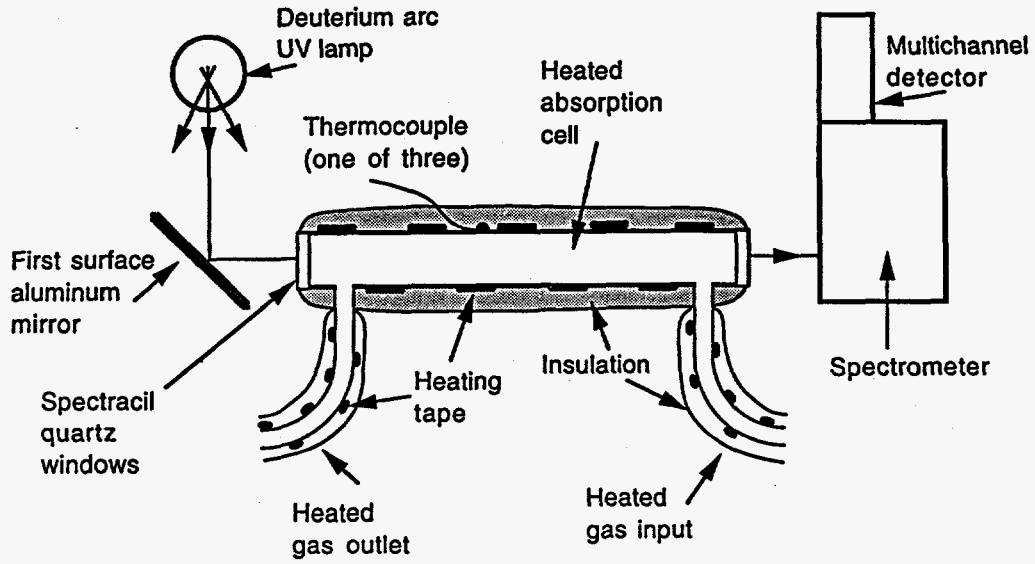

Figure 34. NVUV absorption quick look detector system.

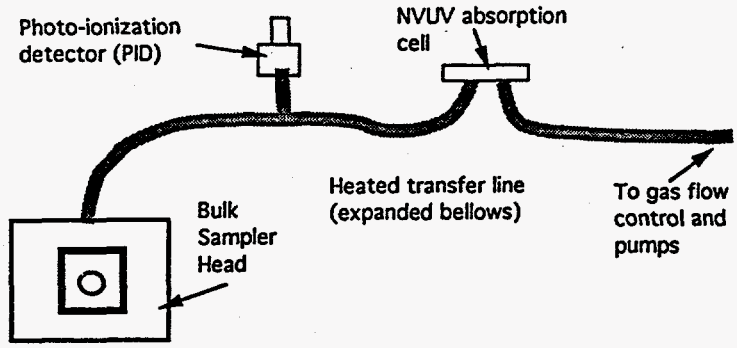

Figure 35. Interconnection of bulk sampler head, photoionization detector and NVUV absorption cell.

More accurate determinations of absolute molar extinction coefficients will be obtained using the equipment illustrated in Figure 36. In this case, two high-temperature capacitance pressure gauges are included inside the oven to determine vapor pressure directly. This configuration avoids the necessity for measuring very small amounts of analyte into the cell, and also avoids the need for assuming that complete vaporization occurs.

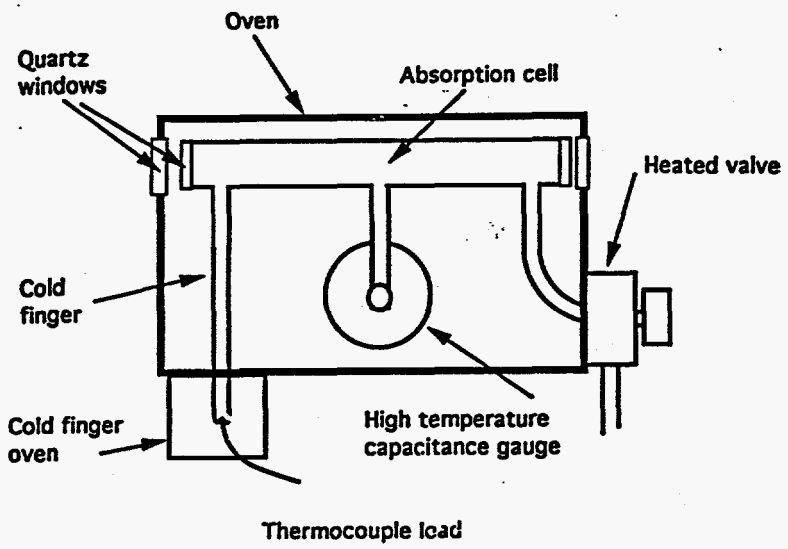

Figure 36. Experimental configuration to determine molar extinction spectra for PCBs and other semivolatile species.

Results

In Table 14 we show absolute peak molar extinction coefficients for a substantial number of PCBs and other species, measured by GE in work prior to this contract, and by others. The molar extinction coefficient $\varepsilon(\lambda)$ is a standard spectroscopic function [9] describing the transmission $T(\lambda)$ of monochromatic light at wavelength λ through a pathlength L of a species at molar concentration ρ moles/liter. When, as in our case, $T(\lambda)$, L and ρ are measured, $\varepsilon(\lambda)$ is calculated from the equation

$$T(l)=10^{-\rho L\varepsilon(\lambda)} \qquad (15)$$

Many of the spectra presented by other investigators were obtained from liquid solutions of the analyte in a solvent, but the results are not much different than the vapor spectra.

The proof-of principle experiments with the bulk sampler head, the photo-ionization detector (PID), and 25-cm UV absorption cell allowed clear observation of analyte amounts as small as 10 μg. Solutions of the chosen analytes were made using pesticide grade methylene chloride. The solution concentrations were on the order of 1 μg/μL for phenyldodecane (base oil constituent), anthracene (base PAH), and for trichlorobiphenyl (PCB congener). In a typical experiment, a base UV spectrum was obtained first with no sample in the system. Then 10, 20, and 40 μL of the appropriate constituent was pipetted into 6-mm-diameter aluminum dishes and allowed to dry for a maximum of 15 minutes prior to placement into the bulk sampling oven. With the flow rate set to 0.4 SCFH, the sample was introduced into the bulk sampling oven. The PID indicates the onset and

Table 14

Peak molar extinction, location of the peak, and its full width at halfmaximum for some selected species including major species found in oils and PCBs. The peaks shown here are those closest to 200 nm wavelength. The fact that so many of the important components have comparable extinctions makes ultraviolet absorption in the 200 nm range a good candidate for a quick-look detector. The molar extinction is equal to the absorbance divided by the product of the concentration, in moles per liter, times the path length.

Species/Reference/Solvent	Molar Extinction	Peak Wavelength	Peak Width (FWHM)
BENZENE*[1]HEPTANE	4.6E+04	184	23
TOLUENE[1]HEPTANE	5.5E+04	189	24
XYLENES*[1]HEPTANE	6-7E+04	190-193	22
ACETONE[2]VAPOR	3.0E+03	194	4
ETHYLENE[2]VAPOR	1.0E+04	190	15
ACETYLENE[2]VAPOR	6.0E+03	180	14
INDANE*[4]ETOH	5.0E+03	201	NA
INDENES*[7]ETOH	1.7E+04	225	NA
NAPTHALENE*[2]ETHER	1.1E+04	208	20
ANTHRACENE*[6]HEXANE	1.1E+04	217	21
ACENAPHTHALINES*/8/PENTANE	1.6E+04	210	NA
DIPHENYL#[3]HEXANE	4.4E+04	202	40
2,4 CHLOROBIPHENYL#[3]HEXANE	4.2E+04	204	37
2,4 CHLOROBIPHENYL#[5]VAPOR	3.9E+04	185	25
25-2 CHLOROBIPHENYL#[3]HEXANE	6.3E+04	197	28
25-2 CHLOROBIPHENYL#[5]VAPOR	3.9E+04	180	28
25-25 CHLOROBIPHENYL#[3]HEXANE	6.3E+04	204	39
236-25 CHLOROBIPHENYL#[3]HEXANE	1.1E+05	217	30
236-25 CHLOROBIPHENYL#[5]VAPOR	6.3E+04	190	40

References (Note: The references refer to Table 9 only.)

[1] J.R. Platt and H.B. Klevans, Rev. Mod. Phys.16, 202 (1944)
[2] E.A. Braude, Ann. Repts., Chem. Soc. 42, 105 (1945)
[3] James D. MacNeil, Stephen Safe, Otto Hutzinger, Bull. Environ. Cont. and Tox. 15, 1,Springer-Verlag (1976)
[4] L. McElwee-White and D.A. Dougherty, J. Am. Chem. Soc. 106, 98 (1984)
[5] C.M. Penney and A. Ortiz, Jr., GE Internal Report
[6] N. Quast and N. Jehon, Anal. Chem., Leibigs (1984)
[7] H. Siegal, Chem. Berichte 118 (1985)
[8] O. Schweikert, Chem. Berichte 117 (1984)

* Major constituent in many oils
# PCB

time dependence of vapor emission qualitatively as a function of time, as shown in Figure 33. Complete UV spectra were obtained from the NVUV system at 20-second intervals. Spectra were acquired in 10 seconds and transferred to disk in 8 seconds. Although this process could have been accelerated to one spectrum each 10 seconds, we found that the 20 second rate provided adequate time resolution. The UV transmission spectra could be seen changing as the analyte concentration in the UV cell increased. Other flow rates used were 1.0 and 2.0 SCFH.

Figure 37 shows the UV transmission vs. wavelength at maximum analyte absorption for 20.26 μg of phenyldodecane evaporated into a 1 SCFH air stream. The corresponding absorption is shown in Figure 38. Figures 39, and 40 show the UV transmission and absorption respectively for 13.2 μg of anthracene in a 1 SCFH air stream. Figures 41 and 42 show the UV transmission and absorption respectively for 10.3 μg of trichlorobiphenyl. Phenyldodecane, anthracene, and trichlorobiphenyl show distinctly different spectral peaks and other features, allowing some degree of specificity identification in a simple system.

Conclusions

The experimental results demonstrate clearly that minimum actionable levels of PCBs, defined for wipe sampling, are measurable with a conveniently sized NVUV absorption system. Sensitivity to oil and solvent surrogates is lower, which is desirable under expected circumstances, where PCBs are expected to be encountered with oils. Our work to date supports an expectation that a NVUV absorption quick-look system can provide a highly useful indication of the probability of actionably contaminated samples. Further work will provide more accurate absolute extinction coefficients for many of the species we expect to encounter in sampling applications. These data will support certification of this technique.

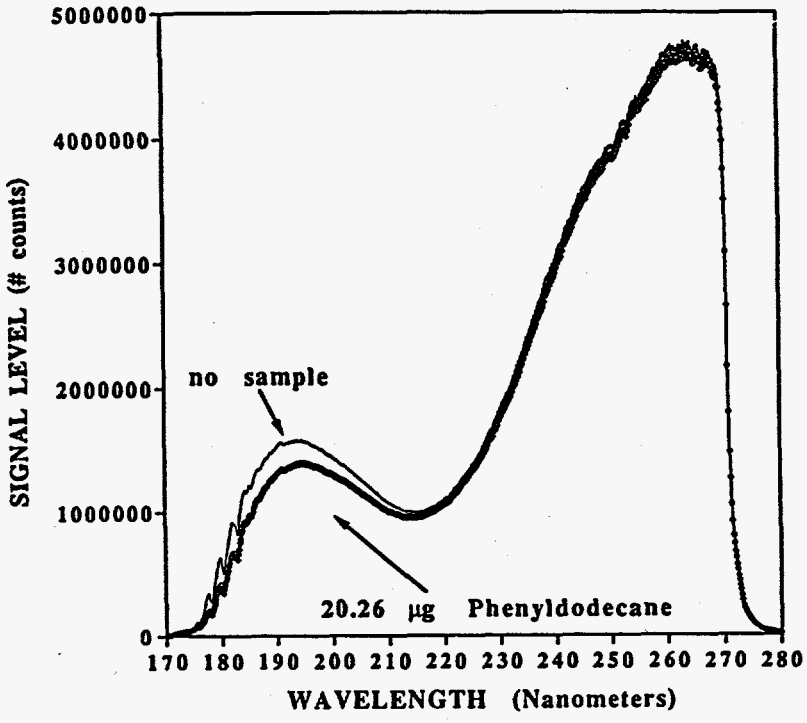

Figure 37. UV Transmission vs. wavelength for 20.26 µg phenyldodecane in a 1 SCFH sir stream.

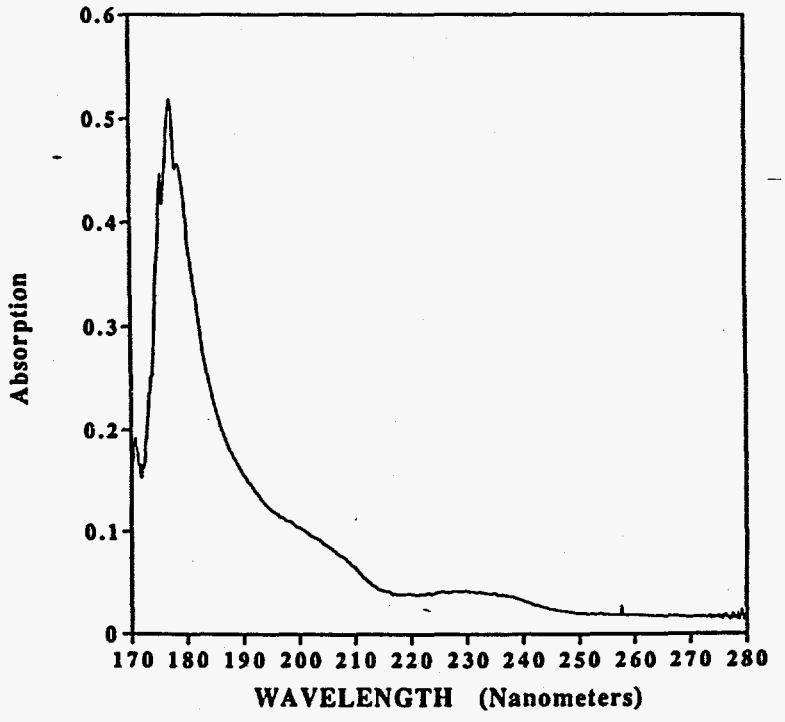

Figure 38. Absorption vs. wavelength for 20.26 µg phenyldodecane in a 1 SCFH air stream.

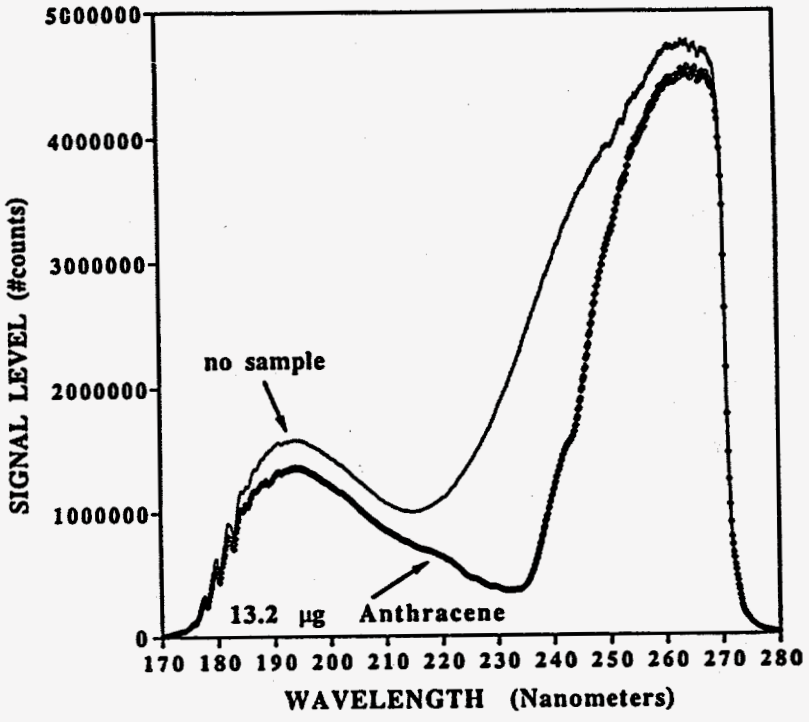

Figure 39. UV Transmission vs. wavelength for 13.2 µg anthracene in a 1 SCFH air stream.

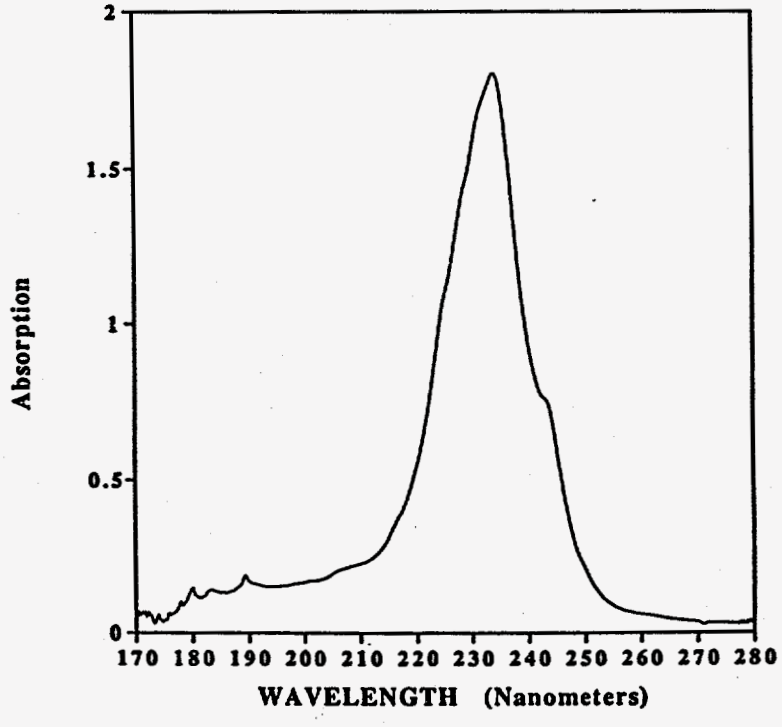

Figure 40. Absorption vs. wavelength for 13.2 mg anthracene in a 1 SCFH air stream.

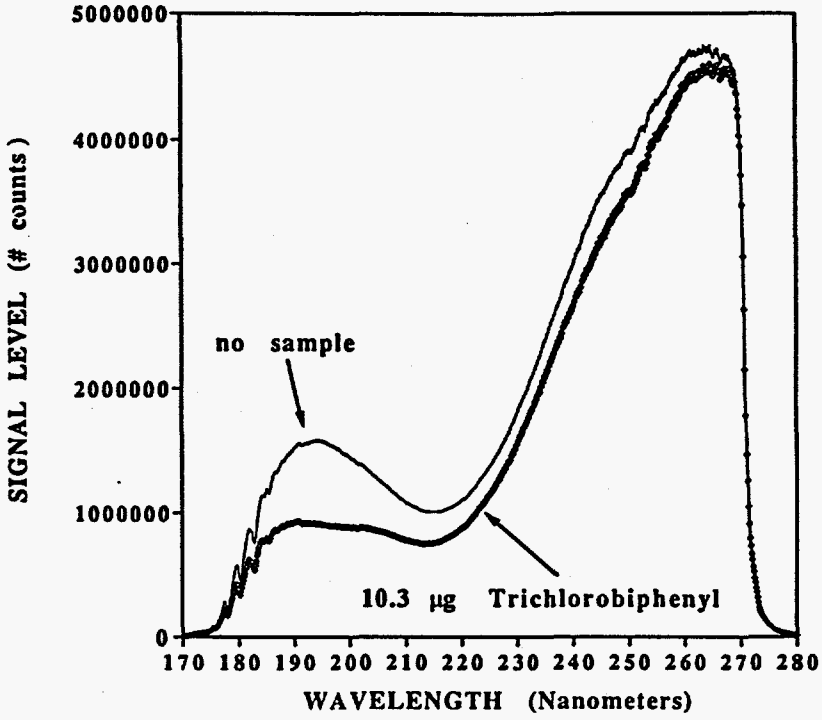

Figure 41. UV transmission vs. wavelength for 10.3 µg trichlorobiphenyl in a 1.0 SCFH air stream.

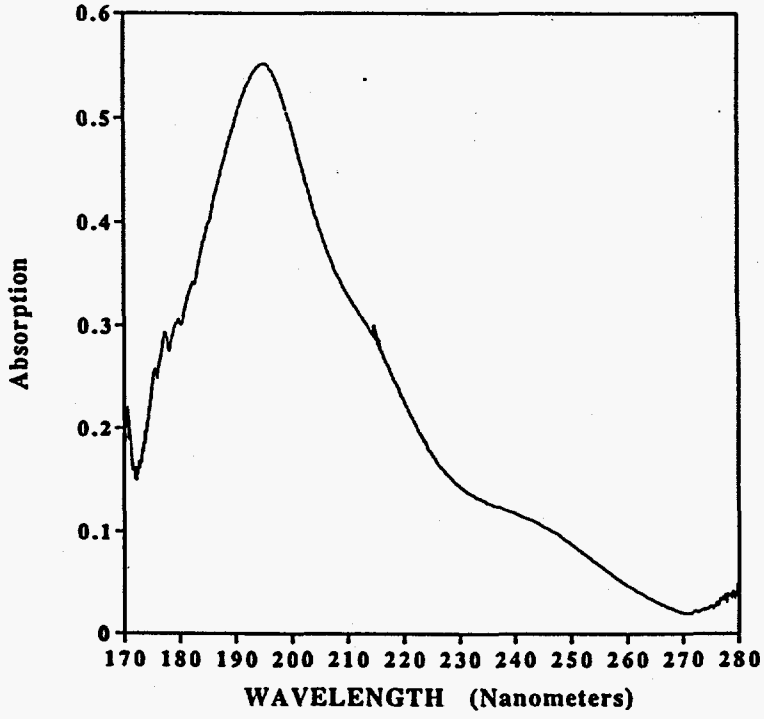

Figure 42. Absorption vs. wavelength for 10.3 mg trichlorobiphenyl in a 1 SCFH air stream.

Task 1.5.3 Trapping Efficiency

A key component of the RSSAR System is the sample trapping module that holds a cassette of sampling tubes containing solid phase sorbent materials. It is the material in these tubes that traps the thermally desorbed contaminants and effectively archives them in a convenient form suitable for later analysis.

The sorbents must have properties suitable to the sampling task at hand. They must be able to efficiently trap the contaminants from a vapor stream that might initially be at high temperature and that might contain high levels of water vapor. These sorbents must be able to efficiently release the contaminants by a secondary thermal desorption step in a manner allowing them to be analyzed and quantified. In addition, they must possess the requisite thermal and oxidative stability to retain their physical integrity. Figure 43 shows a pictorial representation of the sample trapping process.

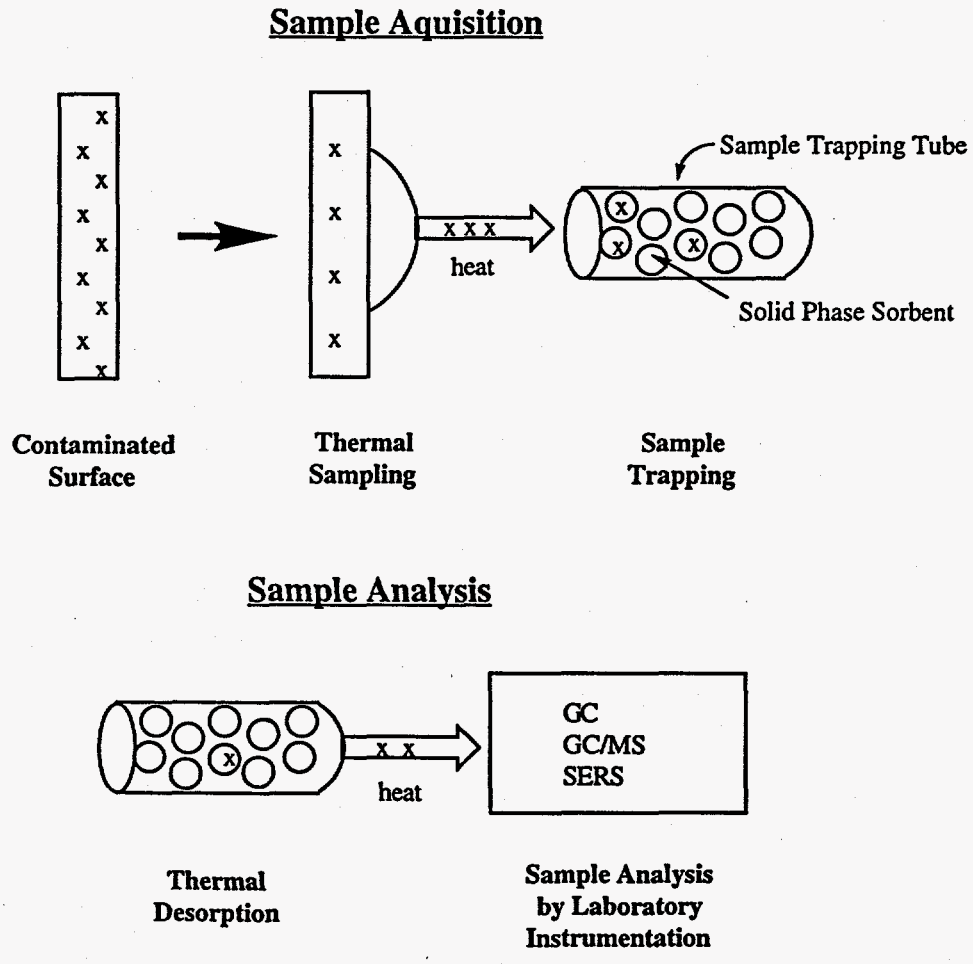

Figure 43. Sample trapping using solid phase sorbent tubes.

A large body of literature describes the technology associated with solid-phase sorbents, including their use in scrubbing contaminants from gas streams [10 through 17]. Some work in this area has been done by GE-CRD under a US DOE contract [18]. Rather than experiment further with new materials for this application, Task 1.5.3 involved testing several commercially available solid-phase sorbents under a variety of experimental conditions to identify materials and conditions suitable for use with the RSSAR system.

Some of the important parameters which were examined in order to optimize the trapping efficiency included

- testing a variety of the sorbent materials
- examining the effect of vapor flow rate
- determining the effect of added water
- selecting the best location for cooling/condensing the sample

Experimental Methods

Five different commercially available sorbents were examined for their ability to trap anthracene, 2,4,5-trichlorobiphenyl, and phenyldodecane from a vapor stream. They are Carbopack™ B and C (graphitized carbon black), Supelpak-2™ (a modified amberlite XAD-2 resin), Tenax-GR™ (a graphitized diphenyl polyphenylene oxide), and Carbotrap 370™, a mixed bed tube containing Carbopack™ sorbents F, C and B. Each has been chosen based on manufacturer recommendations for the trapping of semivolatile compounds. A methylene chloride solution of the three components was used to deposit the materials onto an aluminum pan. After the solvent evaporated the aluminum pan was then inserted into the bulk sampling oven which was maintained at 250°C. The air flow rate drawn from the bulk sampling oven through the sorbent tube was 60 ml/min.

Results

Initial problems were encountered with respect to recovery of a satisfactory fraction (>70%) of contaminants through the bulk sampling oven, as described in the section on Task 1.5.1. These difficulties were traced to recirculating flow paths in the sampling oven, background hydrocarbon chemical emissions from insulation, chemical reactions catalyzed by metals in the sample transfer tubes, an air leak through the seals in the photoionization detector (PID) and excessive flows through the sorbent tubes. The transfer tube and connectors were replaced by glass-lined tubes, and reinsulated by quartz fiber held in place by aluminum foil, involving a rebuild of much of the hot transfer system. In addition, the bulk sampling oven was redesigned to improve vapor removal, and air flows were split to reduce flow rates through the sorbent tubes. These actions improved collection fractions to the point where leakage through the PID accounted for remaining difficulties. Since the PID and UV cells have already been shown to be sufficiently sensitive to the model compounds, the PID was removed from the system for subsequent tests under this task.

™ Carbopack B, C, F, Supelpak-2, and Carbotrap 370 are trademarks of Supelco, Inc.
™ Tenax-GR is a trademark of Altech, Inc.

Results from subsequent trapping experiments which were carried out with the bulk sampling oven connected to a sorbent tube containing Carbotrap 370 indicated that we can efficiently trap volatilized compounds. With this configuration, trapping efficiencies, corrected using the internal analytical standard, ranged from 77.8 to effectively 100% as shown in Table 15. Small amounts of anthraquinone, an oxidation product of anthracene,were also detected in the analysis. Other sorbents were less effective in trapping the model contaminants.

In a separate series of trials, the effect of water vapor on sorbent trapping efficiency was examined. For these experiments, ten milligrams of water was placed in a separate aluminum pan. Condensation of the water vapor on the sorbent tube was observed. Carbotrap 370 was efficient (85-100%) at trapping the anthracene, phenyldodecane, 2,4,5-trichlorobiphenyl. Three of the sorbents examined (Tenax GR, Carbopack B, Carbopack C were even less effective at trapping the analytes of interest in the presence of water vapor. XAD-2 gave highly variable trapping results (Table 16).

In additional duplicate trials, 10 μg of Aroclor 1242 and 10 μg of transformer oil were volatilized in the bulk sampling oven assembly and trapped on Carbotrap 370 . Using the thermal desorption unit, the trapped Aroclor 1242 and oil were desorbed into a solution of hexane. The hexane was analyzed by GC-ECD. The ECD was not sensitive to the transformer oil. Thus, there was no interference from the transformer oil. The average trapping efficiency for the trials was 73.5 %.

The possibility of breakthrough must be considered because of its effect upon sampling efficiency and downstream contamination. This effect depends upon the analyte to sorbent mass ratio, among other factors. Typically, 100 mg of sorbent was packed into an 11 × 0.2 cm (ID) sorbent tube, and less than 100 micrograms of analytes were collected, such that the total analyte to sorbent ratio was on the order of 0.1% or smaller. In the literature, efficient trapping has been reported for analyte sorbent ratios as high as 10%, and in some cases, 50%. Thus our loading is well within general efficient trapping experience.

However, efficient trapping also depends upon chemical affinity and upon site competition between analytes, for example, and water vapor or oil. Therefore, we monitored for breakthrough in selected experiments by inserting a second sorbent tube, or a solvent trap, in series with the primary initial sorbent tube, and then comparing analyte concentrations in these back up traps with that in the primary trap.

When the less efficient sorbents (Tenax GR, Carbopack B, Carbotrap C, XAD-2) were used, significant breakthrough was observed, both in the presence and absence of water vapor. However, no detectable breakthrough was observed with the use of Carbopack 370, including the cases where water vapor was evaporated along with the analytes, and the experiment where Arochlor 1242 and transformer oil were trapped together. Based on these experiments this material is the most effective sorbent for use in the RSSAR system, among those tested, and exceeds Phase 1 performance requirements (>70% trapping efficiency) in all tested categories.

Table 15. Percent Recovered by Thermal Desorption[1]

Sorbent	load (µg)	Anthracene	245-TCB	Phenyldodecane
Carbotrap 370	10	77.8	86.1	78.7
Carbotrap 370	20	81.3	83.6	79.5
Carbotrap 370[2]	40	85.0	82.4	80.7
Carbotrap 370[2]	20	87.2	87.4	84.4
Carbotrap 370[2]	20	101	100	96.2
Tenax GR	10	79.2	80.1	81.3
Tenax GR	20	106.4	93.1	78.6
Tenax GR	40	55.8	70.8	65.3
Carbopack B	10	85.4	98	85.7
Carbopack B	20	91.7	91.6	81.9
Carbopack B	40	53.1	55.6	47
Carbopack C	10	47.8	81.8	51.9
Carbopack C	20	57.4	86.2	68.2
Carbopack C	40	10.3	85.9	11
XAD-2	10	1.5	0	0
XAD-2	20	89.6	88.9	85.8
XAD-2	40	51.4	50	50.7

[1]Average of two trials

[2]numbers obtained from one run

Table 16. Percent Recovered by Thermal Desorption[1]

Sorbent	load (μg)	water (mg)	Anthracene	245-TCB	Phenyldodecane
Carbotrap 370	10	10	92.5	103.5	99.7
Carbotrap 370	20	10	86.2	88.6	90.3
Carbotrap 370	40	10	83.9	89.3	85.1
Tenax GR	10	10	15.6	39.8	34
Carbopack B	10	10	4.7	19.6	10.3
Carbopack C	10	10	28.2	70.2	52.8
XAD-2	10	10	96.8	108	105

[1]Average of two trials

Task 1.5.4 Surface-Enhanced Raman Scattering (SERS) Analysis

Summary of Results

Key results are summarized here:

- Raman spectroscopy is capable of distinguishing individual congeners and Aroclor mixtures. Common to all the spectra is a large feature near 1600 cm^{-1}.
- Using SERS, we have demonstrated quantitative detection of tetrachlorobiphenyl on a pentachlorothiophenol (PCTP) coating. On this coating, a typical oil interference near the 1600 cm^{-1} PCB feature was not present. The SERS response was reasonably linear for samples ranging from 1 to 25 ppth tetrachlorobiphenyl in o-xylene (with 1% oil added). The amount of PCB in the sampled area ranged from 20 ng to 0.5 µg.

Introduction

The most commonly used technique for quantification of PCBs in environmental samples employs gas chromatography (GC), either alone or in combination with a mass spectrometer (GC/MS). While GC analysis provides legally defensible data and is the basis for several EPA-approved analytical methods, it suffers from a number of drawbacks. These difficulties are manifest in long measurement times, high per sample analysis costs, the need for expensive equipment, and requirements for highly trained operators and arise largely from the nature of the technique. The analysis task is exacerbated by the complexity of the PCB congener family that contains 209 members. The analysis is made still more challenging by alterations in the standard Aroclor congener distribution patterns, which result from the aging and weathering of the environmental matrices and from interfering substances commonly found in environmental samples. While advances in equipment and methodology are constantly being made, GC analysis methods present a bottleneck in optimization of large-scale site characterization that can be resolved only with considerable expense. Furthermore, in site decommissioning GC provides more information than is necessary, by analyzing which congeners are present in the sample. A method which yields a fast, reasonably accurate estimate of the total PCB present could provide a major cost advantage in determining whether a sample is over the action limit and what level of remediation or disposal is appropriate.

Task 1.5.4: SERS Analysis – represents an effort to find a PCB quantification technique that is much faster, much less expensive per measurement, and provides a reliable (and certifiable) total PCB quantification. Success in this effort, although not essential to the RSSAR system concept, would substantially enhance its performance. The SERS approach was chosen as one of the most promising available approaches to investigate because it has an adequate margin of sensitivity, and capabilities are developing for chemical-family-specific coatings applied over a SERS substrate that are expected to allow detection of the chemical family (e.g., PCBs) in relatively high concentrations of

other species (e.g., oils). In previous work at Detection Limit Technology, LC, Keith Carron developed a SERS technique that passivates SERS substrates against oxidative or corrosive deterioration. The technique involves the use of a coating that protects the silver, allowing multiple reuse of the substrate. Several coatings have been tested for their response to PCBs. The potential purposes of the coatings are threefold: (1) they stabilize the surface, (2) they may respond selectively to the analyte of interest, allowing better detection in the presence of interferences, and (3) they provide an internal standard that may be used for quantification.

A successful quantitative instrument must meet the following requirements:

1. The SERS signal from a suitable substrate gives a signal with adequate sensitivity, quantifiability, and specificity when exposed to various PCB mixtures in oil.
2. The signal properties are not compromised by the presence of other chemical species that may occur along with the PCB/oil samples.
3. The measurement technique is amenable to economic instrumentation.

Requirement No. 1 (above) was the subject of the Phase I research in Task 1.5.4. GE has subcontracted a major portion of this investigation to Keith Carron, a professor at the University of Wyoming and principal researcher at Detection Limit Technology, LC, because Dr. Carron heads an accomplished research program in selective SERS coatings.

Raman Scattering

Raman scattering is a technique whereby light within one narrow color band is directed onto, or into a substance, and that part of the light shifted in a scattering process to other color bands is observed. The distribution of these color bands provides detailed information about the molecular composition of the target, a characteristic that has made Raman scattering a favorite chemical analysis technique. The major problem with this technique is that Raman scattering is extremely weak; consequently, minor species are difficult to measure in the background of Raman scattering from major species and fluorescence. Surface-enhanced Raman scattering, discovered in the 1980's, provides a way to solve the weak signal problem. In this technique, the analyte is allowed to coat a surface that has been subjected to fine-scale roughening. The roughening process creates high curvature surface sites, which according to one prevalent hypothesis, enhance the electric field intensity of the incident *and* scattered light. As a result, the scattering per molecule can be increased by orders of magnitude (typically 10^4 to 10^8). Stable, selective coatings can be placed over this prepared surface. These coatings may allow the analyte to preferentially approach the surface, such that Raman scattering from the analyte can be increased relative to other species in the initial sample. Initial data from our subcontractor can be interpreted in terms of partitioning of PCBs from an oil solution into a SERS coating. This type of preferential partitioning would substantially enhance the use of SERS in this application. Thus the combination of SERS and selective coatings could provide a major improvement in both sensitivity and selectivity. The goal of this project

is to determine if surface-enhanced Raman spectroscopy (SERS) can detect and quantify PCBs and Aroclor mixtures in oil matrices. Identification of the congener set or Aroclor mixture at a particular site would be beneficial; however, it is more important to be able to reliably quantify how much PCB is present in a complex matrix. Other spectroscopy techniques such as absorption and fluorescence suffer severely from background signals because of the oil and other natural organic contaminants in the matrix. At least under some conditions SERS is known to preferentially excite Raman scattering over fluorescence and therefore might overcome some of the difficulties caused by the presence of the oil. Finally, SERS may be well suited for use with vapor samples, such as those desorbed from sample cartridges planned for the RSSAR system. Vapor may be condensed on a solid substrate, concentrating the analyte and enabling detection at or below the action level for site cleanup.

Experimental Details

SERS Substrate Fabrication

Many methods have been demonstrated for fabricating SERS substrates. Because of the ease of fabrication in this research, silver foil (99.9%) is etched in 30% nitric acid to produce a roughened (SERS active) substrate. After etching, the silver foil becomes gray-white in color.

Coating Procedures

For much of the research, secondary coatings with an affinity for PCBs were applied over the etched silver substrate. In all cases, the coated substrates were found to be very stable. They were repeatedly washed with THF, ethanol, and methanol to remove oil and PCB for further testing. Coated silver substrates stored for 1.5 months showed no deterioration in signal intensity. A summary of the coatings and a comment of the effectiveness of each is shown in Table 17.

Table 17. Coatings Tested on SERS Substrates for their Effectiveness in PCB Detection

Coating	Soak Time	Solvent	Self-Assembled Monolayer	Evaluation
Pentachlorothiophenol	2 minutes	ethanol	no	Quantitative results; Quenched oil signal
Tetrachlorododecane Disulfide	36 hours	ethanol	yes	Photochemical degradation
Biphenyl Analog	2 minutes	tetrahydrofuran	no	Spectral interference
Benzyl Mercaptan	2 minutes	ethanol	no	Spectral interference
Octane Thiol	24 hours	ethanol	yes	Low sensitivity
Isopropyl Thiol	24 hours	ethanol	no	Good sensitivity *
Decane Thiol	24 hours	ethanol	yes	Low sensitivity

* Slight interference from substrate due to impure silver

Pentachlorothiophenol Coating

Pentachlorothiophenol (PCTP) was purchased from TCI chemicals. A saturated ethanolic solution was used to coat the substrate. Coating was virtually instantaneous, so a two minute soak time was used. After soaking, excess PCTP was removed by washing with ethanol and then methanol. These were extremely stable surfaces.

Decane Thiol Self-Assembled Monolayer Coatings

The decane thiol self-assembled monolayer is a low-energy surface and is expected to have an affinity for the nonpolar PCBs. The decane thiol self-assembled monolayer coatings are produced from a 10-mM ethanol solution. The etched silver foil is gently washed with Millipore water and rinsed with 100% ethanol. The ethanol is allowed to evaporate and the foils are immersed in the decane thiol solution for 24 hours; then the coated substrates are removed from the decane thiol solution and washed with ethanol to remove physisorbed decane thiol. Sufficiently long immersion times are critical to the formation of true self-assembled monolayers. The SERS spectrum of the coating matches the spectrum of solid decane thiol, which is taken as proof of self-assembly on the surface.

Biphenyl Analog Coating

To detect PCBs in natural matrices, it may be beneficial to have a coating that mimics the structure and physical properties of the analyte. The purpose of the biphenyl mimetic is twofold. First, it should have a higher affinity for PCBs since it has the appropriate amount of aromatic character, which is lacking in the decane thiol coating. Secondly, previous research has shown greatly improved sensitivity when the analyte and coating have similar Raman spectra—designated "active detection" because the spectrum of the coating is actively involved in the detection process.

The synthesis is carried out with a 4,4'-biphenyldisulfonylchloride (BPDS) and 4-aminophenyl disulfide (APDS). One hundred mg of APDS is mixed with 150 mg of BPDS in a 50-ml aqueous bicarbonate solution. As illustrated in Figure 44, upon heating, the crude product, **1**, in the form of a yellow precipitate, is formed and is filtered. The product (probably polymeric) is a resinous material that can be pulled into long fibers. It is soluble in DMF and THF and is insoluble in chlorinated solvents, hydrocarbons, alcohols, or acetone.

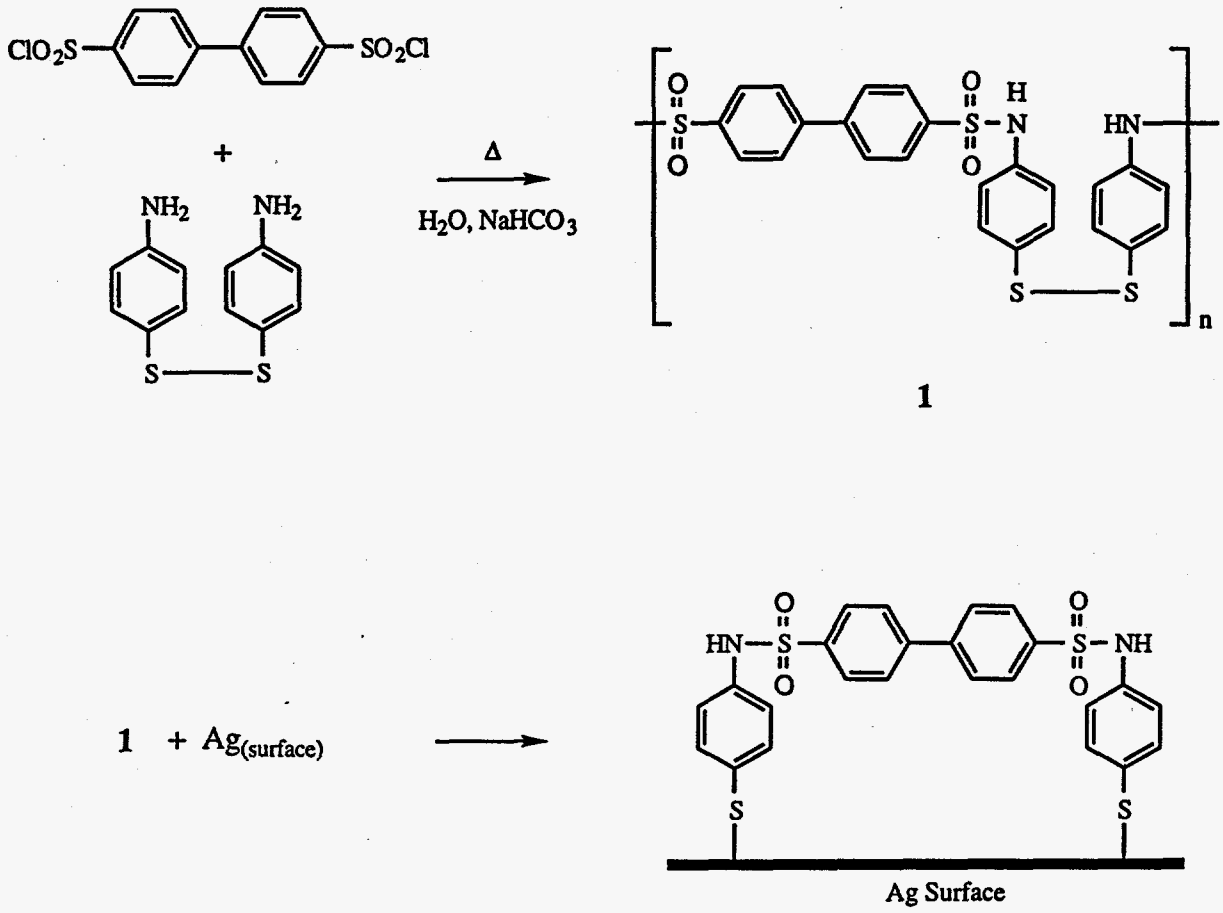

Figure 44. Synthesis of a biphenyl mimetic coating for use in SERS substrates.

TCDDS Self-Assembled Monolayer Coating

Tetrachlorododecane disulfide (TCDDS) was synthesized under a project funded by the Oak Ridge National Laboratories. TCDDS was prepared from a free radical reaction between 11-undecene disulfide and carbon tetrachloride. It was found that TCDDS has an enhanced adsorption coefficient for chlorinated ethylenes over a straight alkyl thiol. The hope was that an enhanced adsorption would also be found for PCBs, but such was not observed. TCDDS required a 36-hour soak time to self-assemble on the SERS substrate.

Other Coatings

Benzyl mercaptan, octanethiol, and isopropylthiol were also tested as coatings for detecting PCBs. All were purchased from Aldrich.

PCB Samples

All samples were purchased from Accustandard, Inc. Six neat congeners (ranging from lightly to highly chlorinated) and two neat Aroclor mixtures were tested for their SERS response. In addition, the Aroclor mixtures were diluted in 10C transformer oil provided by GE-CRD to test the ability of SERS and coated substrates to detect PCBs in

the presence of oil. The PCB samples comprised congeners 44′, 24′5, 33′44′, 22′44′55′, 22′33′566′, and 22′33′4′55′6, and Aroclors 1248 and 1260.

Application of Neat PCBs to the SERS Substrate

To obtain meaningful SERS spectra, a uniform method of presenting the sample is necessary. First, 2 mg of a PCB sample is dissolved in 400 µl of o-xylene. Ten µl of this material is applied to the silver substrate and the o-xylene is allowed to evaporate. The quantity of material applied to the surfaces in this manner should produce 1×10^{17} molecules/cm^2 on the surface, more than enough for a detectable signal. A monolayer of PCB should contain 1.6×10^{14} molecules/cm^2. In monolayer equivalents, the surface has been covered with 625 monolayers.

Application of PCB Oil Mixtures to the SERS Substrate

A series of tetrachlorobiphenyl mixtures with 1% oil content were made in o-xylene. Standard serial dilutions of a 25 ppth solution of tetrachlorobiphenyl were used to make 12.5, 6.25, and 3.125 ppth samples; each solution (including the 25 ppth sample) was spiked with 1% oil. In addition, a 1:25 dilution was used to make a 1 ppth, 1% oil mixture in o-xylene. As with the neat PCBs, 20 µL of the mixture is applied to the substrate and the o-xylene is allowed to evaporate. The relative concentration of oil to PCB ranged from 10:1 for the 1 ppth sample to 2:5 for the 25 ppth sample. It is noteworthy that we were still able to discern a PCB signal on a PCTP coating even in the sample containing the smallest PCB concentration, which had 10 times as much oil as PCB.

SERS and Raman Measurements

SERS and Raman spectra are obtained with a conventional 90° scattering configuration. A cylindrical lens is used to focus the laser beam on the sample, thus serving to match the image on the sample with the rectangular slits on the spectrograph. The Raman optical system is shown in Figure 45. For SERS, the samples are applied to the substrates as described. The coated substrate is placed in a cuvette and the spectrum is obtained by direct illumination of the front, coated SERS surface. For samples containing oil, spectra are taken through a film of oil.

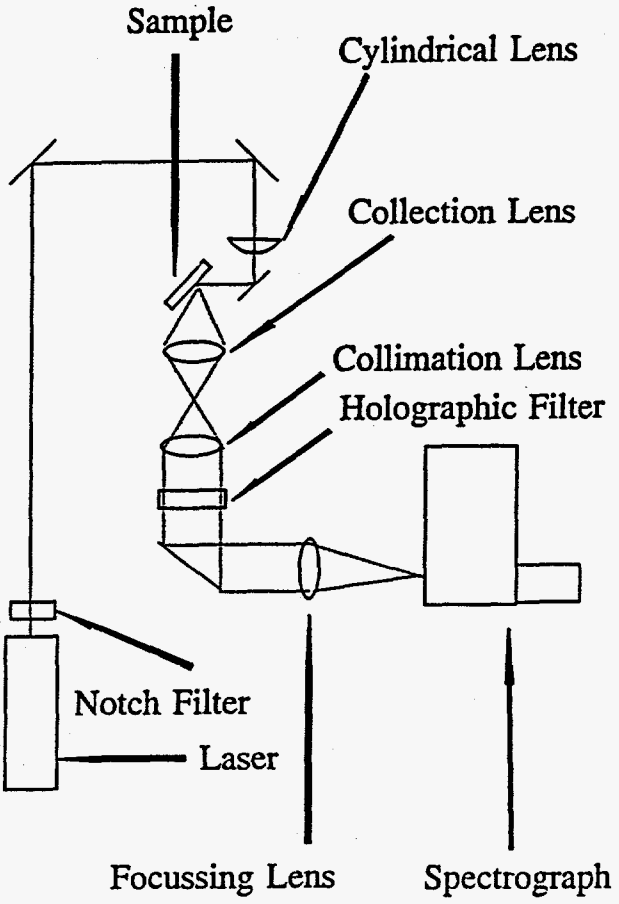

Figure 45. Raman optical system.

Normal Raman spectra of the PCBs or the oil are taken at 90° using a fluorescence cuvette. At the excitation wavelength used (647 nm), fluorescence is not a serious problem.

The spectra are analyzed and plotted with LabCalc (Galactia). In the quantitative studies the blank is a substrate coated with PCB free oil. However, since the substrate is removed for cleaning and coating with PCB mixtures, it does not represent a true blank; slightly different locations on the substrate are sampled with each measurement. Since there are variations in the SERS intensity across the surface of the substrate, subtracting the "blank" from a PCB sample leads to inaccurate results. This problem will be alleviated in the eventual instrument. In the laboratory, liquid samples are analyzed, and the substrate must be removed and cleaned between measurements. In the envisaged system, the sample will be desorbed from sorbent cells and deposited onto SERS substrates from the vapor phase. The instrument to be designed for DOE will capture the vapor on a fixed substrate so that the same location will be sampled with each measurement and much of the sample-to-sample variation should be eliminated.

Test Sequence

The following tests were undertaken in an effort to develop a coating that would stabilize the SERS surface, preferably allow a reusable surface, detect PCBs in the presence of oil, and ultimately allow a determination to be made of the PCB concentration in a real, environmental sample. The tests and reasoning behind each test follow.

- Obtain bulk Raman spectra of neat PCB congeners and Aroclor mixtures. This test is important to establish baseline spectra and to verify that the Aroclor spectra make sense in light of the spectra of individual congeners.

- Obtain bulk Raman spectra of 10C transformer oil and of PCBs dissolved in oil. Real samples are expected to have high oil concentrations, and oil is the most interfering contaminant in PCB spectroscopy because of its high fluorescence. The purpose of the bulk spectra is to determine whether it is possible to detect a PCB signal over the oil background and to determine whether the Raman signal changes in the presence of oil.

- Obtain SERS spectra of neat PCB congeners and Aroclor mixtures on unaltered, silver foil coatings. This test highlights any changes in the SERS spectra (when compared to the bulk spectra) and determines whether the PCBs and silver interact with each other.

- Obtain SERS spectra of neat PCB congeners and Aroclor mixtures on silver foil covered with specialized coatings. Test the SERS coatings using samples of PCBs in oil. The ideal coating would selectively enhance the PCB signal over the oil background. The coatings need to be tested for this ability as well as for their stability in oil solution. In addition, the effect of oil on the SERS spectra must be determined. Detection limits need to be determined for PCBs in the presence of oil.

- Perform a series of quantitative tests, using both neat PCBs and PCBs in oil to determine whether the coating selected in the previous experiment allows a correlation between PCB concentration and Raman signal. Determine whether a total PCB concentration may be obtained without a priori knowledge of the congeners or Aroclor mixtures present at the test site. Determine whether it is possible to identify individual congeners or Aroclor mixtures and their concentrations based on their SERS spectra. The outcome of this test should be calibration curves and detection limits.

In a continuation of this test series, in Phase II we would

- Perform a series of quantitative tests on environmental samples containing PCBs to verify that the additional contaminants present still allow analysis based on the previously derived calibration curves. Determine whether an extraction method is necessary to provide an initial partition between the PCBs and all other compounds.

Discussion

Raman and SERS Spectra for Neat Single Congener PCBs and Aroclor Mixtures

The purpose of the initial experiments with PCB congeners and mixtures is to compare the SERS spectra to those obtained using bulk Raman spectroscopy, to identify spectral features with which to identify the PCBs, to calculate the PCB detection limit, and to identify promising coatings that could be used to detect PCBs in the presence of oil. Bulk Raman spectra for the congeners and Aroclor mixtures are found in Figure 46. The Aroclor spectra look reasonable when compared to the spectra of the congeners. The most dominant feature is a large Raman band in the 1600 cm^{-1} region.

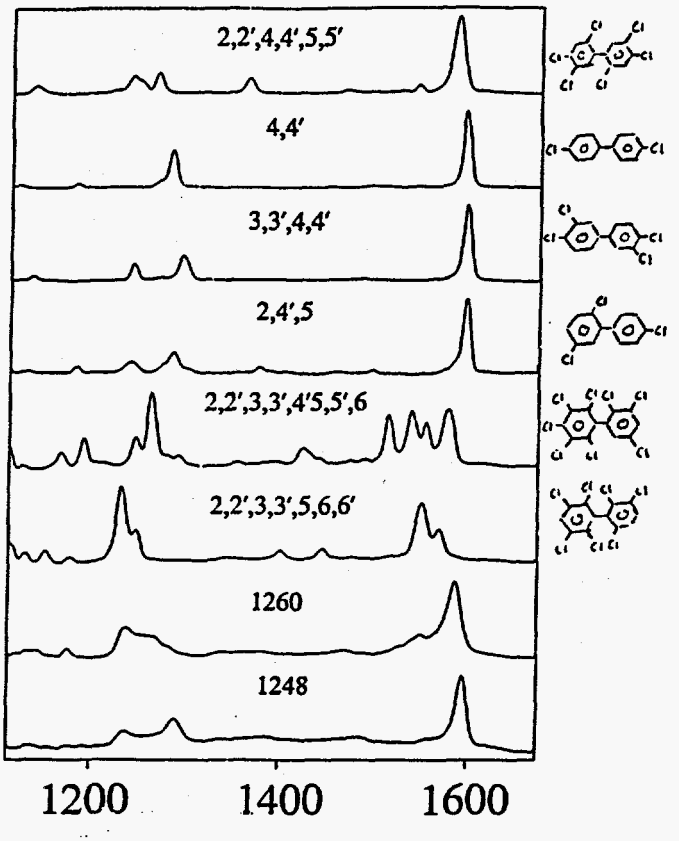

Figure 46. Bulk Raman spectra of PCBs.

Poor SERS spectra were obtained for PCBs on uncoated silver, since uncoated etched silver is not sufficiently protected to prevent oxidation and loss of signal. The first coating tested, a self-assembled coating of decane thiol, stabilizes the surface. Figure 47 shows the spectrum of a decane thiol-coated silver surface ("blank"), the same surface with tetrachlorobiphenyl ("PCB raw"), and a subtraction to remove the coating peaks. This procedure was repeated for all of the PCBs and they are shown in Figure 48. Overall, the spectra match those obtained for pure PCBs. The spectra were obtained with 100-second integrations and 50-mW laser power. The excitation wavelength was 647 nm and the slit width corresponded to 6 cm^{-1}.

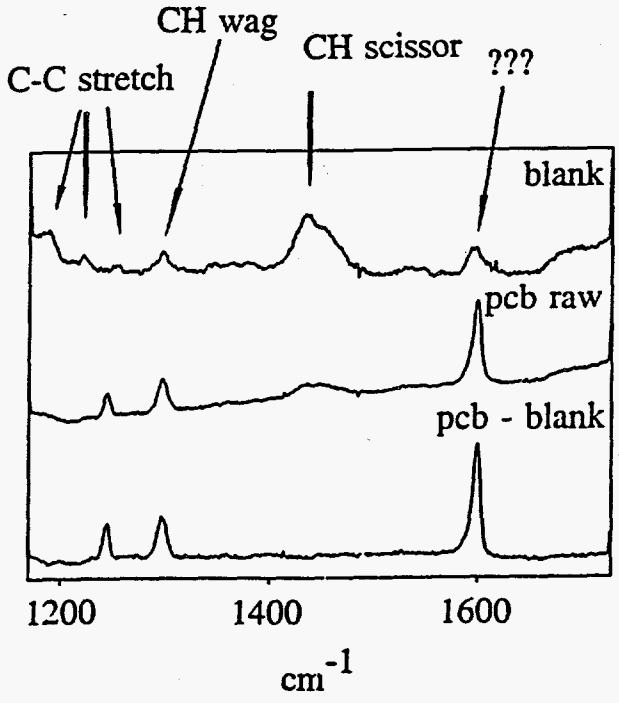

Figure 47. Spectrum of tetrachlorobiphenyl on a decane thiol-coated silver surface.

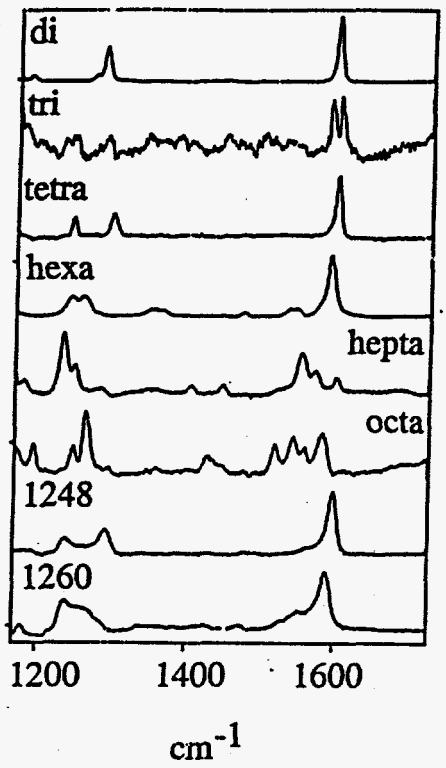

Figure 48. SERS spectra of the same PCB congeners and Aroclor mixtures as in Fig. 46, on a decane thiol-coated silver surface.

The procedure for applying PCBs in o-xylene to the decanethiol coated SERS substrate produced approximately 625 monolayers of PCB on the surface. In real situations using real samples far fewer monolayers are expected to be deposited on the surface. Therefore, it is necessary to correct the results such that they represent the signal that would be observed for one monolayer. A calculation is necessary since there are no simple methods of producing single monolayers.

It can be shown [19] that the relationship between distance from the surface and signal is

$$I_n = I_1(n)^{-2.8} \tag{16}$$

where I_n is the signal at a distance from the surface, I_1 is the signal at the surface, and n is the number of C-C bonds. This has been verified in several independent experiments using self-assembled monolayers of various carbon-backbone chain lengths. Thus, the observed signal, I_{PCB}, for a thick layer of PCBs beginning 10 carbon units (about 1.4 nm) away from the surface may be found by summing by threes from 10 to 1875 (the surface coverage was estimated as equivalent to 625 monolayers and each PCB monolayer takes up as much space as three C-C bonds).

$$I_{PCB} = I_1 \sum_{10}^{1875} (n)^{-2.8} = I_1(0.0038), \quad n = 10,13,16... \tag{17}$$

Substituting eq. (17) back into eq. (16), we find that the signal for a single monolayer of PCBs at a distance of 10 carbon bonds from the surface is

$$I_{10,PCB} = \frac{I_{PCB}}{0.0038} 10^{-2.8} = 0.42 I_{PCB} \tag{18}$$

Thus, a single monolayer at 10 C-C away from the surface is predicted to account for 42% of the observed signal.

Detection of PCBs in 10C Transformer Oil

Experiments to detect PCBs in oil were performed using Aroclor 1260 and 3,3',4,4' tetrachlorobiphenyl.

Raman spectroscopy of bulk samples of transformer oil and transformer oil with 50 ppth PCB present was done using a 100-second integration and 50 mW of 647-nm radiation. The samples were weakly fluorescent at this wavelength. Due to aromatic components in the oil, we observed strong Raman features around 1600 cm^{-1}. These features occurred at frequencies only slightly higher than those observed for PCBs. Therefore, only after subtraction of the oil spectrum from the oil and PCB spectrum was it apparent that there was a small PCB peak on the shoulder of the oil feature near 1600 cm^{-1}. The fact that it was necessary to subtract a blank oil spectrum from the signal spectrum suggests that this will not be a robust detection mechanism. Generally, it will not be possible to anticipate the particular oils and interferers present in a sample, and therefore we will not know what to subtract. Standard Raman scattering techniques appear to be a poor approach for measurement of PCBs in oil.

Several coatings were tested for their ability to selectively excite Aroclor 1260 in 10C transformer oil. One method by which to obtain selective excitation is to provide a surface that will selectively partition or concentrate PCBs out of the bulk solution. The rule of thumb to partition materials out of a matrix is "like dissolves like." In addition, with this type of coating it is sometimes possible to detect an analyte by observing changes in the spectrum of the coating rather than detecting the analyte itself. A biphenyl coating synthesized by reaction of 4,4'-biphenyldisulfonylchloride (BPDS) and 4-aminophenyl disulfide (APDS) was tested first. Strong spectral interference caused by the similarity of the coating to the PCBs made it an undesirable coating material. Benzyl mercaptan was tested as an aromatic coating. The same spectral interference was found to be due to the spectral similarity between biphenyl rings and phenyl rings.

Next, alkane thiol coatings were tested since their structural dissimilarity with biphenyl was expected to alleviate problems with spectral interference. A chlorinated alkane thiol, bis-12,12,12,10- tetrachlorododecane disulfide (TCDDS), was tested. This

coating has been found to have about 100 times higher affinity for chlorinated ethylenes than straight alkane thiols. This material could detect PCBs in 10C transformer oil. However, this coating appeared to photochemically degrade under laser irradiation.

Octanethiol and isopropylthiol were tested as simple alkylthiol coatings. SERS is known to have a strong distance dependence from the surface. Isopropylthiol holds the sample to be tested at a distance of only 2 carbons from the silver surface. By comparison, octanethiol holds the sample 8 carbons away. Referring back to eq. (16), this fourfold improvement in distance from the surface is expected to lead to nearly a sevenfold increase in detected signal. However, neither coating was effective for detecting PCBs in the presence of oil without subtracting an oil blank from the SERS spectrum.

The final coating tested was pentachlorothiophenol (PCTP). PCTP was tested because of its chemical similarity to PCBs and the flat background in the 1600 cm^{-1} region. PCTP was found to have good properties for the detection of PCBs.

Figure 49 illustrates the quantitative capacity of SERS for detecting PCBs in the presence of oil on a substrate coated with PCTP. The spectra show the increase in the 3,3',4,4' tetrachlorobiphenyl 1595 cm^{-1} band for 20 μg to 0.5 mg of PCB congeners deposited on the SERS substrate with area of approximately 1 cm^2. These spectra were taken on a single substrate which was washed between samples with o-xylene, ethanol, and methanol. This series illustrates the robustness of the substrates. The samples were prepared using 3,3',4,4' tetrachlorobiphenyl and 1% 10C oil in o-xylene solvent. A 20 μL sample was placed on the substrate and the xylene was allowed to evaporate. Figure 50 shows an expanded view of the oil blank and of the spectrum obtained for 20 μg PCB. The PCB feature at 1600 cm^{-1} is clearly visible over the PCTP background, and there does not appear to be any interference from the aromatic components of the oil in this region. It is not yet fully understood how the PCTP coating quenches the oil signal (near 1600 cm-1) and whether the coating partitions PCBs out of the oil containing mixture. Figure 51 shows the results of the quantitative study. A ratio of the height of the large PCTP peak at 1518 cm^{-1} (internal standard) vs. the 1595 cm^{-1} peak for 3,3',4,4' tetrachlorobiphenyl shows a reasonably linear dependence as a function of the PCB mass per volume of oil. The R^2 for the line is 0.97. In P hase 2, we expect to repeat this experiment with Aroclors 1248 and 1260 in order to test whether the apparent linear dependence will still be present in PCB mixtures. If the linear dependence is robust, it appears that SERS will be a feasible method for PCB detection at levels of interest to DOE.

The action limit for PCB remediation corresponds to 10 μg from a 100 cm^2 surface. A 20-μl sample of 1 ppth PCB corresponds to about 20 μg of PCB on the SERS substrate, which has a surface area of approximately 1 cm^2. The actual area sampled by the laser beam, however, is only 3 mm × 100 μm, or 3×10^{-3} cm^2. Thus, the mass of PCB seen by the SERS system is only 60 ng. Although the concentrations used in the laboratory experiments seem high, the absolute quantity of PCB detected is well within the range of

interest to DOE. Stable, quantitative results will require sampling a larger substrate area, in order to average out effects due to nonuniformity of the substrate. A sample area of 3 mm on a side, or 9 mm^2, at the same PCB density on the surface, would correspond to a PCB sample of less than 2 μg.

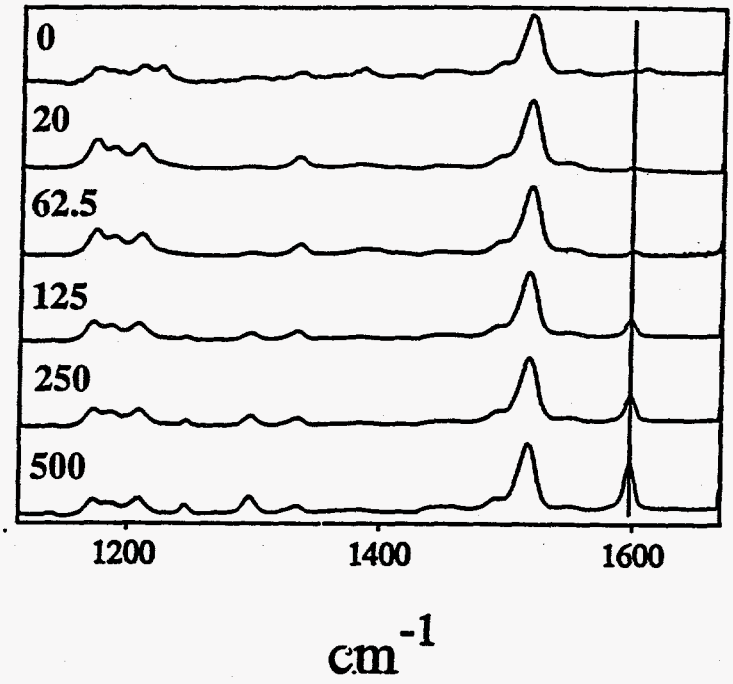

Figure 49. SERS spectra for tetrachlorobiphenyl in the presence of oil. Sample preparation is described in the text. PCB quantity given in mg.

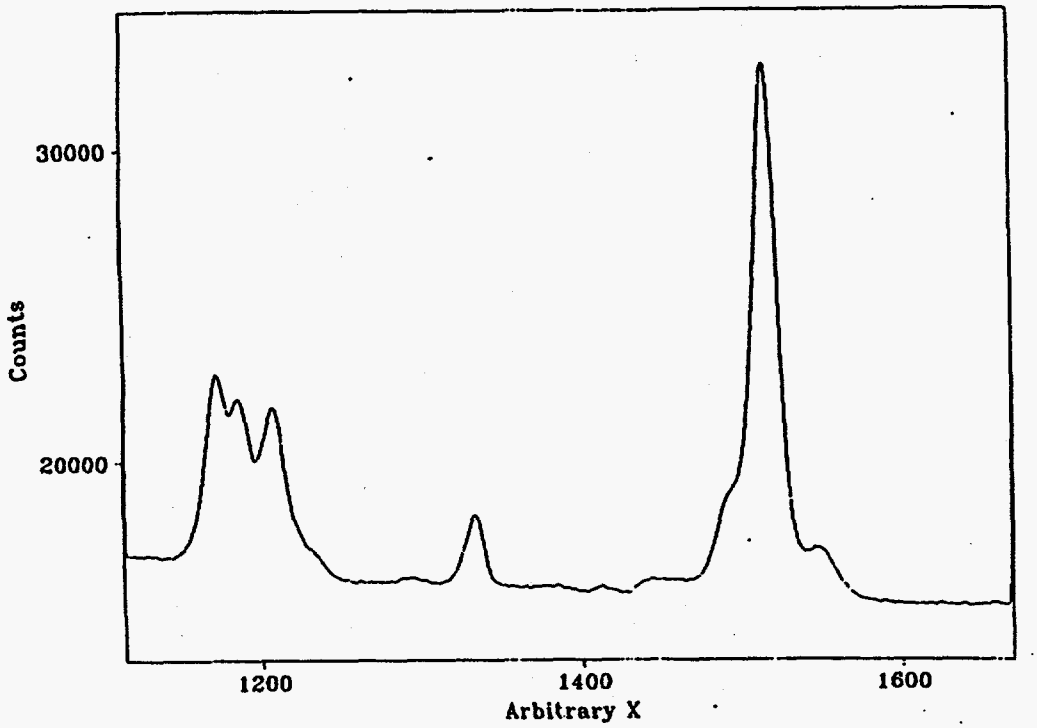

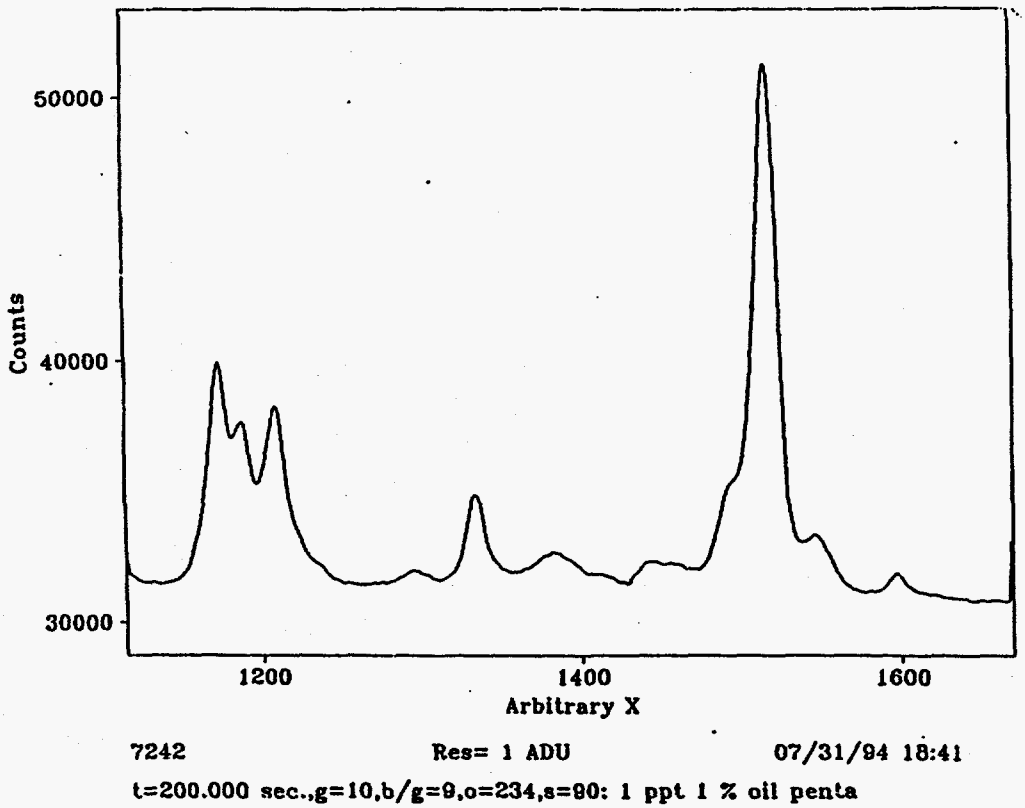

Figure 50. An expanded view of the oil blank and of the spectrum obtained for 20 mg PCB shown in Figure 49.

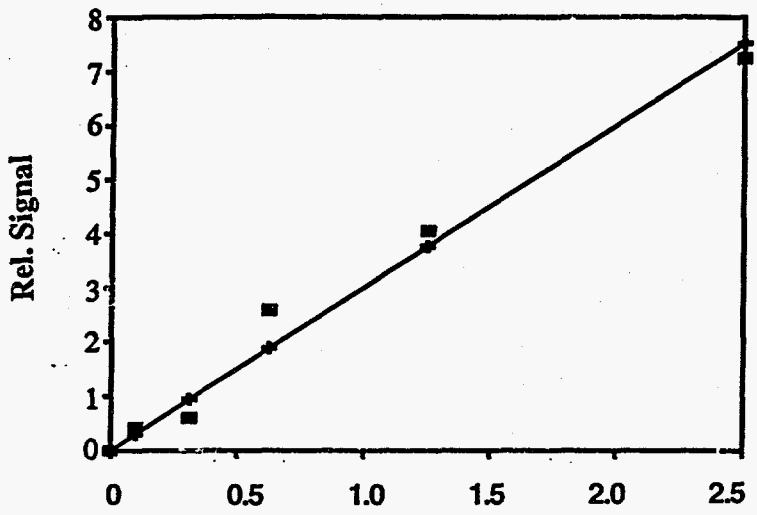

Figure 51. Linear SERS response to tetrachlorobiphenyl in the presence of oil.

Conclusions

A PCB congener has been detected in solutions containing up to 10 times as much transformer oil as PCB using SERS. The coated substrates have been demonstrated to be reusable, eliminating the expense of single use, disposable elements and reducing the number of substrates that need to be kept available in the laboratory. Sample introduction for liquids is simple. Quick screening may be done by dipping the substrate into the sample. More controlled sampling is possible by using a pipette to spot a known amount of the sample onto the center of the substrate. A more elaborate instrument would allow desorption of PCB vapors from a solid phase adsorbent cartridge onto the substrate, eliminating any complicated sampling by the operator. Using clear, quartz substrates (coated with a silver SERS surface and overcoated with one of the coatings identified here), it will be possible to examine the sample from the back rather than the front surface and to allow automated sample presentation to the substrate while protecting the optical elements from contamination.

SERS presents advantages over normal Raman in the sharpness and clarity of the spectra attainable, in the ease of (automated) introduction of very small samples, in its ability to quench fluorescence that would otherwise interfere with analyte detection, and in its ability to partition the analyte from a mixed matrix. In phase II, we will investigate the realization of these advantages for a quantitative instrument to evaluate environmental samples.

Task 1.6 Conceptual Design of the Archival Multisample Trapping Module (MSTM)

Background

The goal of the RSSAR system is to provide an efficient means for characterizing surface and subsurface contamination on very large areas. The system includes thermal sampler heads, a quick-look detector and an archival multisample trapping module. The sampler heads extract contaminants from surfaces through thermal desorption, providing samples in the vapor phase. The quick-look detector provides a real-time, semiquantitative analysis of the vapor sample to determine the presence of subject contaminants in a significant quantity. This detector serves as a guide for sampling strategy and to estimate contamination levels for personnel safety.

To more accurately identify and quantify particular contaminants and levels, an archived sample is required. Solid sorbent technology provides a proven, reliable means for collecting and storing samples for subsequent detailed analysis through the use of a thermal desorption unit (TDU) and conventional analytical instruments (GCs and/or GC/MS).

There are currently numerous commercial systems available for collecting individual solid sorbent samples. The systems are typically not automated and do not lend themselves to efficient sampling of large areas that require a significant number of samples. There are also a number of systems available to collect multiple solid sorbent samples (up to 24). These systems are not fully automated and lack a direct interface to existing analytical instruments.

Objective

The objective of Task 1.6 is to provide a conceptual design for an automated, multisample trapping module (MSTM). The conceptual design addresses interfaces to the sampler heads and quick look detection module on the front end of the system and to the analytical instruments on the back end. Critical design issues and uncertainties are identified relating to the operating performance requirements and to the functional description of the multisample trapping module.

General System Performance Requirements

Conventional solid sorbent air sampling is a proven technology. In the simplest of terms, sample tubes are packed with an absorbent material and samples are collected by drawing air through the tubes. The technology has been used successfully for sampling a wide array of compounds in a variety of applications.

The RSSAR system and the applications for which it is being designed present several unique requirements that must be addressed in the design of a multisample trapping module to fulfill its function as part of an overall system. The first issue relates to the very large number of samples that will likely be required and, hence, the need for a fully automated and efficient sampling system. A second critical issue relates to interfacing the

multisample trapping module (MSTM) to the front and back ends of the RSSAR system, i.e., the sampler heads and quick-look detector on the front end and the analytical instrumentation (TDU and GC/MS) on the back end. As in any fully automated system, additional attention to detail is required to ensure that the quality and integrity of the collected samples are maintained in the sampler, particularly since the analytical results may be used to certify regulatory compliance. In addition, a modular system design will provide for increased versatility and enhanced commercialization potential for applications beyond the RSSAR program.

Fully Automated System

The RSSAR system is being designed for an application that will require surface and subsurface contaminant characterization of large areas. The tasks for which it is being designed will require a very large number of samples to be collected. Current sampling methods are labor-intensive with the attendant quality control problems.

To efficiently perform the sampling operations that will be required, the MSTM must be automated. The system should require minimal input from the user and must have the "intelligence" to track all pertinent sampling information. This "intelligence" will facilitate record-keeping, minimize handling and training requirements, reduce errors caused by operator fatigue in the highly repetitive sample acquisition tasks, and expedite the process of attaining quality analytical results.

Interface to Sampler Head and Quick Look Detector

The front-end interface of the MSTM to the sampler heads and quick-look detector presents a unique situation in that the sample vapor stream will likely be at very high temperatures and will contain a significant moisture content. A heated transfer line will be used to carry the vapor sample from the sampler head, through the quick look detector and to the MSTM inlet. The vapor sample stream will need to be cooled at some point prior to, or at impact point with, the adsorbent material. Otherwise, the possibility exists that the sample will break through the absorbent bed.

A potential problem arises when liquid condenses at the point in the transfer line when cooling is allowed. Depending on the sorbent material, significant condensation in the sorbent bed could impact on sampling efficiency. Condensation prior to the sorbent bed could leave residual contamination in the transfer line that could be inadvertently transferred to the next sample (cross-contamination).

The optimum cooling point will be determined through testing and analysis. Factors to be evaluated are sampling efficiency (percent capture, percent breakthrough), transfer line contamination, and cross-contamination. During Phase I testing, we have discovered that 0.1 ml of water introduced into the bulk sampling oven along with 30 to 120 micrograms of analyses has no negative effects on sampling efficiency. This result was obtained with sorption tubes holding only 0.1 grams of sorption material. The tubes contemplated for RSSAR system use can hold at least 4 times this amount, and should thereby handle at least 0.4 grams of water. Further, we have identified sorbents which are

efficient at collecting PCBs at temperatures up to, and over 100 °C, where water vapor condensation is not likely to be a problem. Should condensation be a problem, a number of options exist for minimizing its effects, including incorporation of a "back-flush" or "bake-out" cycle into the MSTM to purge the transfer line between samples.

Interface to Automated Thermal Desorption (TDU) System

An efficient collection of a large number of samples is only one part of achieving cost effectiveness in sampling and analysis. A more critical element impacting cost effectiveness is the ability to efficiently transfer the samples to analytical instrumentation. For this reason, it is crucial for the RSSAR system, and specifically the MSTM, to provide a means for a direct, automated interface between the sample tubes and the analytical instruments that will be providing quantitative results on the back end.

Sample transfer from the MSTM to the TDU should require minimal, if any, operator-handling. Sorbent tube samples should be protected against cross-contamination, passive sampling, and sample loss at all times. All data collected during the sampling process, including quick look detector results, should be directly integrated and transferred into the analysis system to provide timely historical and accurate results.

Quality Assurance / Quality Control (QA/QC)

Analytical results used to certify regulatory compliance must be accurate and follow thorough QA/QC procedures. As in any fully automated system, additional attention to detail will be required to ensure that the MSTM acquires the necessary data to ensure the quality and integrity of the collected samples.

Each sample must be identified and tracked throughout the sampling and analysis procedure. Appropriate administrative data for each sample must also be recorded, to include the name of the operator taking the sample as well as the location, the time, and the date the sample was taken, i.e., the chain-of-custody.

Numerous environmental factors could also impact analytical results and must be monitored and recorded for each sample. These parameters include sample temperature, relative humidity, atmospheric pressure, and vacuum pressure.

In addition, a number of critical sampling parameters must be measured and recorded to ensure accuracy of the analytical results. In any air sample taken via solid sorbent tubes, the total mass and volume of air collected is critical. These data can be measured and verified by using a calibrated pump in conjunction with measuring actual volume and/or mass flow rates. System leak checks should also be performed and recorded.

Modular Components

The design of the MSTM should be modular, which will improve eventual manufacturing and maintenance procedures as well as provide for a flexible system. For example, it is likely that the MSTM will have great utility outside the RSSAR system as a stand alone ambient air sampling system.

Thermal Desorption Unit (TDU) Literature Review

After reviewing initial design issues and system requirements it was determined that the most significant issue impacting the design and development of the MSTM was the interface to the thermal desorption unit (TDU). TDUs and their associated interfaces to GC and GC/MS systems are complex instruments and have evolved over the past ten years to provide accurate thermal desorption of solid sorbent samples for subsequent analysis.

For the RSSAR system to operate efficiently, it is critical that the TDU system be capable of automated multitube thermal desorption. The samples generated by the RSSAR system and the MSTM specifically must be capable of directly interfacing with the TDU and the analytical system through a common sorbent tube and the sorbent tube magazine.

A literature search identified a number of TDU vendors. The vendors have been evaluated with regard to the objectives of this project. The literature search identified the following vendors which sell TDU type devices:

Vendor	Instrument
CDS/Dyantech	CDS 6000/PTA-30
Chrompak	TCT/PTI
Dyantherm	DYNA-ACEM
Envirochem	810TD/8916
Gerstel	Gerstel TDS
Perkin-Elmer Corporation	ATD-400
Scientific Instruments Services, Inc.	TD-2
SGE, Inc.	CHIS
Tekmar	5010 GT

Criteria were then developed to evaluate the suitability of these instruments to meet the requirements of the RSSAR system. The criteria in order of priority include

- Automated multitube desorption
- Interface capability with MSTM
- Temperature range
- Cost
- Technical support
- Service support
- Availability of spare parts

Five of the nine vendors and systems were eliminated when the first criterion was applied. Most of these systems are single-tube, manually loaded systems that do not lend themselves to automated runs. Of the remaining four systems, Dyantherm and Envirochem have a multitube desorption capability but only to a maximum of 16 tubes. In addition, samples are loaded in a rack type configuration by tightening two threaded end caps around the sorbent tube that is surrounded by the desorption oven. As in the single desorption systems, these designs do not lend themselves to automation and interface to a MSTM.

The CDS/Dyantech system has a 30-tube capacity, with the tubes arranged in a carousel. Samples are manually placed in a "positioner" that places each tube in the correct orientation relative to two needles that pierce the two septa sealing the sorbent tube. The whole assembly is elevated into an oven for the desorption. While the system has nearly twice the capacity as the Dyantherm and Envrochem systems, an automated approach must overcome the procedure that is currently handled manually, namely, placing the tube in the positioner. Additionally, the system has a maximum temperature of 180°C which severely limits its use in TDU applications.

The Perkin-Elmer system meets the criteria best for the project. Perkin-Elmer has been manufacturing TDU units longer than any of the vendors evaluated. As a result Perkin-Elmer also owns the largest share of the TDU market. Perkin-Elmer's latest generation instrument, the ATD-400 has the capability to perform unattended desorption and analysis of up to 50 tubes. Samples are loaded by simply placing the tube on the analyzer's carousel. For the analysis, the system rotates the tube into the unit, removes the tube end caps, seals the end of the sorbent tube, pressure-checks it, and then desorbs the sorbent tube, all automatically. The system has a maximum desorption temperature of 400°C. This high degree of automation lends itself readily to interfacing with the RSSAR and MSTM. As Perkin-Elmer is one of the largest analytical instrument manufacturers in the United States, they bring an extensive service and technical support network to the project.

A contact was established with Perkin-Elmer personnel to discuss a possible interface between the RSSAR system and their ATD-400. Perkin-Elmer personnel were interested in the possibilities and expressed a willingness to participate.

Concept Design

A fully automated, modular, and versatile concept has been developed for the MSTM portion of the RSSAR system. The concept will allow for RSSAR operations to be conducted with minimal operator input and virtually no operator handling of individual samples. Sorbent tubes will be housed in a transportable magazine that will interface to both the RSSAR system and the TDU system. Samples will be protected prior to, and subsequent to, sampling to minimize contamination and cross-contamination potential.

During sampling, sensors will monitor all relevant parameters to ensure reliable, accurate samples. Data generated from sensors during sampling and RSSAR quick-look

detector results will be stored in nonvolatile electronic memory resident in the sorbent tube magazine. The data will then be available to the TDU and analytical instruments to facilitate timely and accurate analysis. Figure 52 depicts the three major components comprising the field portion of the MSTM and the TDU that will reside in the laboratory.

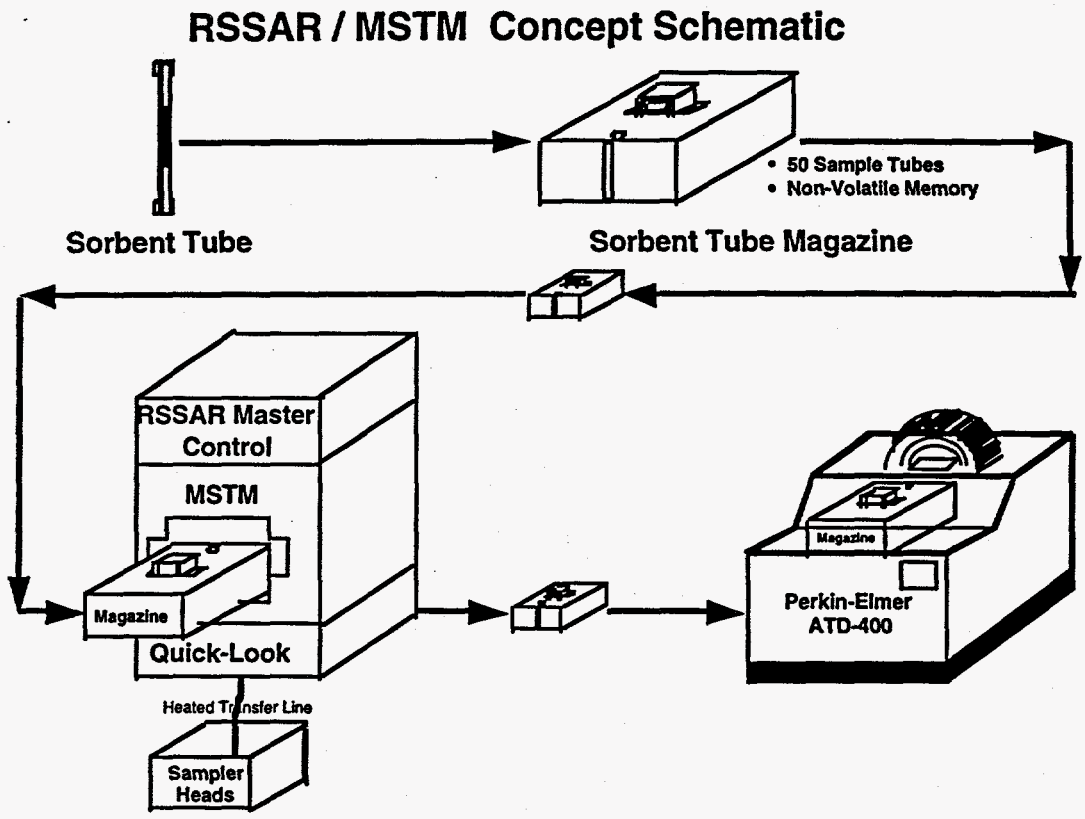

Figure 52. Three major components comprising the field portion of the MSTM and the TDU that will reside in the laboratory.

Interface to the Perkin-Elmer TDU will require a sample transfer device that will reside on top of the ATD-400, or the ATD-400 could be modified to accept the sorbent tube magazine directly. The sample transfer device will be relatively straightforward and is the preferred approach, at least through the prototype stage. Modifications to the ATD-400 to accept the MSTM magazine are possible but would require a significant development effort by Perkin-Elmer. Perkin-Elmer is willing to consider that option.

The RSSAR system will have the capability to perform both quick-look detection and sorbent tube sampling at each location. However, a sorbent tube sample is not required for each location. Algorithms will be developed to determine if an archived sorbent tube sample will be required. Sufficient memory will be in the magazine to store data for all 50 archived sorbent tube samples plus 500 quick-look detector samples.

Sorbent Tube and Sealing Means

The first major component of the MSTM is the sorbent tube itself. To ensure compatibility with the ATD-400, the dimensions of the MSTM's sorbent tube must be precisely the same as Perkin-Elmer's tube. The ATD-400 uses stainless steel or glass sorbent tubes (3.50 in. long with 0.250 in. OD). The ATD-400 sorbent tubes also include teflon end caps designed to seal the tube prior to and subsequent to desorption (the end caps are automatically removed prior to desorption).

The tube cap removal and the sealing mechanisms included in the Perkin-Elmer ATD-400 do not lend themselves readily to a portable, rugged sampling system. The ATD-400 system uses pneumatic systems to remove the tube caps and to seal the tubes for desorption. In addition, the mechanism is quite complex and costly.

A concept was developed for modifying the Perkin-Elmer tube cap to facilitate sampling. The concept would allow the MSTM to seal the sorbent tube during sampling with the new end cap remaining on the tube, as depicted in Figure 53. The new tube cap will keep the same overall dimensions of the original cap, but will include a custom septum seal. Septa are routinely used in gas chromatograph operations and are made of relatively inexpensive inert materials.

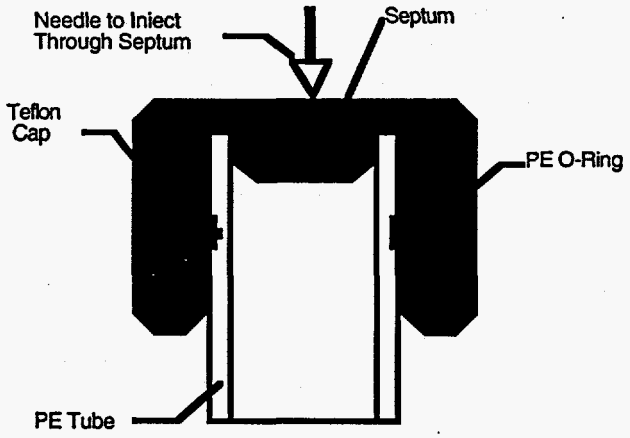

Figure 53. Sorbent tube cap

During sampling a hypodermic needle controlled by the sampler will be injected through the septum seal into the inner diameter of the tube. The needle will be sealed to the septum material and the septum material will be sealed to the teflon cap, tube top, and tube inner diameter. Figure 54 depicts the arrangement during sampling.

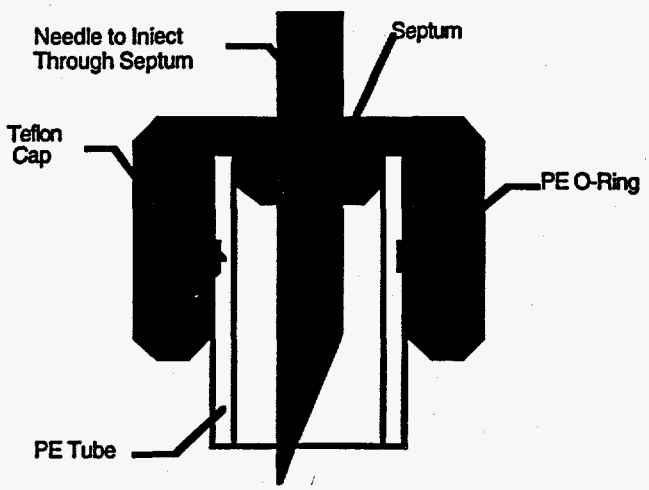

Figure 54. Tube sealing arrangement during sampling

This concept provides numerous advantages. While not being sampled, the tube remains isolated from the outside environment, thus minimizing passive sampling, sample loss and cross-contamination. The sampler mechanisms are kept relatively simple, less expensive and rugged, and the system will not require excessive power and compressed air for pneumatic devices. The tube and new cap will be directly compatible with the existing ATD-400.

Sorbent Tube Magazine

The second critical component of the MSTM is the sorbent tube magazine. The sorbent tube magazine is critical to the operation of the entire RSSAR system, since it will serve as the interface between the field sampling system and analytical instrumentation. Figure 55 depicts an isometric view of the sorbent tube magazine (outside housing). Once the magazine is loaded with "clean" sorbent tubes, operators will not be required to handle any sample tubes until analysis of the samples is completed in the laboratory.

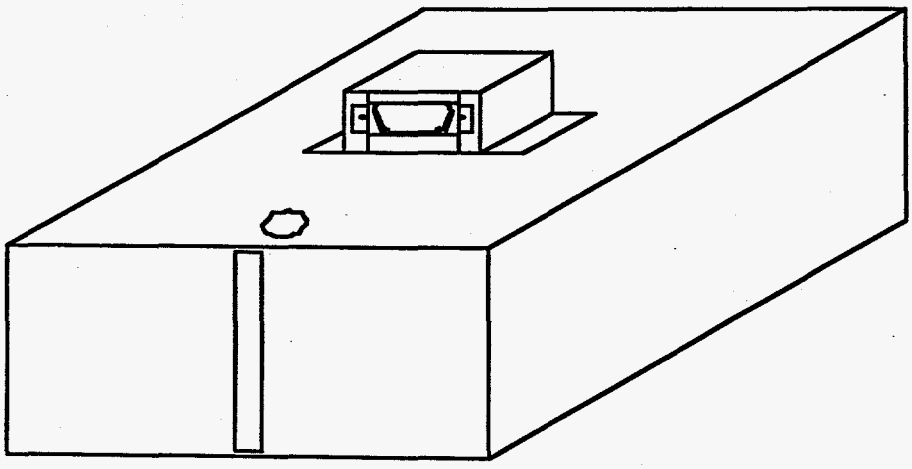

Figure 55. Magazine schematic

The magazine (dimensions approximately 9 in × 9 in. × 4 in.) will house 50 sorbent tubes in a circular arrangement within a transportable housing. The magazine simply inserts and locks into the sampler. A single point on the circle will serve as the sampling location, i.e., the point where the injection seals are to be made to the sample tube. The magazine will contain mechanics to allow rotation of the sorbent tubes, thus allowing all 50 tubes to be indexed to the sampling position.

In addition to housing the sorbent tubes, the magazine will have on-board nonvolatile electronic memory sufficient to store all pertinent sampling data. An electrical connection is made between the sampler electronics (note connector on top of magazine in Figures 55 and 56) and the magazine memory during insertion of the magazine. During sampling operations the magazine memory will continuously receive data from the MSTM microcontroller. Following sampling, the magazine will be removed from the MSTM and transported to the analytical laboratory.

Once in the analytical laboratory, the magazine will directly interface with the ATD-400. An automated device will transfer the tubes from the magazine to the ATD-400 carousel. Operators will not be required to handle sample tubes prior to analysis. The magazine will electronically interface with the ATD-400 and/or a PC computer to allow for the retrieval of all pertinent sampling data stored in the magazine memory during sampling operations.

Auto-Sampler

The auto-sampler will be a modular component of the overall RSSAR system, as shown in Figure 52. Figure 56 depicts a schematic of the multisample trapping module. The sampler accepts the sorbent tube magazine, locks it in place, seals the sample tube, and draws sample flow through the tube. The sampler will also interface electrically to the magazine. In the RSSAR configuration, it will be transmitting all relevant sampling data and quick-look detector results to the nonvolatile memory resident in the magazine.

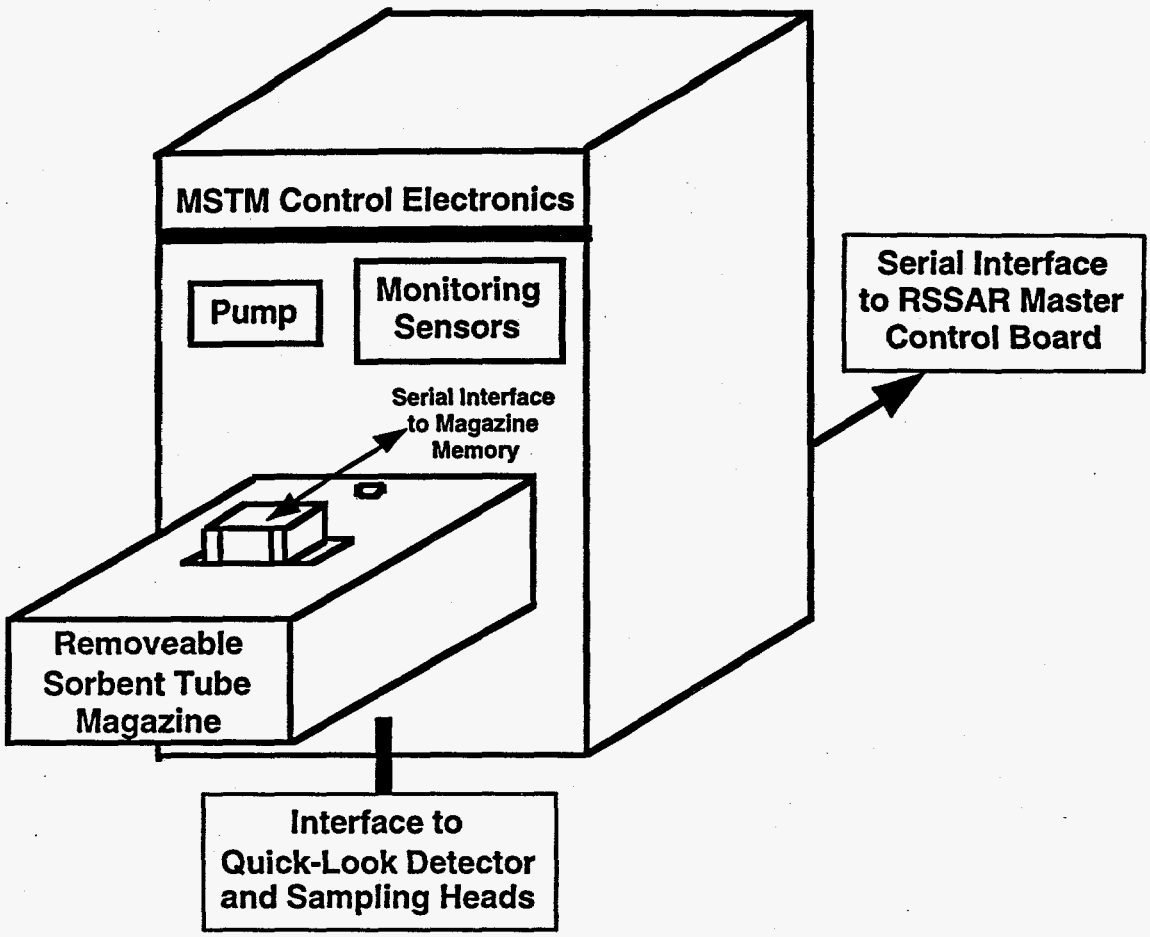

Figure 56. MSTM schematic

The sampler will also interface electrically to the RSSAR master control circuitry, as shown in Figure 57. Through that interface the sampler will receive instructions for sampling. The sampler air pump will be capable of drawing sample air through the quick-look detector only or through both the quick-look detector and sorbent tube, as shown in the flow diagram shown in Figure 58. The RSSAR master control board will also transmit sensor data that it is processing (transfer line temperatures, head temperatures etc.) to the sampler and through to the magazine memory for storage.

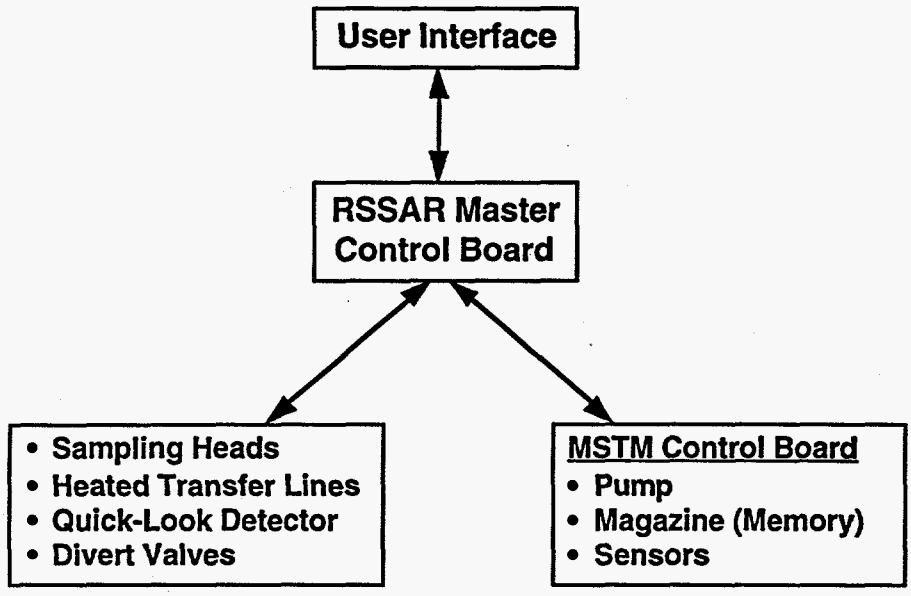

Figure 57. RSSAR control organization

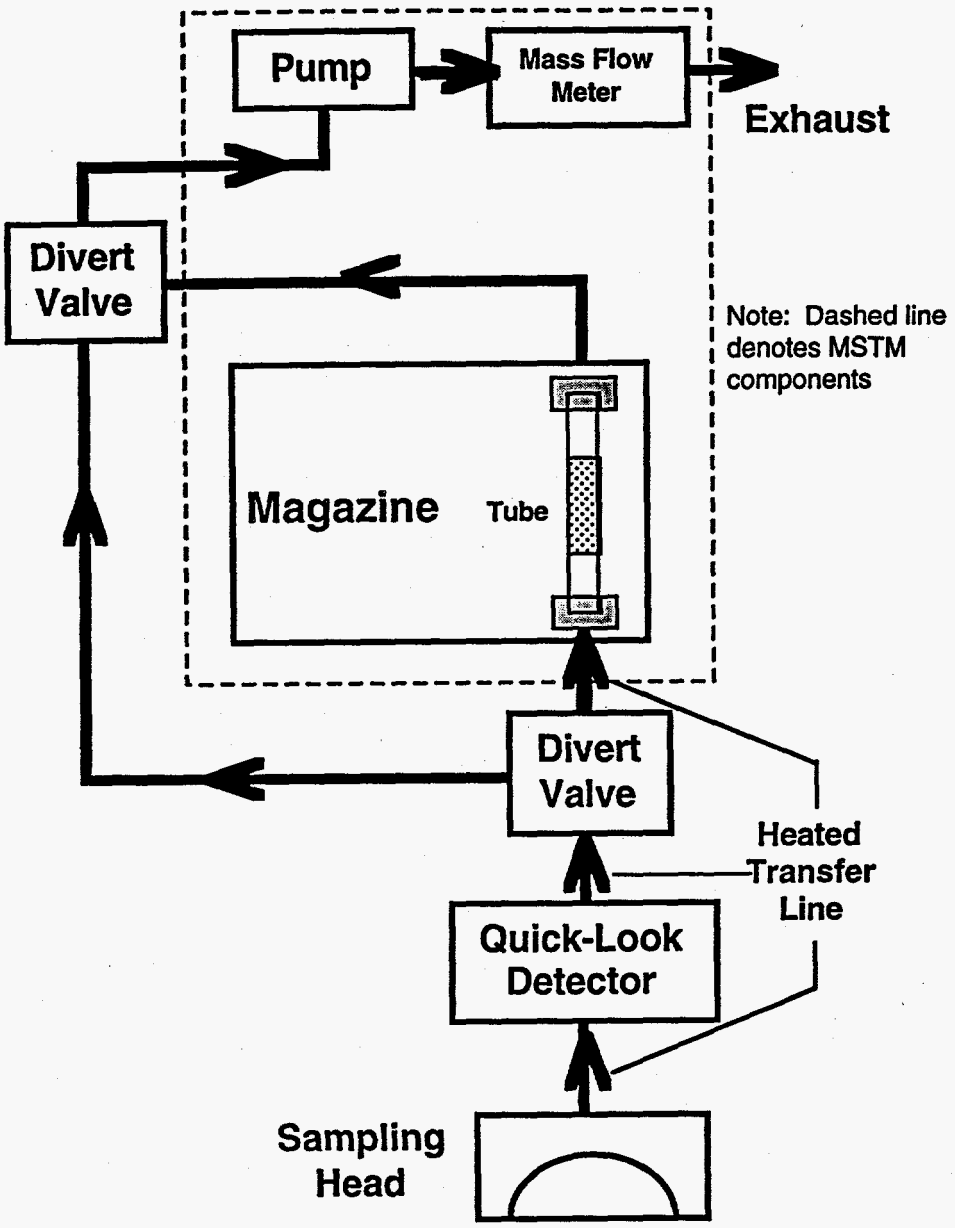

Figure 58. RSSAR sample flow path

Major components of the sampler include

- Electronic Control Circuitry
- Calibrated Air Pump
- Mechanism for Accepting Sorbent Tube Magazine
- Control Mechanism for Indexing Sorbent Tube Magazine
- Control Mechanism for Injection Seal to Sorbent Tube
- Sensors to Monitor Sampling Parameters
- Non-Volatile Memory Resident in Sorbent Tube Magazine
- Serial Interface to Communicate with RSSAR Master Control

In commercial applications different from the RSSAR system, the modular auto-sampler can serve as a standalone, fully automated air sampling system, as shown in Figure 59. This configuration would be particularly suited to applications requiring time-profiles of atmospheric conditions over extended periods of time.

In this mode, sampling instructions can be programmed directly into the sorbent tube magazine. The magazine can then be transported and inserted into the sampler. The sampler circuitry then reads and executes the programmed test sequence. All critical sampling parameters will be monitored during sampling and stored in the magazine's nonvolatile memory. For outdoor environmental sampling scenarios, the sampler will be capable of accepting data from external weather sensors. Battery operation and radio or telecommunication interface for remote operation are additional capabilities that can be added.

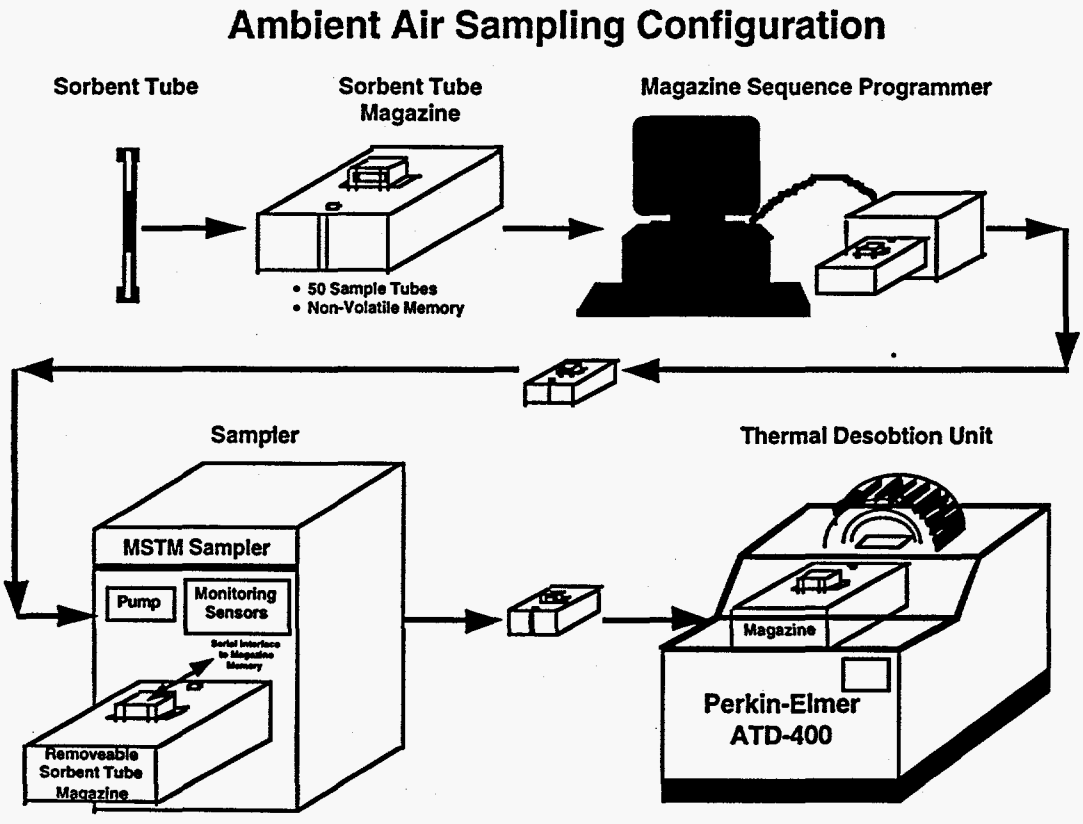

Figure 59. MSTM in ambient air sampling configuration

Performance Requirements / Specifications

Performance specifications have been developed for each of the three major components of the MSTM, including the sorbent tube, magazine, and auto-sampler.

Sorbent Tube Specifications

1. Compatible with Perkin-Elmer ATD-400 tubes
2. 0.250 in. Outer diameter (OD) by 3.50 in. long
3. Stainless Steel or Glass Material
4. End caps protect sample, but allow for injection of needle during sampling
5. Tube sealed prior to sampling
6. Tube protected subsequent to sampling

Sorbent Tube Magazine Operating Specifications

1. House and protect 50 sorbent tubes
2. Transportable
3. On-board nonvolatile memory to store all sampling information (64 Kbytes)
   - Per Sorbent Tube Sample (Up to 50 per magazine)
     - Operator Name
     - Date Start/Stop
     - Time Start/Stop
     - Location ID 1
     - Location ID 2
       - Lat (deg,min,sec)
       - Lon (deg,min,sec)
     - Quick Look Detector Result(s)
     - Set Flow Rate
     - Measured Flow Rate (Avg. over whole sample)
     - Ambient Temperature (Avg. over whole sample)
     - Ambient Relative Humidity (Avg. over whole sample)
     - Wind Speed / Wind Direction (if applicable)
     - Light Intensity (if applicable)
     - Rainfall (if applicable)
     - Atmospheric Pressure (At start of sample)
     - Sample tube pressure drop (Avg. over whole sample)
     - Error Codes / Fault Indicators (2)
       Power Interrupt
       Flow Leak
     - Operator comments (Code ???)
     - Vapor Train Temperatures (10) (from master control board in RSSAR System) (Avg. over whole sample)
     - Error Codes (2) from RSSAR system

- Non-Sample Quick Look Results (Up to 500 per magazine)
    - Operator Name
    - Date Start/Stop
    - Time Start/Stop
    - Location ID 1
    - Location ID 2
    - Lat (deg,min,sec)
    - Lon (deg,min,sec)
    - Quick Look Detector Result(s)
    - Operator comments (Code ???)
    - Error Codes (2) from RSSAR system
4. Communications interface to sampler control board
5. Mechanical system to interface magazine to sampler
6. Mechanical system to allow tubes to be positioned for sampling

Auto-Sampler Operating Specifications

1. Microprocessor controlled
2. On-board real-time clock
3. Accept magazine containing up to 50 sorbent tubes
4. Mechanical interface to magazine to align tube for sampling
5. Tube sealing mechanism
6. Sequential sampling (1 tube at a time)
7. Communications interface to magazine memory
8. Serial interface to RSSAR master control board
9. Auxiliary serial interface
10. Serial Output Only
11. Vacuum Pump
    - Variable flow rate (electronically set)
    - Calibrate flow (+/- 5%)
    - Flow rate range: 20mL/min to 1000mL/min
    - True constant flow (flow independent of pressure up to 40"H2O pressure drop)
12. Mass flow meter (verification of pump flow rates)
13. Ambient temperature sensor (-40 °F to 150 °F, +/- 1 °F accuracy)
14. Relative Humidity (RH) sensor
15. Atmospheric pressure sensor
16. Wind speed & wind direction sensors
17. Precipitation Sensor

Prototype Design

Initial prototype design has been undertaken on some multisample trapping module components. Efforts to date have focused on the sorbent tube cap, magazine and tube sealing mechanism and initial circuit board flowcharting. Table 18 shows a list of the prototype drawing figures and an associated description. These drawings appear in Appendix 2

Table 18. Prototype Drawings

Drawing	Description
Figure A2-1	MSTM Circuit Board Schematic
Figure A2-2	End Cap Design
Figure A2-3	Sorbent Tube Comparison
Figure A2-4	Magazine (Top View)
Figure A2-5	Magazine (Side View)
Figure A2-6	Sampler Magazine Receiving Structure and Sealing Mechanism (Side View)
Figure A2-7	Magazine and Sampler Structure and Sealing Mechanism (Side View)
Figure A2-8	Magazine and Sampler Structure and Sealing Mechanism (Top View)

Technical Risks

The condensation of water vapor at the inlet to the MSTM remains a legitimate concern. Condensation could contaminate the flow path in and around the injection needle that is to be used to seal the sorbent tube. The condensation could result in sample loss and/or cross contamination (residual sample remaining in flow path and subsequently transferred to next tube). This risk is compounded by the automatic nature of the system as condensation may go undetected for any number of samples taken by the 50 tube magazine.

Prototype testing conducted as early as possible in Phase II would determine the extent of the problem, if any. If testing reveals that condensation is causing contamination problems, a "backflush" or "bake-out" mode could be incorporated to purge the sampling line between samples, a smaller sample could be taken, or a sorbent selected whose analyte retention characteristics are unaffected by water that can subsequently be removed by purging.

Results and Conclusions

A concept design has been developed for the multisample trapping module (MSTM). The design allows the module to interface directly to the sampling heads and quick-look detector through a heated transfer line. The design also allows for a seamless interface to a commercially available thermal desorption unit, specifically the Perkin-Elmer ATD-400.

A magazine housing 50 individually capped sorbent tubes serves as a link between the field sampling and laboratory analysis. Individually capped sample tubes provide maximum protection against passive sampling and sample loss. In addition to housing the sample tubes, the magazine contains on-board nonvolatile electronic memory to record and store all pertinent information associated with each sample.

The field sampler sequentially samples up to 50 sorbent tubes. During sampling, sensors on-board the sampler monitor and record all pertinent sampling data, including sample time, set and measure flow rates, temperature, relative humidity, atmospheric pressure, and tube pressure drop (leak test). Following sampling the magazine may simply be removed from the MSTM and transported to the laboratory. In the laboratory the magazine will interface to the TDU device, delivering not only the sample tubes but all data recorded during sampling.

The concept design provides almost fully automated operation with minimal operator input required. Virtually no sample handling is required by the operator, thus enhancing QA/QC, reducing to chain of custody discrepancies, and providing for efficient and accurate sample analysis.

The modular design concept will enhance the commercialization potential of the system, extending it beyond the scope of the RSSAR system. Without the RSSAR master control board, heated sampler heads and quick-look detectors, the MSTM will be an efficient, automated standalone sampler that could serve numerous applications.

Conclusions

GE, with DOE support has completed Phase I of a four-phase program to develop a Rapid Surface Sampling and Archival Record (RSSAR) System. The objective of this effort is to provide instrumentation for the detection of semivolatile organic contaminants on concrete, transite and metal surfaces as well as bulk materials such as concrete drillings. The RSSAR System will be a modular instrument made up of several components:

- Sampler heads for thermally extracting the contaminants from concrete surfaces, steel surfaces and bulk materials.
- Quick-look detectors to give a real time assessment of contamination levels.
- Multisample trapping module to trap and store vaporized contaminants in a manner suitable for subsequent detailed lab-based analyses.

GE and its subcontractors, EAI Corporation, Inc., and Detection Limit Technology, LC, have completed the Phase I tasks and have met the objectives in the RSSAR proposal. The Phase I portion of the equipment has been designed, constructed and tested. Information about critical operating conditions for the samplers has been obtained, and a concrete model to aid in understanding the sampling process has been developed. In addition, the feasibility of using surface-enhanced Raman spectroscopy (SERS) to provide rapid information about contaminant identity has been demonstrated and a preliminary design of a multitube sample trapping module has been developed. Conclusions are as follows:

- PCB sampling can be conducted at 250°C with no detectable formation of dibenzofurans. However, the potential for formation of dibenzofurans at lower temperatures must be tested further, since this possibility has been suggested by some of our experiments at 200°C.
- A thermal concrete sampler head with appropriate heating rate and heat distribution characteristics has been designed, built, and tested. It is suitably rugged for laboratory and limited field testing, providing uniform heating over >60% of sampling areas. A concrete model to aid in understanding the sampling process has been developed. No insurmountable difficulties have been encountered.
- A bulk sampler head for characterizing loose materials such as floor sweepings and materials drilled from bore holes has been designed, built, and extensively tested. It is convenient to use as a workhorse instrument for calibration and recovery fraction measurements Flow rates have been optimized at 2 SCFH for recovery of three major classes of pollutants—oil, PCBs, and PAHs. Several problems common to thermal sampling techniques, dealing with incomplete recovery and chemical conversion, have been encountered, and solved.

- A commercially available photoionization detector has been demonstrated to be viable for providing a "quick-look" indication of surface contamination using the RSSAR system. It has more than adequate sensitivity to detect <10 μg PAHs, PCBs and oil, the action level for many contaminants.
- A Near Vacuum Ultraviolet (NVUV) detector has also been designed, built and demonstrated to be a viable quick-look indication of contamination. In addition to having adequate sensitivity to detect <10 μg of contaminants, it may provide a useful degree of speciation based on the absorption spectrum.
- Testing of commercially available solid phase sorbents for use in trapping and archiving thermally desorbed pollutants has produced good results, indicating collection efficiencies generally over 80% with the best sorbents, even in the presence of a substantial amount of water vapor.
- The feasibility of using surface-enhanced Raman spectroscopy (SERS) as an analytical tool for detecting PCBs (Aroclor mixtures and single congeners) in the presence of excess oil has been investigated with encouraging results. Detecting PCBs is best done by using SERS coating technology in which PCBs are partitioned from oil to a pentachlorothiophenol coating on a silver substrate. It has been demonstrated that for a single congener in an oil contamining mixture, quantitation at the detection limits of interest can be done.
- A preliminary design has been developed for the multitube sample trapping module that will house solid phase sorbent tubes and that will allow for simple, automated subsequent analysis of samples while providing direct transfer of sampling data for data handling simplification.

Phase I development of the RSSAR system has been completed. In Phase II, the team will develop the steel sampling head and the multisample trapping module and will construct a fully integrated lab scale system. In Phase III, a portable prototype system suitable for field use will be constructed. In Phase IV, the design of a production system will be completed and production units will be built.

The RSSAR system will provide DOE with a new tool to dramatically lower the costs associated with building decontamination and decommissioning activities. It will allow surfaces to be rapidly sampled for the presence of semivolatile organic contaminants and will provide the means for quickly identifying clean surfaces. It will archive samples in a form that will easily allow automated laboratory analysis and will automatically associate the sampling data with the lab analytical results.

References

[1] C. Rappa, S. Marklund, P.-A. Bergquist and M. Hanson in "Chlorinated Dioxin and Dibenzofurans in the Total Environment," (G. Choudhary, L.H. Keith, and C. Rappa, eds.) Butterworth Publishers, Boston, p. 99-124, 1983.

[2] H.R. Buser, H.P. Bosshardt, C. Rappa, and R. Lindahl, *Chemosphere*, 5, 419-29 (1978).

[3] M.M. Grade, Personal communication of unpublished results.

[4] M.D. Erickson, *Chemosphere*, 19, 161-165 (1989) and references cited therein.

[5] B.R. Frieden, ed., "The Computer in Optical Research," Springer-Verlag, NY, 134-137 (1980).

[6] H.S. Carslow and J.C. Jaeger, "Conduction of Heat in Solids," Oxford, p. 75, 1959.

[7] A. Dayan and E. Gluekler, "Heat and Mass Transfer within Intensily Heated Concrete Slab," Internation J. Heat Mass Transfer, 25, 1461-7 (1982).

[8] O. Hutzinger, S. Safe, and V. Zitco, The Chemistry of PCBs, CRC Publishing Co.

[9] R.A. Friedel and M. Orchin, "Ultraviolet Spectra of Aromatic Compounds," John Wiley and Sons, Inc., New York, 1951

[10] F. Bruner, G. Bertoni, G. Crescentini, *Journal of Chromatography*, 167, 399-407, 1978.

[11] J.F. Pankow, L.M. Isabelle, T.J. Kristensen, *Analytical Chemistry*, 54, 1815-1819, 1982.

[12] J.F. Pankow, L.M. Isabelle, *Journal of Chromatography*, 237, 25-39, 1982.

[13] G. Bertoni, F. Bruner, A. Liberti, C. Perrino, *Journal of Chromatography*, 203, 263-270, 1981.

[14] K. Schoene, J. Steinhanses, A. König, *Journal of Chromatography*, 514, 270-286, 1990.

[15] J.F. Pankow, T.J. Kristensen, *Analytical Chemistry*, 55, 2187-2192, 1983.

[16] J.H. Raymer, E.D. Pellizzari, *Analytical Chemistry*, 59, 1043-1048, 1987.

[17] R.H. Brown, C.J. Purnell, *Journal of Chromatography*, 178, 79-90, 1979.

[18] U.S. DOE Contract No. DE-AC21-92MC29110 entitled Organic Sponges for Cost-Effective CVOL Abatement.

[19] M. Dickey and K. Carron, "Determination of distance dependence of surface enhanced Raman using self-assembeld monolayers," to be submitted to Langmuir.

Abbreviations and Nomenclature for Rapid Surface Sampling and Archival Record (RSSAR) System Final Report.

Abbreviation	Definition
APDS	4-Aminophenyl Disulfode
BPDS	4,4'-Biphenyldisulfonylchloride
CCD	Charge Couple Device
DMF	N,N-Dimethyl formamide
DOE	Department of Energy
DSC	Differential Scanning Calorimetry
EAI	EAI Corporation, Abingdon, MD
GC	Gas Chromatography
GC/FID	Gas Chromatography / Flame Ionization Detection
GC/MS	Gas Chromatography / Mass Spectrometry
GE	General Electric Co.
GE-CRD	General Electric Corporate Research and Development
IR	Infrared
IUPAC	International Union of Pure and Applied Chemistry
mcgm	microgram
ng	nanogram
NVUV	Near Vacuum Ultraviolet
OSHA	Occupational Safety and Health Administration
PAH(s)	Polynuclear Aromatic Hydrocarbons
PCB(s)	Polychlorinated Biphenyls
PCDD(s)	Polychlorinated Dibenzodioxins
PCDF(s)	Polychlorinated Dibenzofurans
PCTP	Pentachlorothiophenol
PID	Photo-ionization Detector
PPM	Part Per Million
PPTH	Part Per Thousand
RSSAR System	Rapid Surface Sampling and Archival Record System
SCFH	Standard Cubic Feet per Hour
SERS	Surface Enhanced Raman Spectroscopy
TCB	Tetrachlorobiphenyl
TCDDS	Tetrachlorododecane Disulfide
THF	Tetrahydrofuran
TC(s)	Thermocouple(s)
UV	Ultraviolet
VUV	Vacuum Ultraviolet

For mathematical symbols used in the development of the concrete model, refer to Table 5 in Section 1.3.1.

Appendix 1

Design Drawings for the Bulk Sampler Oven and Concrete Sampler Head

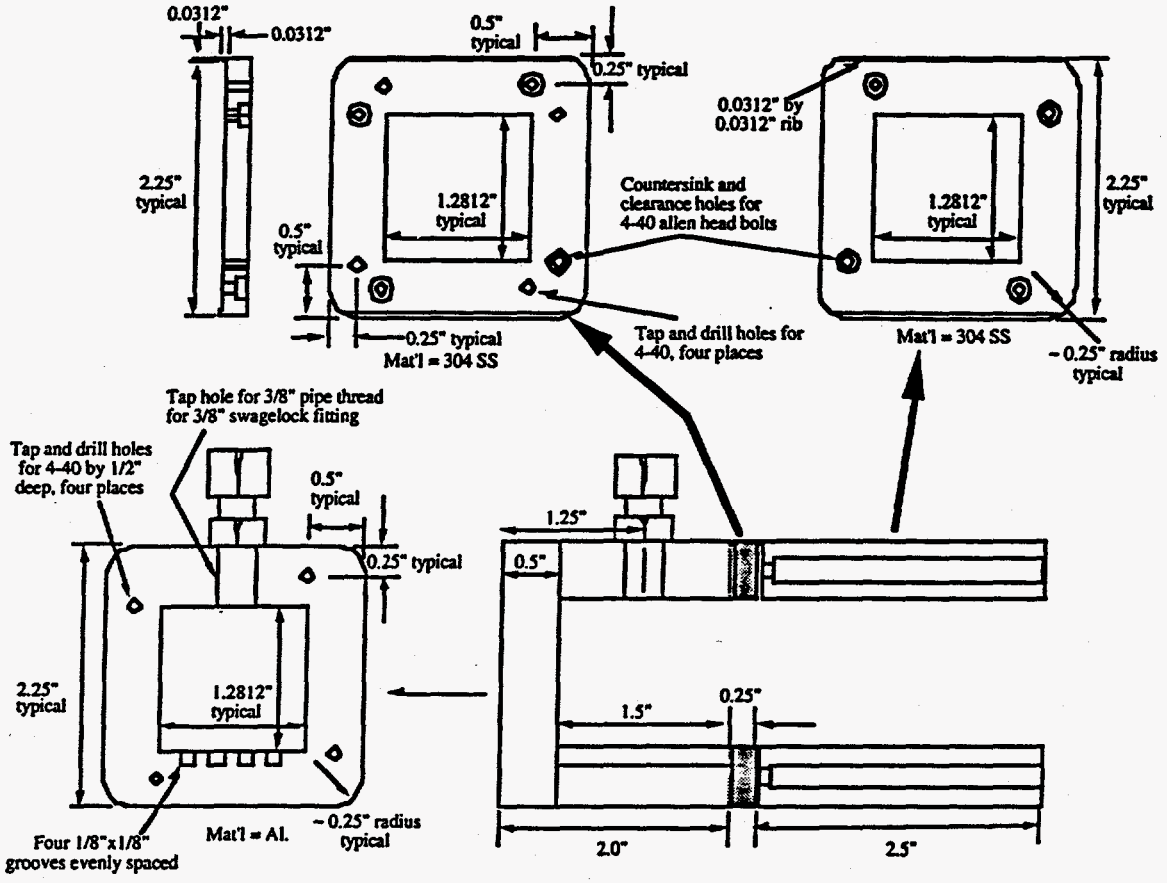

Figure A1-1. Bulk Sampler Oven

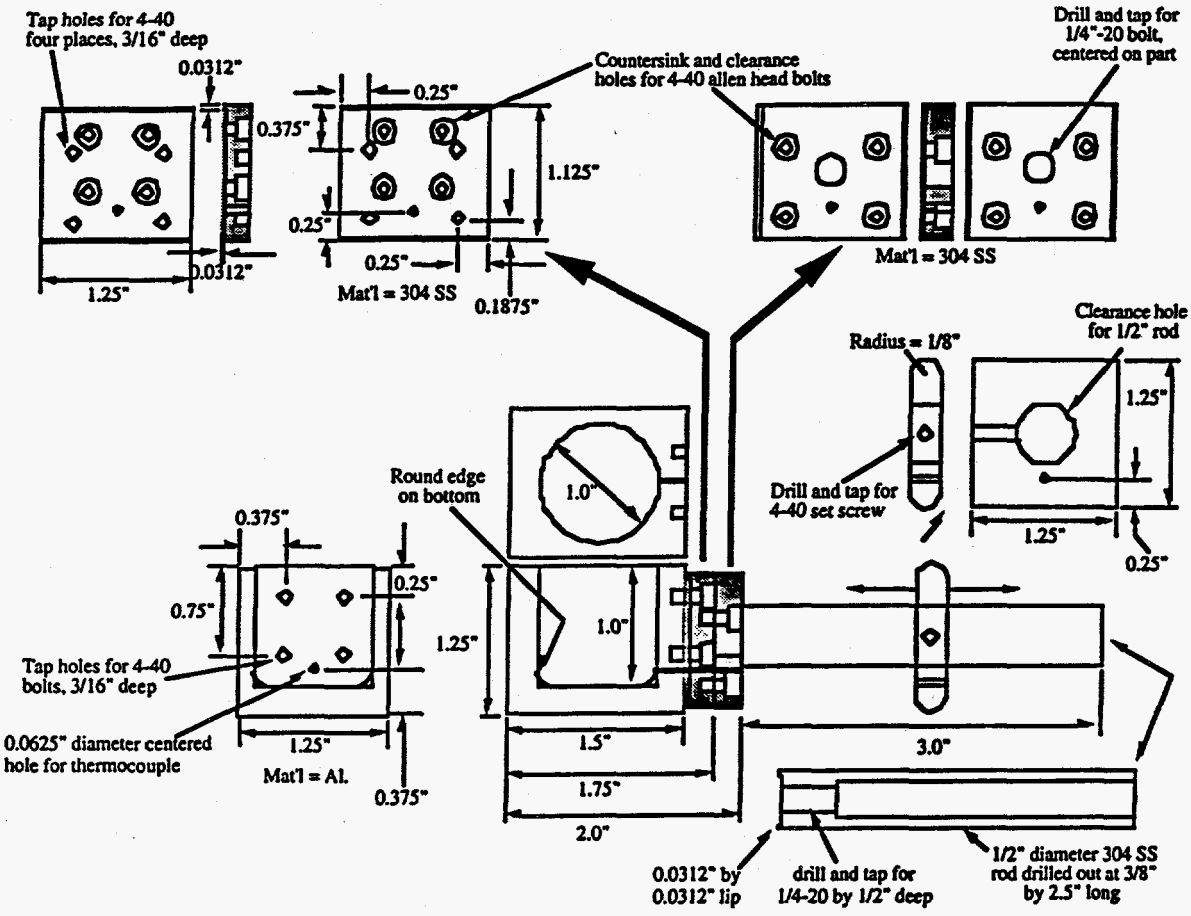

Figure A1-2. Bulk Sampler Oven Tray

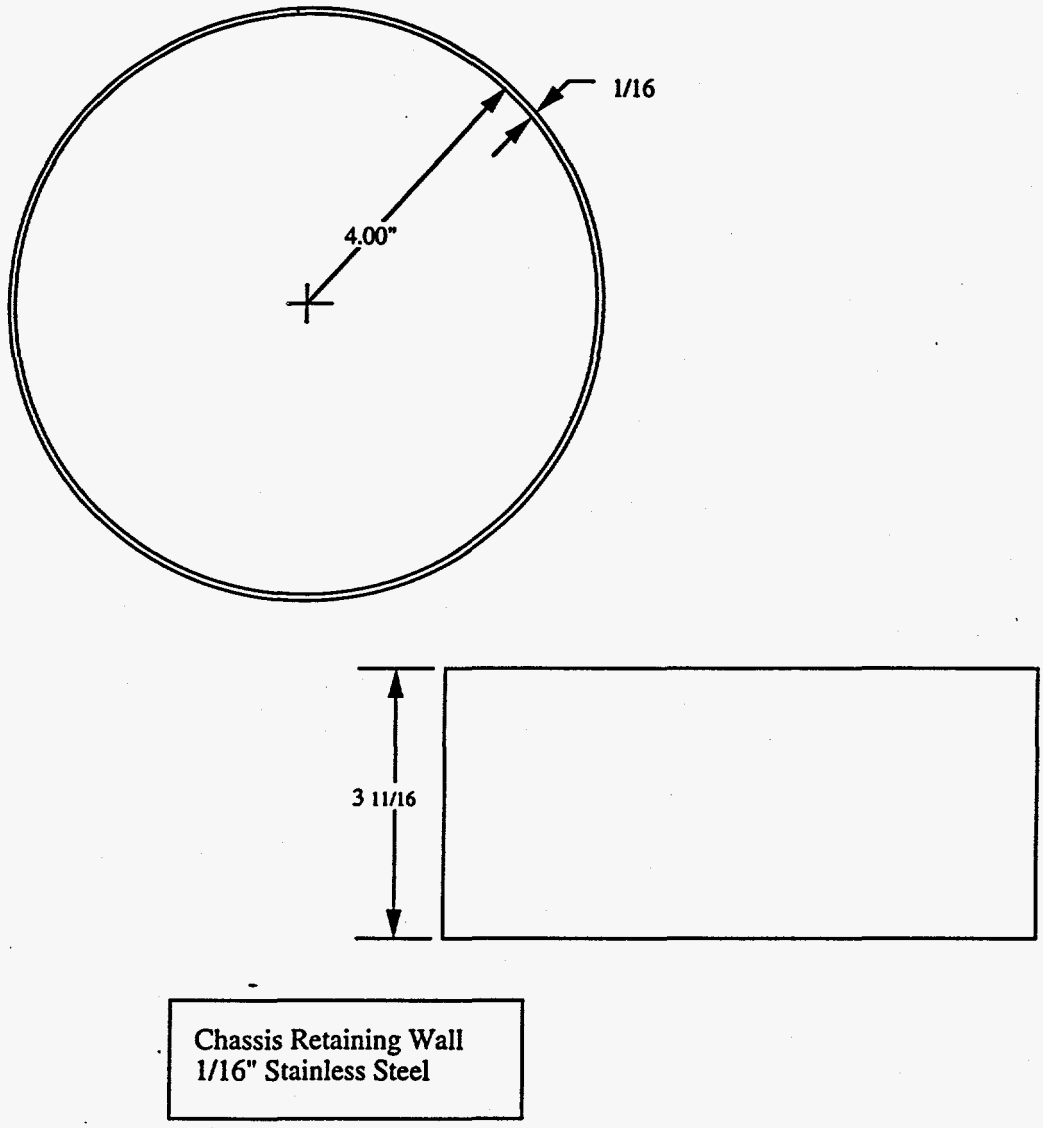

Figure A1-3. Concrete Sampler Chassis Retaining Wall

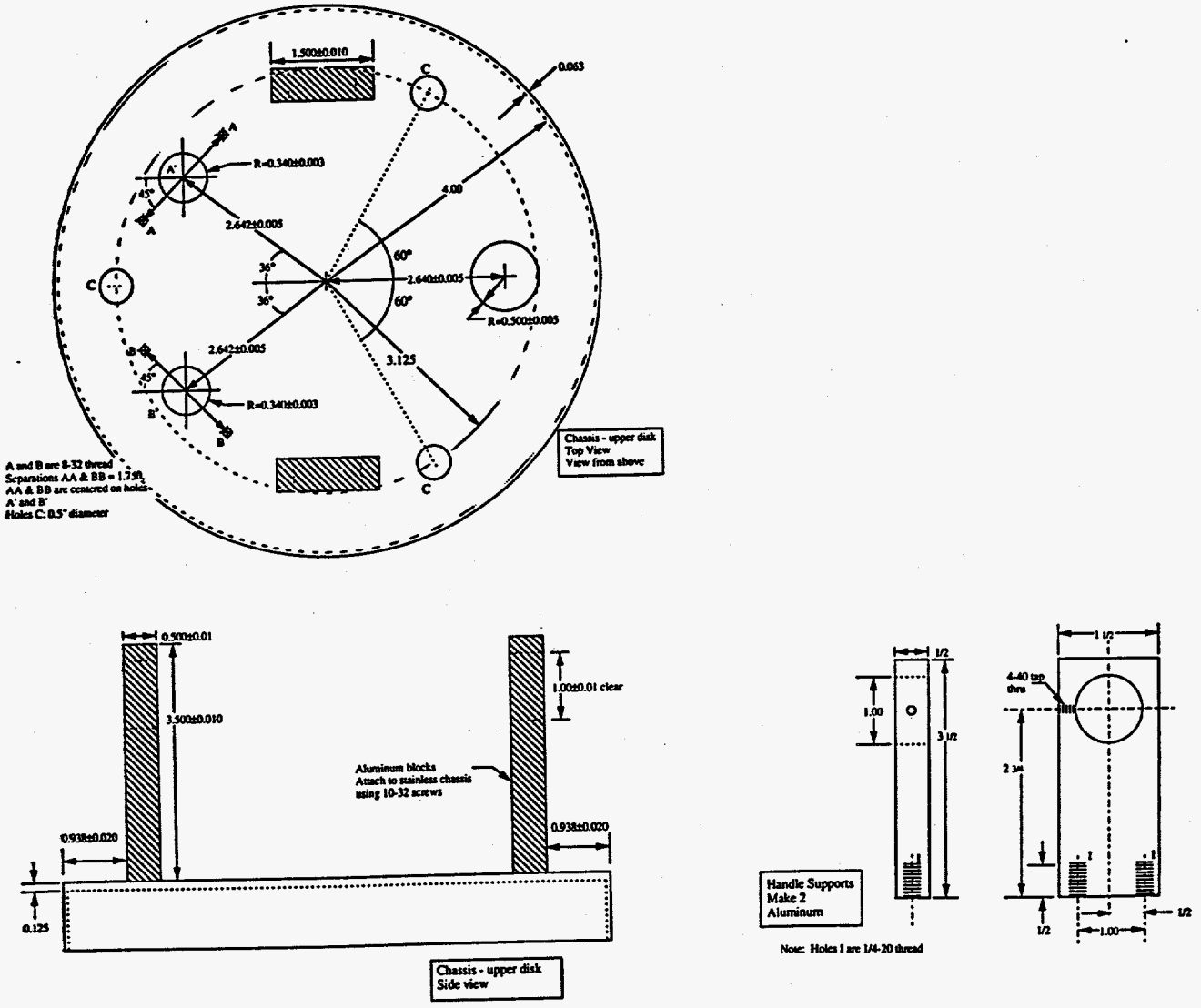

Figure A1-4. Concrete Sampler Chassis Upper Disk

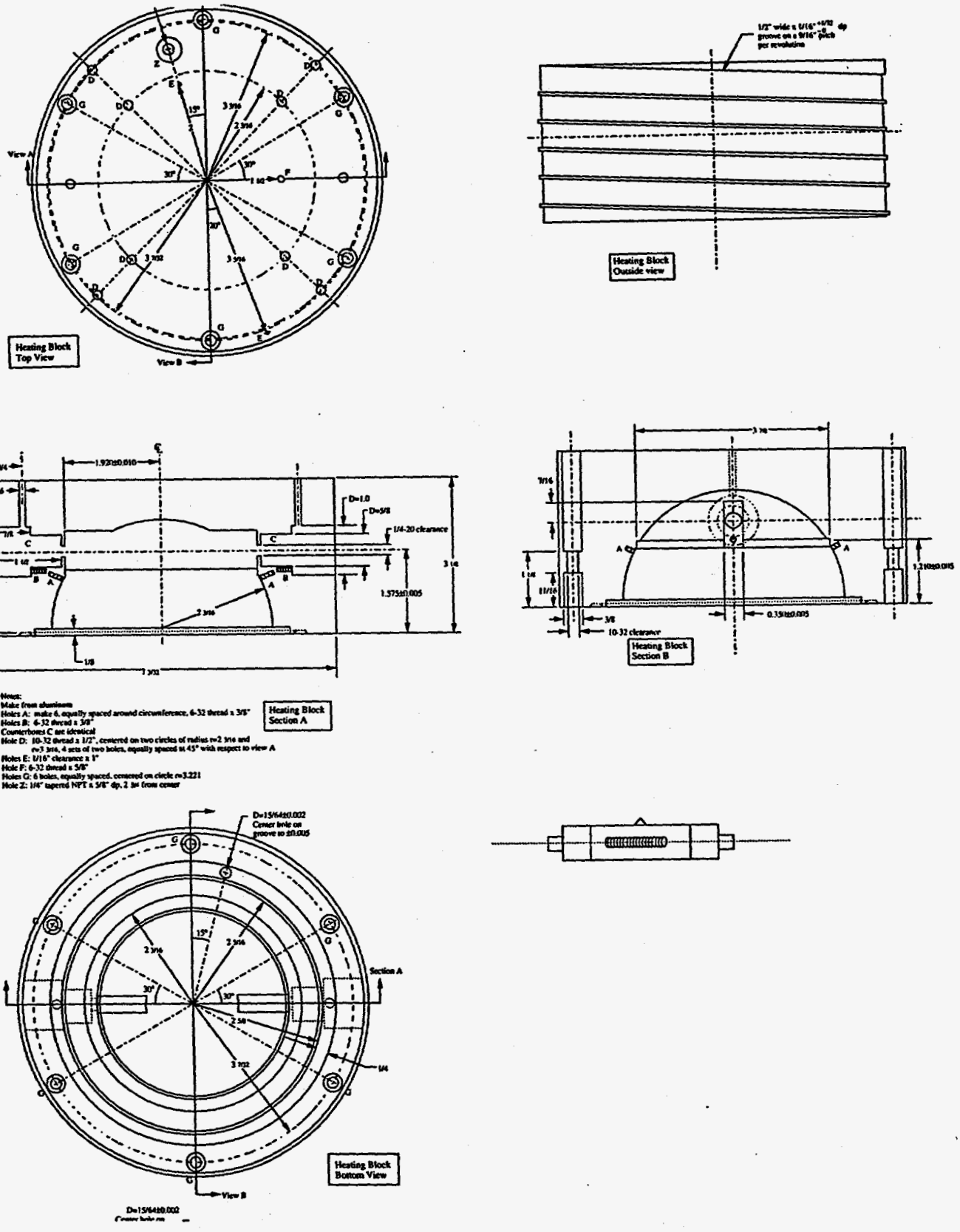

Figure A1-5. Concrete Sampler Heater Block

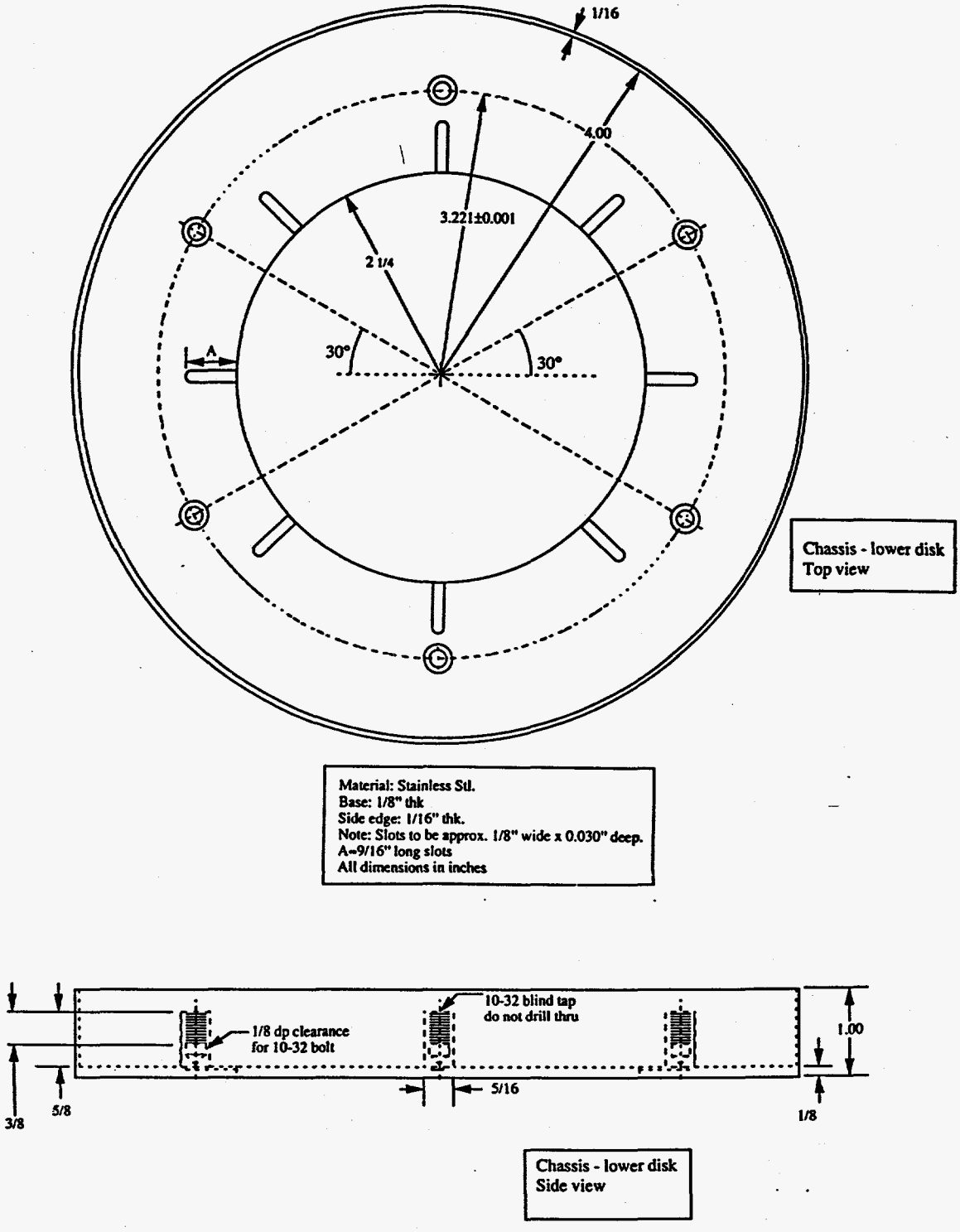

Figure A1-6. Concrete Sampler Heater Lens Holder

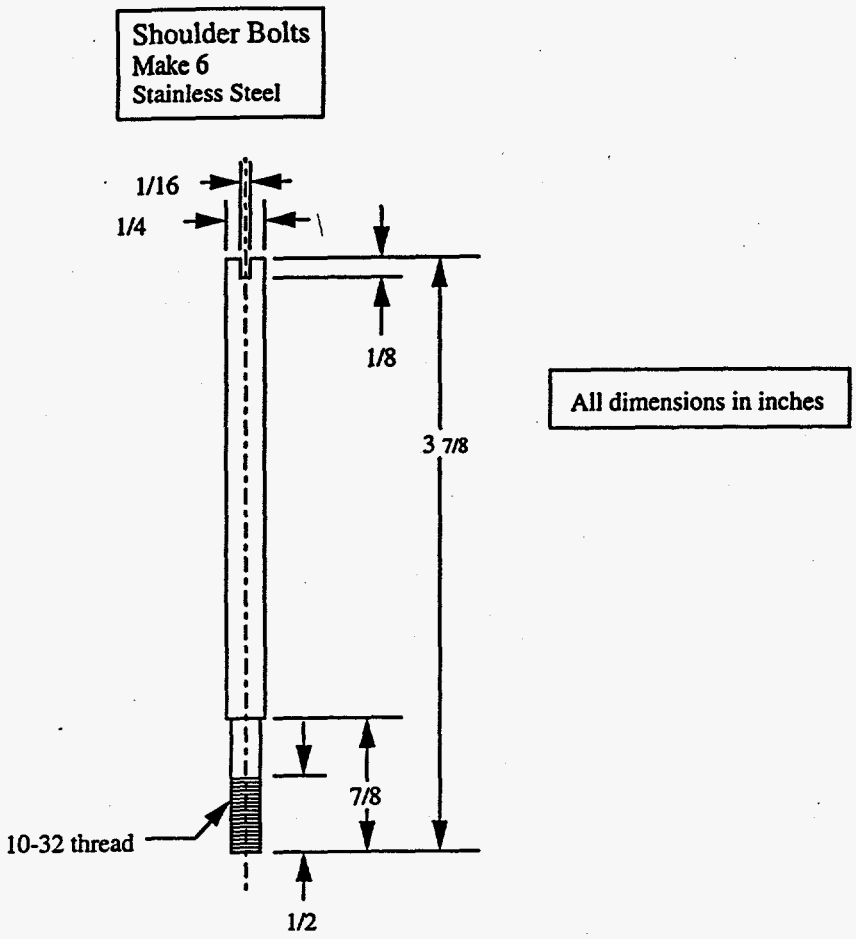

Figure A1-7. Concrete Sampler Shoulder Bolt

Appendix 2

Prototype Drawings

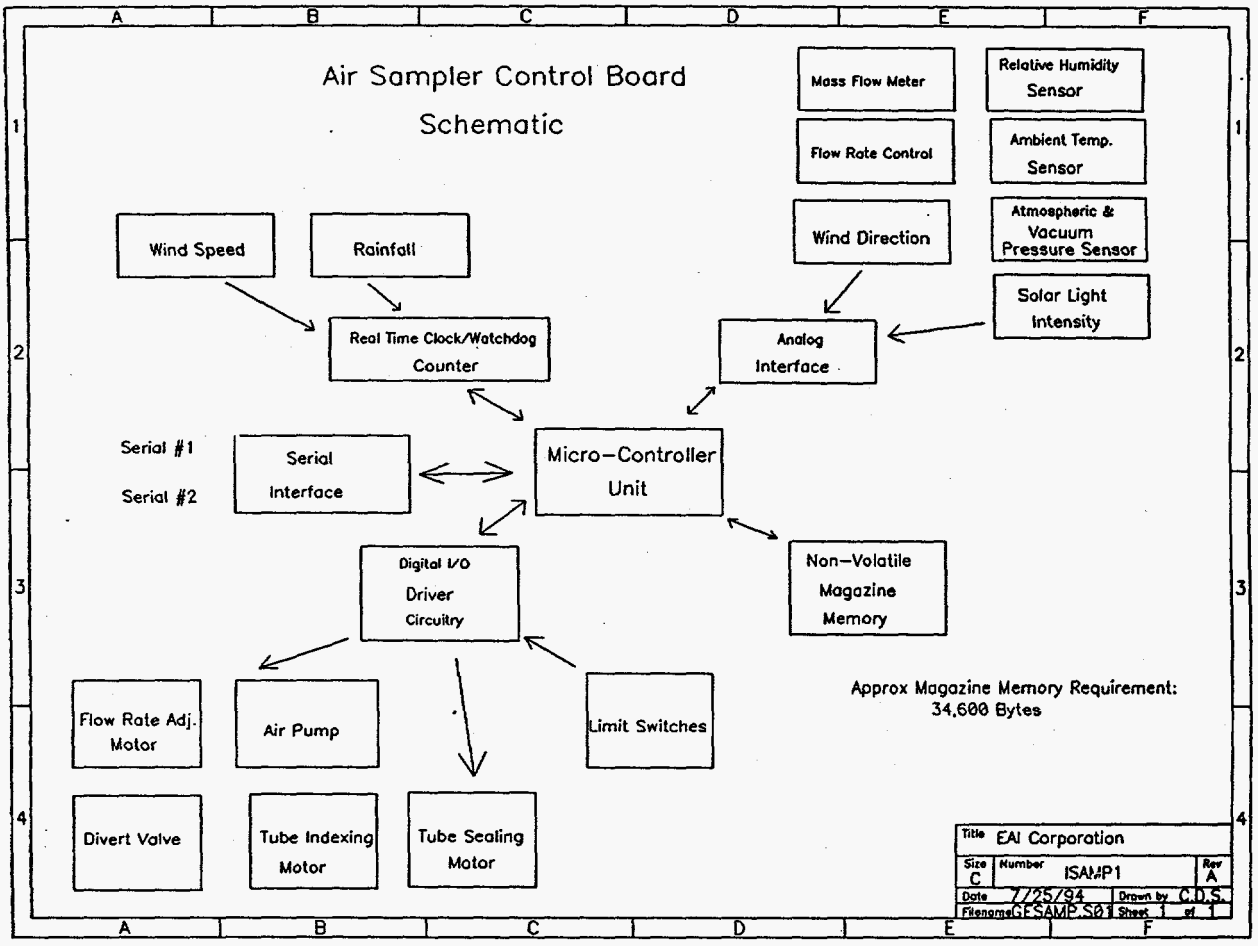

Figure A2-1. MSTM Circuit Board Schematic

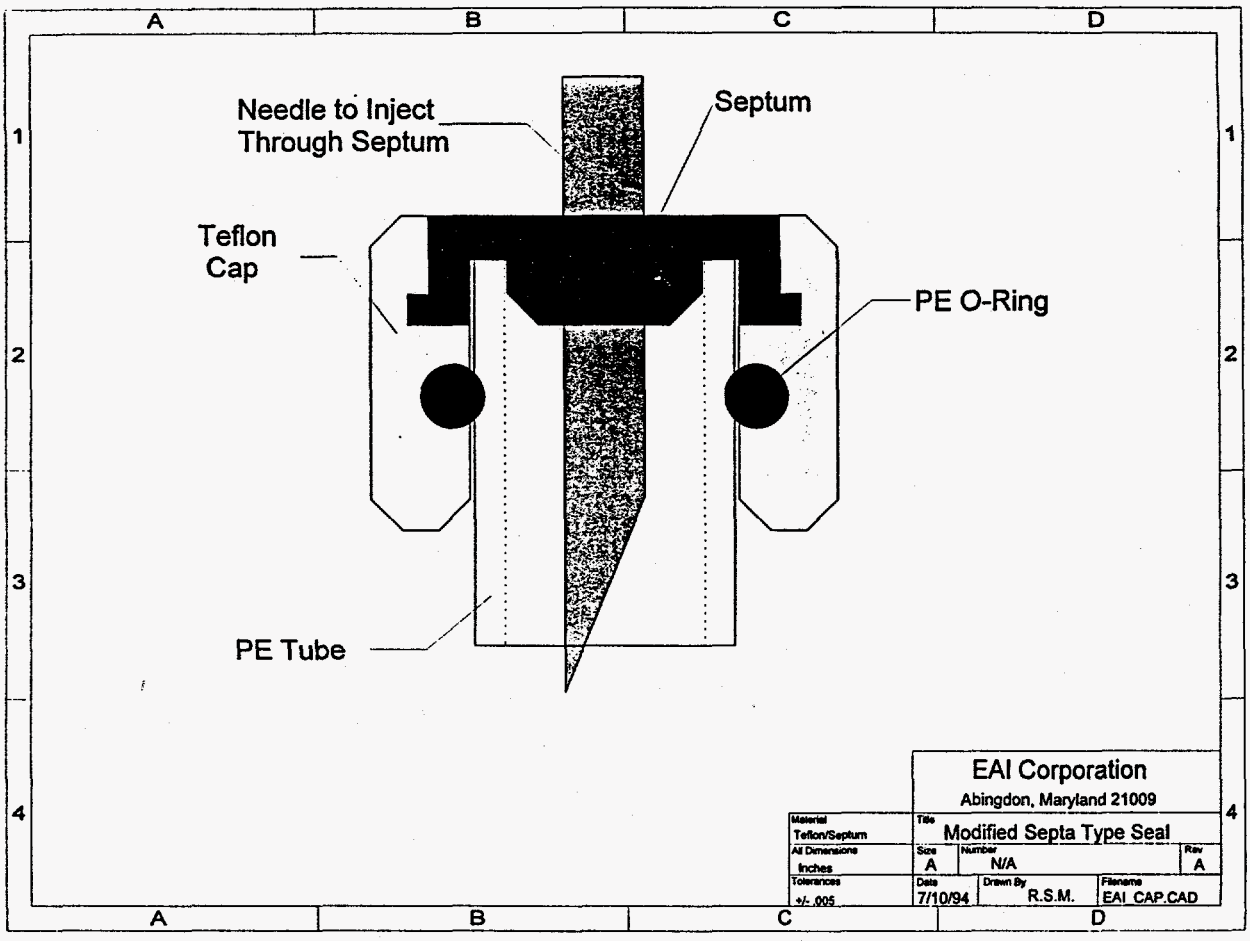

Figure A2-2. End Cap Design

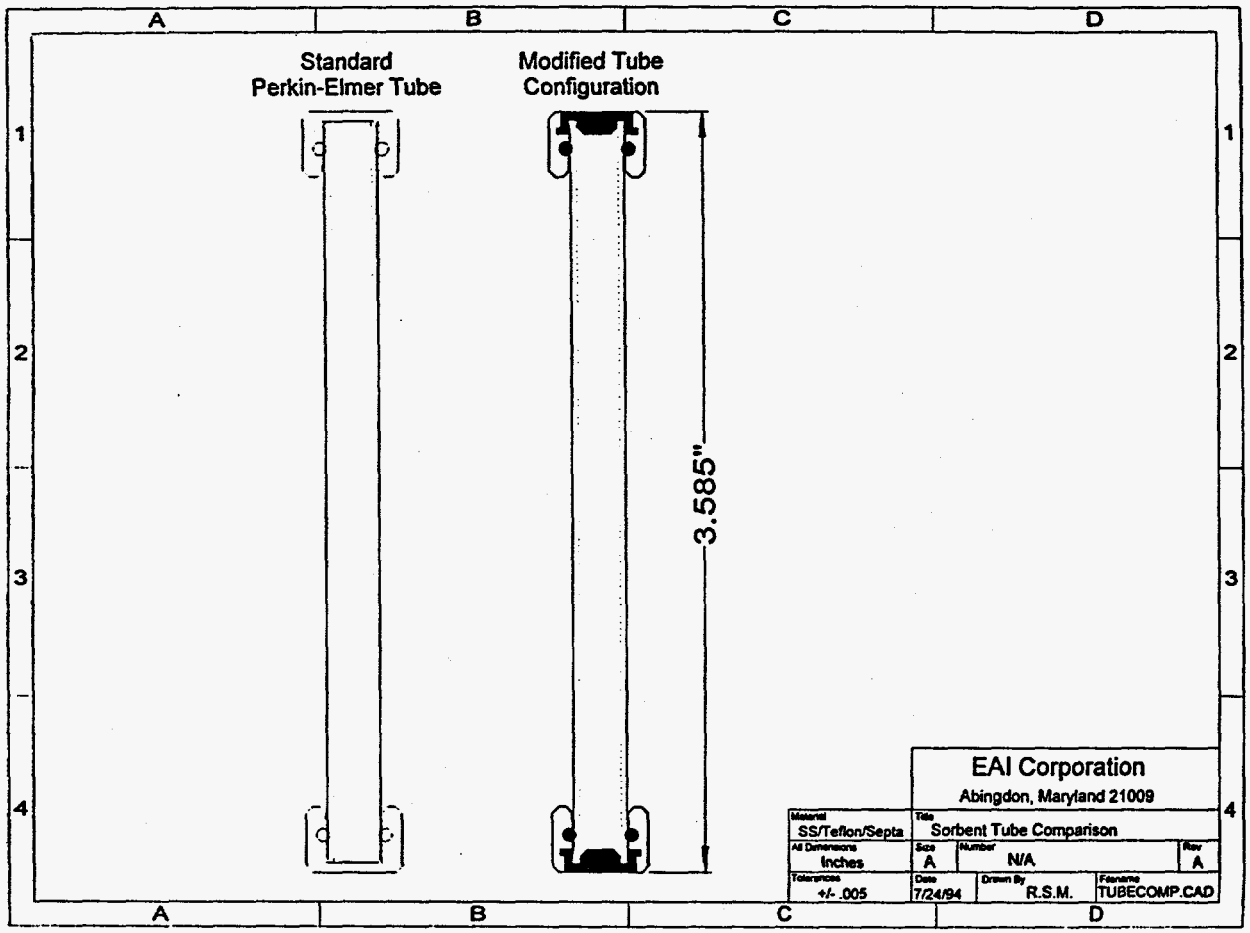

Figure A2-3. Sorbent Tube Comparison

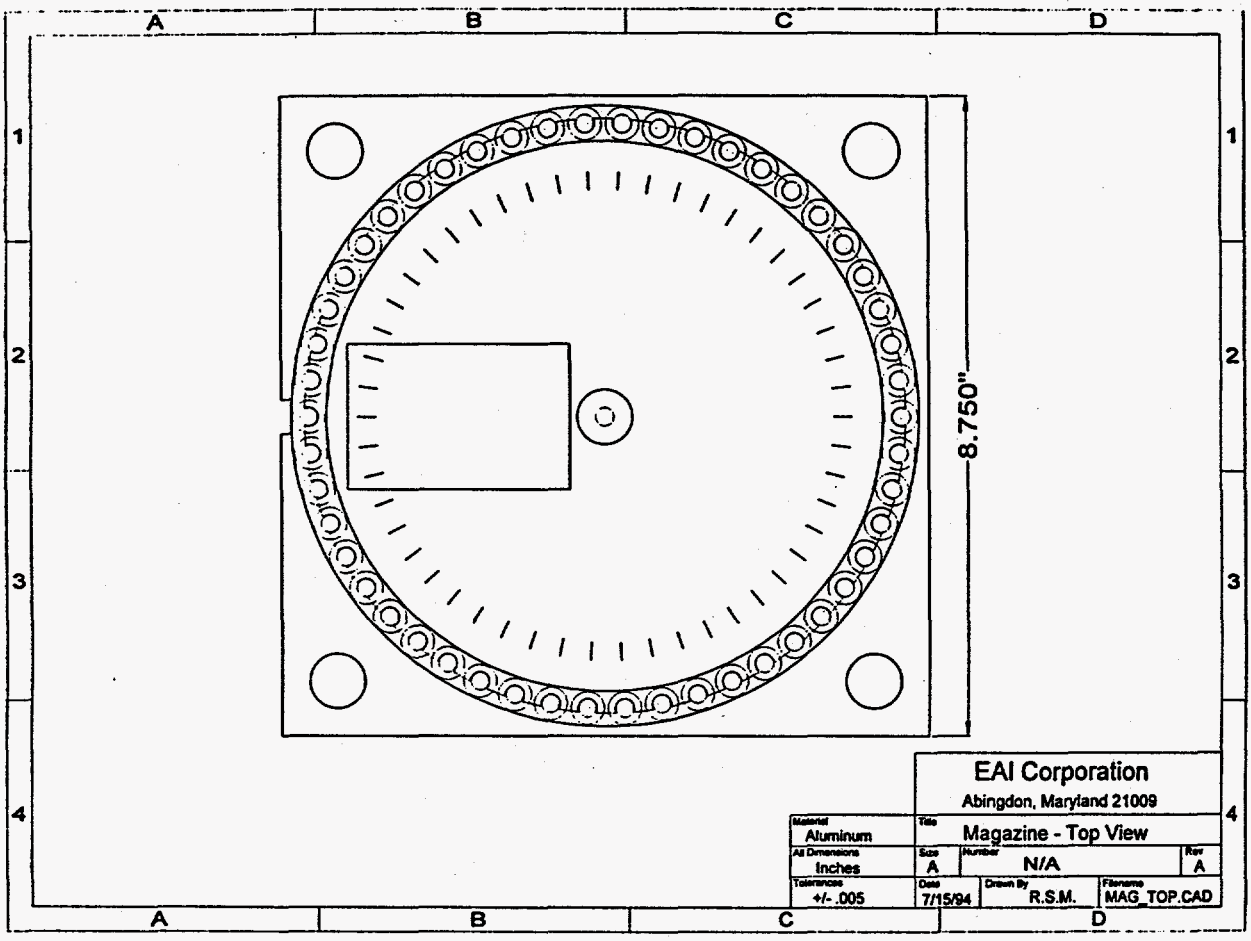

Figure A2-4. Magazine (Top View)

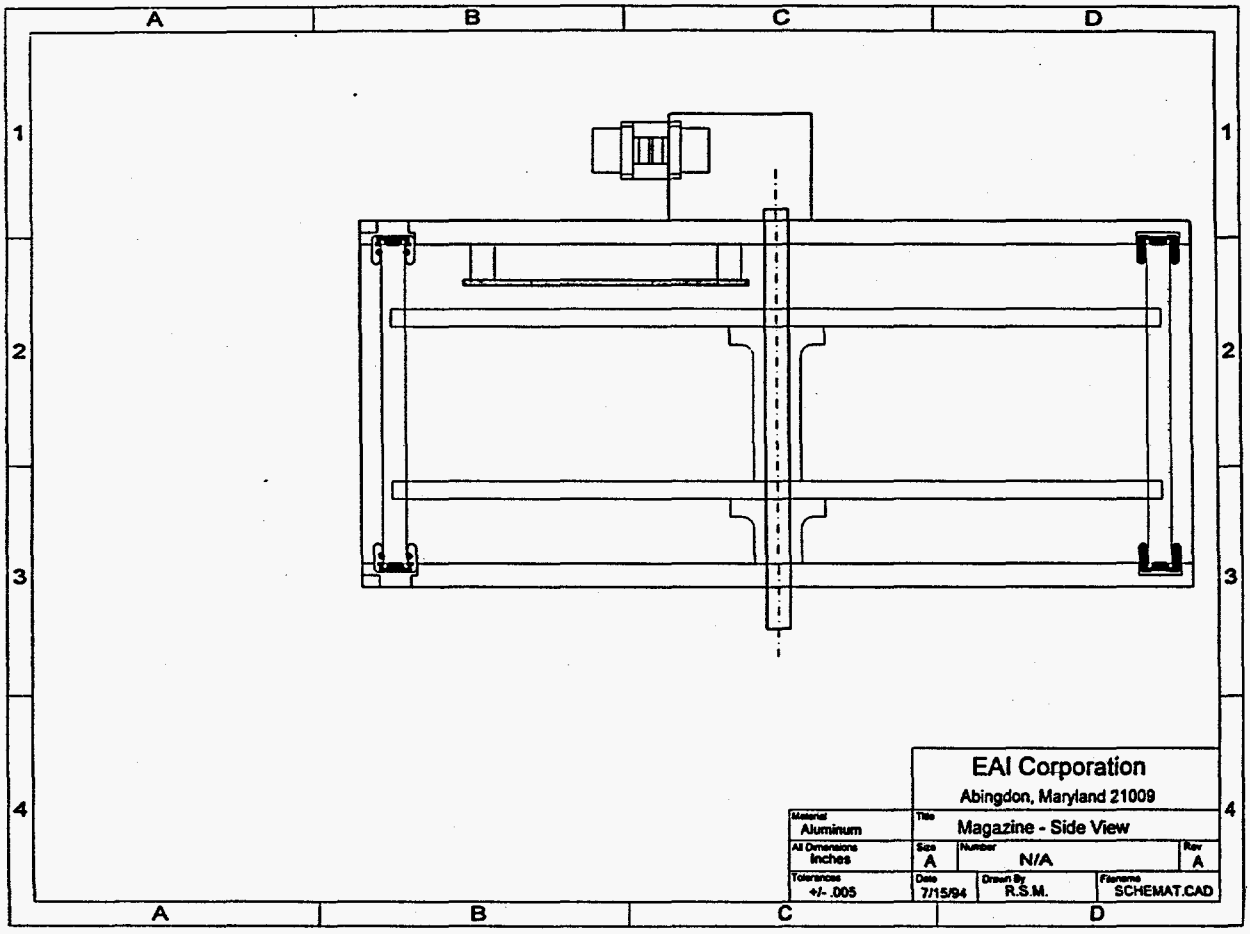

Figure A2-5. Magazine (Side View)

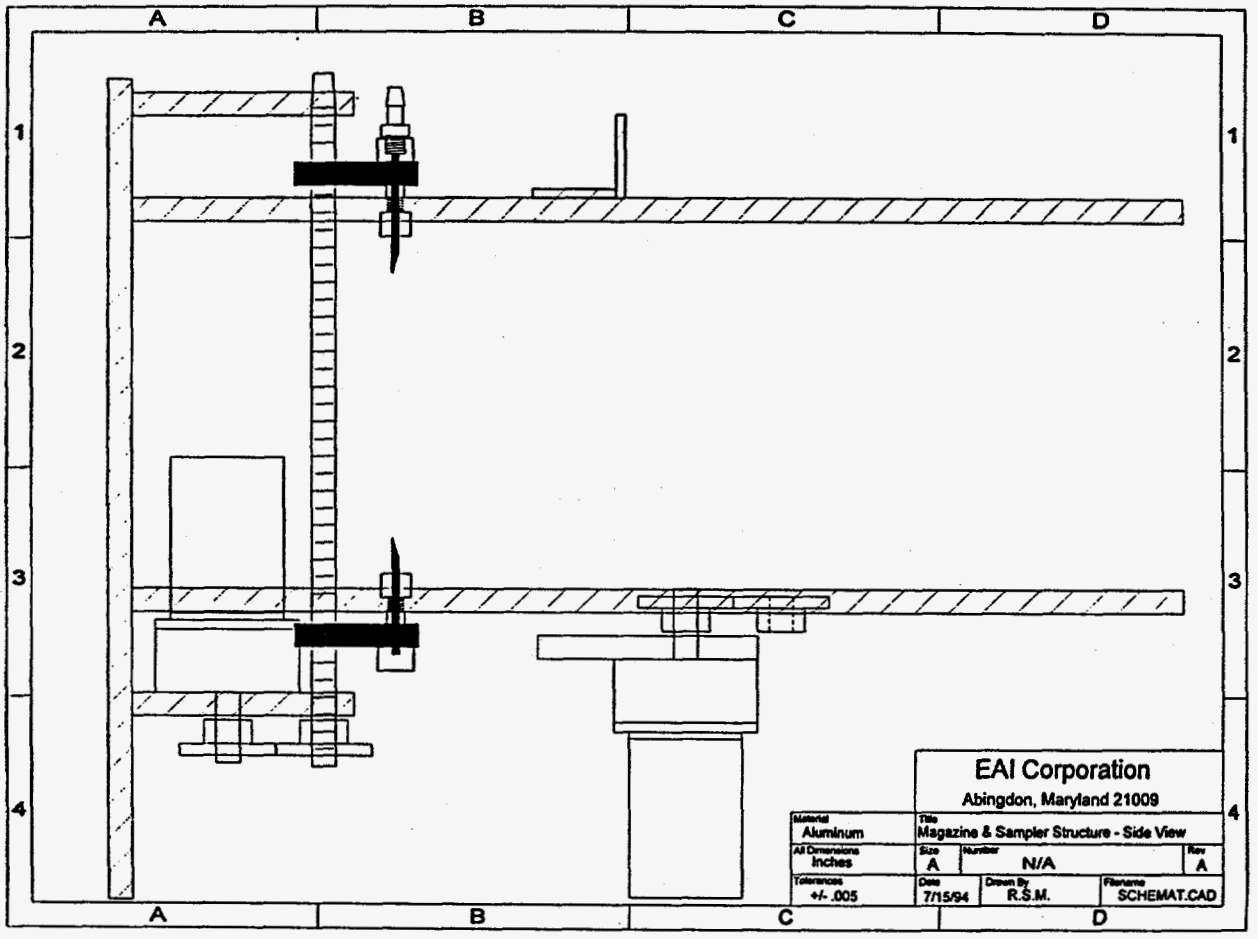

Figure A2-6. Sampler Magazine Receiving Structure and Sealing Mechanism (Side View)

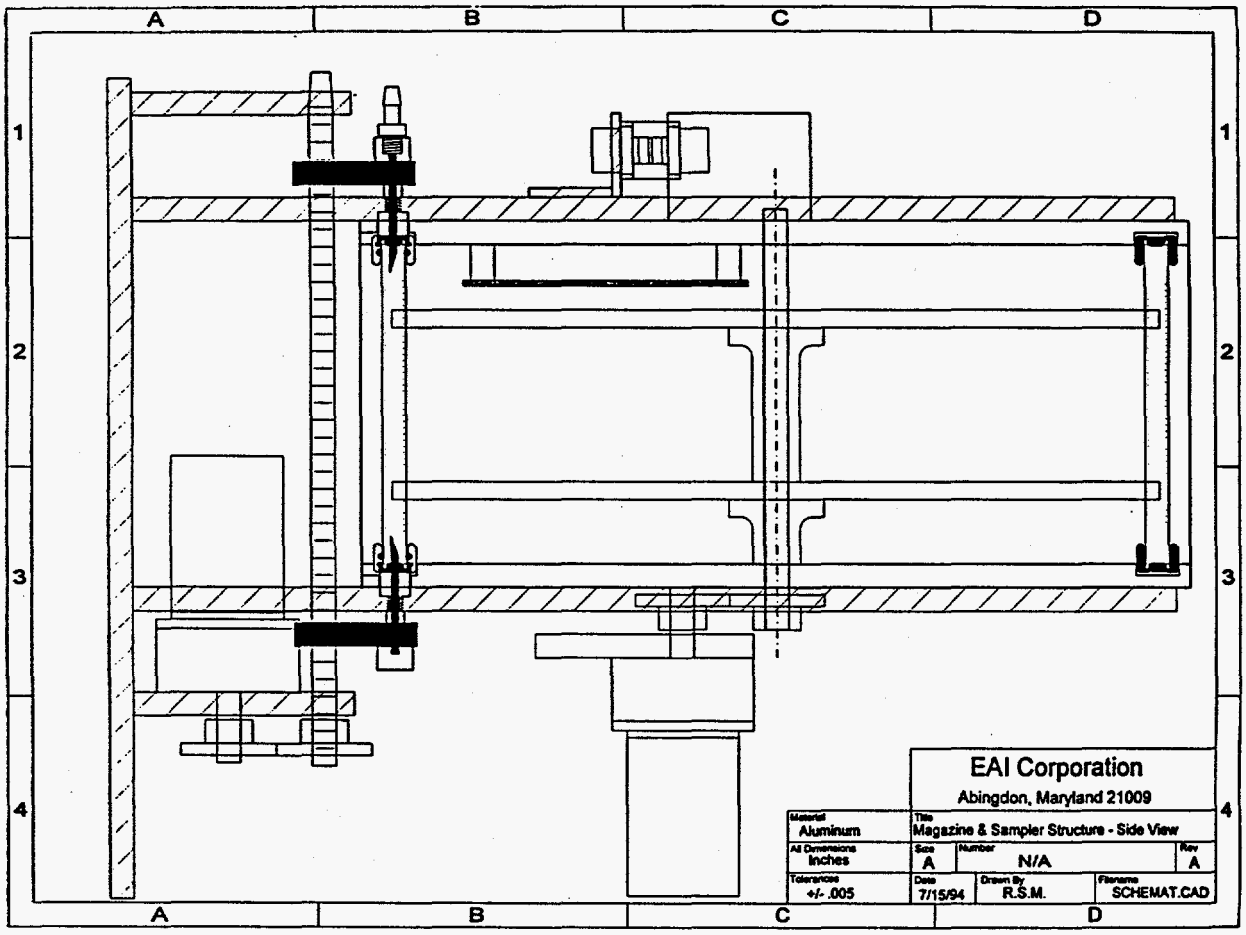

Figure A2-7. Magazine and Sampler Structure and Sealing Mechanism (Side View)

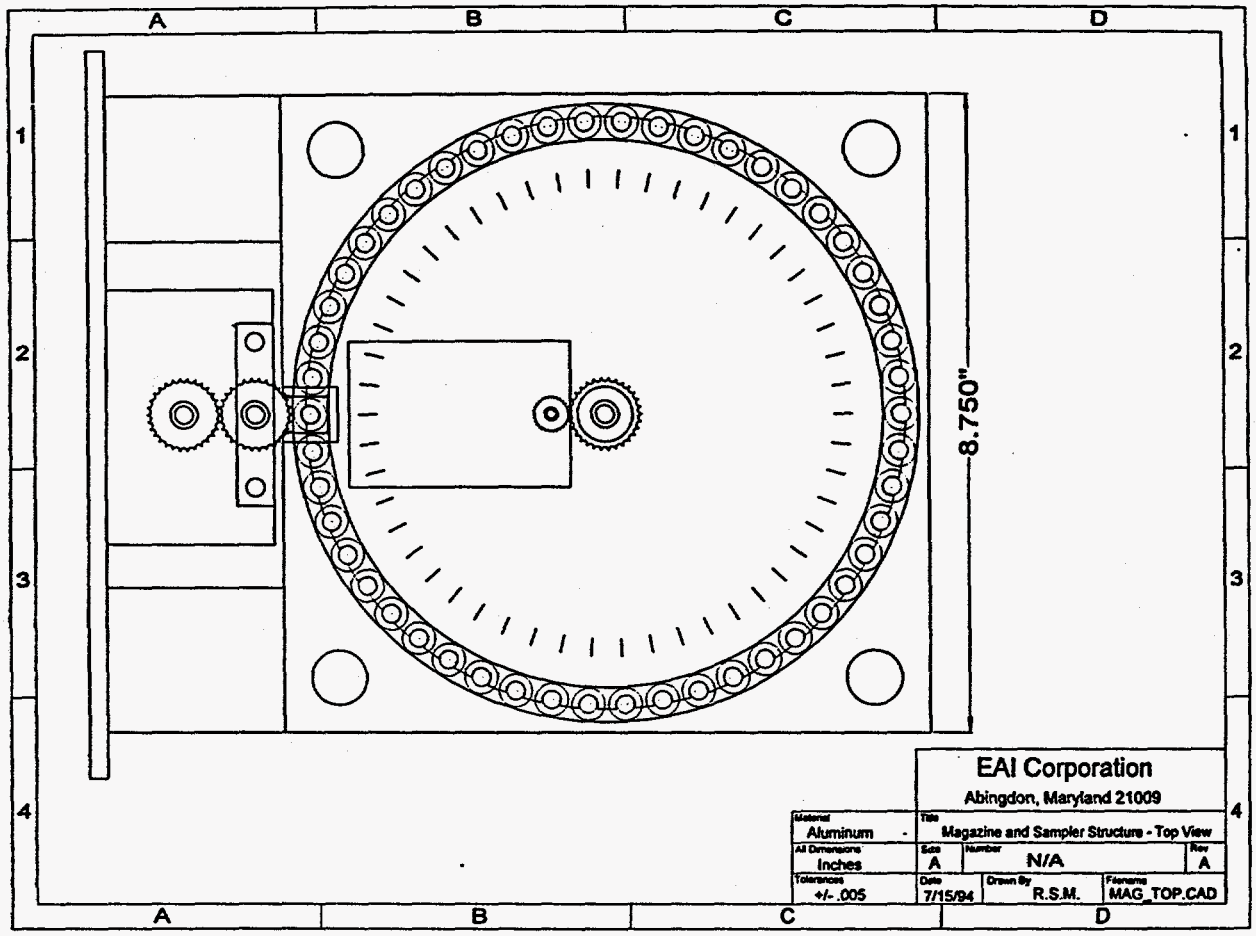

Figure A2-8. Magazine and Sampler Structure and Sealing Mechanism (Top View)